An Investigation into Selenium Geochemistry in Phosphate Mine Soils

Jessica Elizabeth Favorito

Dissertation Submitted to the Faculty of the Virginia Polytechnic Institute and State University

in Partial Fulfillment of the Requirements for the Degree of

Doctor of Philosophy

In

Crop and Soil Environmental Sciences

Matthew J. Eick (Chair)
Paul R. Grossl
Walter Lee Daniels
Kang Xia

April 28, 2017
Blacksburg, VA

Keywords: Adsorption, Bioavailability, Dissolved Organic Carbon, Phosphate Mine Soils, Selenium, Sequential Extraction Procedure, XAFS

An Investigation into Selenium Geochemistry in Phosphate Mine Soils

Jessica E. Favorito

Abstract (Academic)

In the western United States, elevated selenium (Se) levels in soil have resulted in documented cases of ruminant fatalities. This is due to the ingestion of Se-hyperaccumulating vegetation growing on previously reclaimed phosphate mine soils. A field-scale analysis was first conducted to examine Se bioavailability to plants. Soil and plant samples were collected from transects from five study locations in Soda Springs, Idaho. Soils were analyzed for Se speciation and geochemical phases using a sequential extraction procedure (SEP). Additionally, speciation, SEP results, and Se bioavailability in the hyperaccumulator, western aster (*Symphyotrichum ascendens* (Lindl.)), were related using simple linear regression. Soil speciation and the validity of this SEP were then evaluated using synchrotron-sourced X-ray absorption fine structure (XAFS) spectroscopy for both whole and a sequence of extracted soils. Lastly, competitive adsorption of Se with two dissolved organic carbon (DOC) species, citric and salicylic acid, was examined on an amorphous iron oxide mineral surface.

A strong relationship was identified for western aster Se and the first two combined SEP fractions, water-soluble and PO_4^{3-}-extractable Se ($R^2 = 0.85$; $P = <0.0001$). Results also indicated a strong relationship between selenate and water-soluble Se ($R^2 = 0.83$; $P = 0.0002$). This suggests that water extracts could be useful Se bioavailability assessment tools in highly contaminated systems. XAFS analyses indicated that elemental and organic Se were the most predominant phases overall in whole soils. The dominant oxidized species present was selenite sorbed onto iron oxides and calcite. Critical SEP evaluations using XAFS also indicate that oxidized Se species were underestimated by the SEP and elemental Se was overestimated. In extracted soils, XAFS results indicated partial recovery of carbonate, iron oxide and organic Se occurred. Therefore, it is suggested that researchers exert caution when employing SEPs. Additionally, sorption analyses demonstrated the highly competitive behavior of citric acid with both selenite (pH 5-8) and selenate (pH 5-6). Little competition was observed in the presence of salicylic acid for both Se species. Competition and subsequent desorption of both sorbed species in the presence of citric acid suggest a possible mechanism for Se solubilization and bioavailability in seleniferous environments.

An Investigation into Selenium Geochemistry in Phosphate Mine Soils

Jessica E. Favorito

Abstract (Public)

Selenium (Se) is a contaminant found in elevated levels in soils and plants in the Western United States due to phosphate mining. This has caused livestock deaths throughout the mining region following ingestion of plants with particularly high Se levels. Soils and plants were sampled from five study locations and used to assess relationships between soils and plant Se uptake. A sequential extraction procedure (SEP) was used to estimate Se in soils related to soluble, exchangeable, bound, organic, and elemental forms of Se. X-ray absorption fine structure (XAFS) spectroscopy was then used to critically evaluate the validity of these phases and the procedure accuracy. Lastly, the competitive effects of organic acids, which are naturally present in soils, on Se sorption was evaluated in a batch reactor system. From the SEP analysis, higher levels of Se were found in organic and elemental fractions, moderate quantities were observed in sorbed fractions, and smaller abundances were observed in soluble and exchangeable fractions. Relationships between soluble Se and selenate, a highly bioavailable form of Se determined from speciation analyses, indicated that simple water extracts could be used to assess Se "hotspots" in order to prevent further livestock fatalities. The critical evaluation of this SEP using XAFS determined that this procedure was under- and over-estimating bound and organic extracted phases of Se. This was possibly due to mineral and organics that were incompletely dissolved during extraction. It was determined that researchers should exert caution prior to using SEPs and have suggested several recommendations. Lastly, the batch reactor analysis indicated a form of DOC, citric acid, was highly competitive for mineral surface sites with selenite and selenate. Competition from salicylic acid was not obvious. Differences in competition were speculated to be linked to differences in molecular structure. This work suggests possible mechanisms for solubilization of both selenite, which is typically strongly bound, and selenate, which is typically soluble, in soil systems. Results offer an explanation for the exceedingly bioavailable nature of Se in the Western US.

Acknowledgements

I wish to thank a number of people who have assisted me throughout my doctoral research. I would like to express my deepest, sincerest gratitude to my adviser, Dr. Matthew Eick. With his guidance, I have learned far more than I ever thought was possible. I cannot thank him enough for the opportunities that I have been given as his student. I would like to thank the members of my doctoral advisory committee, Drs. Paul Grossl, Lee Daniels and Kang Xia, for their guidance, insight, and support throughout the completion of my dissertation. I especially would like to thank Paul for his time spent with me during my fieldwork in Idaho, his assistance with my projects, and the many phone calls throughout the years. I would also like to thank Dr. Todd Luxton for making my synchrotron work possible and for all of the time he has spent with me on it. This is an opportunity that I am very grateful for. Thank you to the staff and my fellow graduate students in the Department of Crop & Soil Environmental Sciences for their friendship, support, and help over the years.

Most importantly, I owe most of my strength and success to my family and John. Your love, support, and encouragement have pushed me through difficult times more so than anything. To my parents: thank you for all that you have taught me and for always believing in me. I am very lucky to have such an incredible support system!

Table of Contents

List of Figures

List of Tables

Chapter 1: Introduction

Selenium (Se) is a trace element found in elevated concentrations from phosphate mining practices and reclamation in the Western US. Following phosphate mining, Se-rich overburden was used as a topsoil replacement during reclamation prior to 1996 (Blanchard et al., 2002). This material was high in reduced Se species; however, the oxidizing conditions present in semi-arid systems promote Se oxidation to the soluble species, selenite and selenate. Soils in this region are particularly high in Se and have reached levels upwards of 1,000 mg Se kg^{-1} soil (Bennett, 1982; Lakin and Byers, 1941). Plants that are considered Se-hyperaccumulators can absorb in excess of 1,000 mg Se $kg^{-1}_{DW\ (Dry\ weight)}$ (White, 2016). Selenate is the more bioavailable-oxidized species, however, plants can also absorb selenite in smaller quantities (Spallholz, 1994). This has resulted in extensive fatalities in livestock due to acute Se toxicity following grazing on hyperaccumulating vegetation. Western aster (*Symphyotrichum ascendens* (Lindl.)) is the species responsible for grazing fatalities throughout Southeastern Idaho, with unpublished tissue samples in excess of 13,000 mg Se kg^{-1}_{DW}. Selenium bioavailability can be affected by a number of possible factors, such as species and phases present, redox conditions, and soil geochemical and mineralogical conditions, competitive oxyanions, and pH (Geering et al., 1968; USEPA, 1996). Hence, it is imperative that these processes are better understood in order for Se risk to be properly mitigated.

For this work, Se bioavailability was evaluated from a field, spectroscopic, and molecular approach. The objectives of this dissertation are as follows:

A) Chapter 1: To complete a field scale analysis involving both speciation and fractionation of Se in soils sampled from previously reclaimed phosphate mines. Results will be related to plant Se absorption and bioavailability.

B) Chapter 2: To employ spectroscopic methods using synchrotron sourced X-ray absorption fine structure (XAFS) spectroscopy to identify Se speciation in soils and evaluate a sequential extraction procedure (SEP).

C) Chapter 3: To examine Se behavior and adsorption in batch reactor systems in the presence and absence of dissolved organic carbon (DOC) on an amorphous Fe oxide surface. Competitive interactions with organic ligands can promote oxyanion solubility on mineral surfaces.

References

Bennett, B.G., 1982. Exposure of man to environmental nickel - an exposure commitment assessment. Sci. Total Environ. 22, 203-212.

Blanchard, T., Baun, C., Stone, L., Gudgell, D., Hayes, J., 2002. Hardrock and Phospahte Mining in Idaho. A report by the Idaho Conservation League and Boulder-Whites Clouds Council.

Geering, H.R., Cary, E.E., Jones, L.H.P., Allaway, W.H., 1968. Solubility and Redox Criteria for the Possible Forms of Selenium in Soils. Soil Sci Soc Am J 32: 35-40.

Lakin, H.W., Byers, H.G., 1941. Se occurrence in certain soils in the United States, with a discussion of related topics: fifth report. United States Department of Agriculture, Washington D.C.

Spallholz, J.E., 1994. On the nature of selenium toxicity and carcinostatic activity. Free Radical Biol. Med. 17, 45-64.

USEPA, 1996. EPA Environmental Assessment Sourcebook. Ann Arbor Press, Inc., Chelsea, Michigan.

White, P.J., 2016. Selenium accumulation by plants. Ann. Bot. 117, 217-235.

Chapter 2: Selenium Geochemistry and Adsorptive Behavior in Semi-Arid Soil Systems: A Review

Abstract

Selenium is a trace element found naturally in the environment and in exceedingly high concentrations in the Western Phosphate Field of the US. This is notably due to phosphate mine reclamation practices. There is great concern over Se soil contamination in this region because it can be taken up by vegetation at toxic levels to livestock. In turn, this has caused acute toxicity in wildlife and foraging animals that graze on them. Both soil redox chemistry as well as sorption processes control Se bioavailability to plants. Sorption processes involving soil mineral components, including phyllosilicate clays, iron oxides, aluminum oxides, and carbonates as well as organic components play a critical role in plant bioavailability. Competing anions in solution can also promote or impede Se sorption onto these surfaces. This review provides useful information related to Se contamination. Integrating this knowledge into remediation and mitigation plans will prove beneficial for determining mechanisms of sequestration that can reverse adverse impacts in seleniferous soils.

Introduction

Selenium (Se) is a chalcogenic element, with naturally high concentrations found in sedimentary rock. Other chalcogens, such as sulfur (S) and tellurium (Te), are chemically similar and exhibit similar behavior to Se in soils. Many plants cannot differentiate between S (an essential element) and Se (Pilon-Smits, 2015). Origins of Se contamination are generally through mining and agricultural drainage over seleniferous soils (NAS-NRC, 1983). Elevated concentrations of Se in soils contaminated by phosphate mining processes have become a concern in semi-arid regions across the United States. This is largely due to oxidizing conditions

and high pH that reduce sorption on oxide minerals, promoting the bioavailability of Se (Jacobs, 1989; Neal, 1995). This has caused harmful effects on livestock and wildlife that ingest Se-rich vegetation. For most animals, Se is a micronutrient and is used in a variety of physiological processes. However, at high concentrations found in seleniferous regions, it is also a toxin. The species, selenite and selenate, predominate in oxidizing semi-arid environments. They are also the more toxic forms, with selenite considered more toxic than selenate (Cobo Fernandez et al., 1993). The inherent bioavailability of oxidized Se species is dependent on its adsorptive behavior in soils. The purpose of this review is to detail and integrate published literature that observes Se behavior in semi-arid soils and its various adsorptive mechanisms. This information is critical for determining means of Se mitigation in Se contaminated soils.

Geology, Mining, and Distribution of Se in Semi-Arid Environments

Selenium is typically associated with igneous and sedimentary rocks (NAS-NRC, 1983). Within the earth's crust, the average concentration for total Se is 0.05 mg kg^{-1} (Fordyce, 2013). Its average abundance varies depending on rock type and location. The average concentration in igneous rocks is 0.35 mg kg^{-1}, between 0.03 and 0.08 mg kg^{-1} in limestone, and 0.05 mg kg^{-1} in shale. In sandstones, the average is less than 0.05 mg kg^{-1}. In semi-arid locations of the United States, Se content in rock can range from 0.02 mg kg^{-1} to over 1,500 mg kg^{-1} (Lakin, 1961). Concentrations in the higher end of this range are associated with mudstones. Other rocks associated with high Se concentrations are phosphatic rocks, black shale, and coal (Fordyce, 2013). As noted, Se concentration markedly increases between the upper ore and waste rock material (Figure 2.1 ; USGS, 2002).

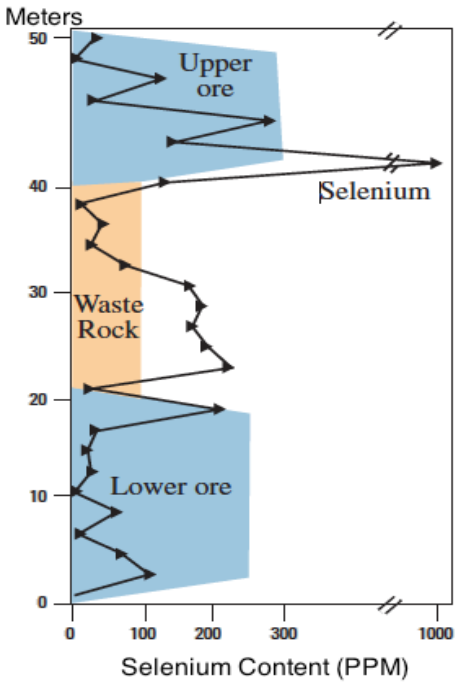

Figure 2.1. The black line indicates selenium concentration (parts per million, ppm) in three layers of the Phosphoria Formation. The upper and lower ore zones are the Meade Peak Phosphatic Shale Member. The waste rock is the middle zone, comprised of low-grade phosphatic shale (USGS, 2002).

Selenium is released into the environment through a number of activities, including: mining of coal, copper, lead, zinc, uranium, and phosphate, coal fly ash from coal combustion, coal and oil combustion facilities, manufacturing of Se-based products; agricultural phosphate fertilizers, agricultural usage of biosolids and manure, and pesticide and fungicide application. Non-anthropogenic releases include Se volatilization from plants and bacteria and volcanic activity (ATSDR, 2003; Fordyce, 2013; USEPA, 2002). In soils, Se contamination is typically related to weathering of bedrock (ATSDR, 2003).

In the western US, the release of high levels of Se is typically initiated by phosphate mining of the Phosphoria Formation (Figure 2.2 ; NAS-NRC, 1983). The process occurs through phosphate bed removal via open pit mining, causing exposure of Se-rich shale. Once exposed to the atmosphere, Se is oxidized to selenite and selenate. Unroofed waste rock and tailings allow

for Se mobilization with sediments through mass wasting and as dissolved loads in surface runoff and groundwater flow. In semi-arid regions, evaporative processes exceed precipitation rates. Drainage is impeded, and thus, Se species accumulate on surfaces (Presser et al., 2004).

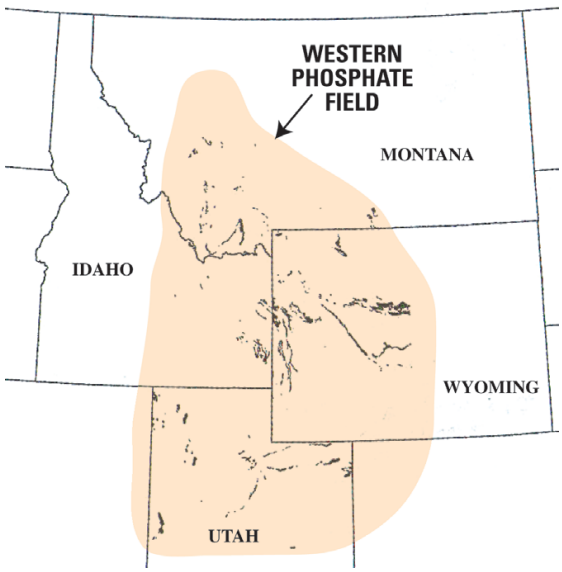

Figure 2.2. Map of the western phosphate field with formation exposures indicated in black (USGS, 2002)

The predominant form of Se found within the Phosphoria Formation is elemental Se, however, other species present include selenate, selenite, and selenide (organoselenides and ferroselite ; Stillings and Amacher, 2010). Within the ore, elemental Se is substituted for sulfur in the minerals bornite, chalcopyrite, pyrite, vaesite-pyrite, and sphalerite (Jensen, 1989; Stillings and Amacher, 2010). There are also organic portions of shale that contain high Se concentrations (Rader and Hill, 1936). Selenides exist as methylated compounds, hydrogen selenide (H_2Se), and metallic selenides. Both reduced species of Se are insoluble and therefore, not as bioavailable. They occur under acidic, reducing conditions. Once exposed to the surface, reduced Se species can oxidize to the soluble oxyanions, selenate (SeO_4^{2-}) and selenite (SeO_3^{2-}; McNeal and Balistrieri, 1989).

The Phosphoria Formation covers a 350,000 km^2 area throughout the west and is a large supplier of phosphate ore. This formation is of concern because of its extensive mining history that began in 1906 (Presser et al., 2004). Large concentrations of Se and other trace elements found originated from ancient seawater. These elements were precipitated, sorbed, or altered from biogenic material during deposition (McKelvey et al., 1959; Piper, 2001; Presser et al., 2004). The average Se concentration observed in phosphate ore of the Meade Peak Member is 30 mg kg^{-1}, with maximum concentrations reaching 800 mg kg^{-1}. Mudstones contain concentrations reaching up to 1,500 mg kg^{-1}(USGS, 1977).

In natural soils, typical Se concentrations range from 0.01 to 2.0 mg kg^{-1} soil (Shacklette and Boerngen, 1984). In seleniferous regions, Se concentration can be found at toxic levels that exceed 1,000 mg Se kg^{-1} soil (Bennett, 1982; Lakin and Byers, 1941). Historically, seleniferous soils are defined as those that allow vegetative accumulations greater than 5 mg Se kg^{-1} of plant tissue (Dhillon and Dhillon, 2000; Lakin and Byers, 1941).

Selenium Redox Chemistry

Depending on the environmental conditions, a variety of Se species can exist in soils. Under alkaline, moist soil conditions with high porosity, selenite is quickly oxidized to selenate (Lakin, 1961). Selenate is considered to be the more soluble form of Se, and is therefore, more bioavailable (Spallholz, 1994). This form predominates in the arid, alkaline soils of the western U.S. (Geering et al., 1968). Selenate is a diprotic weak acid, with a pK_a1 of -3 and pK_a2 of 1.9, where maximum adsorption occurs. Because of this, it is completely deprotonated under most soil conditions (Masscheleyn et al., 1990; Peak and Sparks, 2002). Selenite is also diprotic, with a pK_a1 of 2.5 and pK_a2 of 7.3. This signifies that selenite will exist as $HSeO_3^-$ between pH 3 and

8 (Li et al., 2008). Hence, it is typically sorbed at normal soil pH to a variety of mineral surfaces, while selenate is typically in solution (Abrams and Burau, 1989; Duc et al., 2006; Goldberg and Glaubig, 1988; Hayes et al., 1987; Rajan, 1979; Su and Suarez, 2000).

Several studies have indicated that mineral surfaces, such as iron (II) and manganese (II) oxides, may act as oxidation catalysts or as direct oxidants. Also, oxygen and hydroquinone can act as direct oxidants of selenite and elemental Se in the presence of a variety of oxide minerals. Scott and Morgan (1996) demonstrated that birnessite was able to directly oxidize selenite. The rate of this process was decreased by increasing pH and increased by increasing temperature (Scott and Morgan, 1996).

Selenium transformations are more likely influenced by biotic than abiotic reactions. This is because selenate does not readily undergo reduction with changes in pH and temperature. Selenate is considered more soluble than selenite under most soil conditions, and is therefore, more biologically available (NAS-NRC, 1983; Spallholz, 1994). It is also important to note that microbes that accomplish Se reduction are abundant in many environments. These include:, *Bacillus selenitireducens, Bacillus arsenicoselenatis, Sulfurospirillum barnesii, Aeromonas hydrophila, Thauera selenatis*, and proteobacteria of the strains AK4OH1 and Ke4OH1 (Macy et al., 1989; Macy et al., 1993; Oremland et al., 1994; Switzer Blum et al., 1998). The species *Hafnia alvei* was able to reduce selenate to the less toxic and immobile form, elemental Se (Youssef et al., 2009). Zheng et al. (2014) found that selenite could be reduced to red elemental Se by the bacterium *Comamonas testosteroni* S44 (Zheng et al., 2014). Tan et al. (2016) also found that selenite could be reduced to elemental Se by *Streptomyces sp*. strain ES2-5.

Selenium Sorption

Surface/water interface interactions are critical for Se sorption and potential bioavailability to plants (Sparks, 2003). In soils, Se oxidative states exhibit different adsorptive mechanisms. Studies have indicated that selenate is weakly bound to most mineral surfaces while selenite is bound strongly (Peak, 2006). A variety of soil chemical and physical properties have been studied regarding Se sorption and include pH, ionic strength, competing ions, and soil minerals and their crystalline structure (Benjamin, 1983). Previous studies conducted in this area include those primarily on whole soils, clay minerals, iron and aluminum oxides, and calcareous surfaces.

Whole Soil Sorption.

Pezzarossa et al. (1999) examined selenate sorption and desorption on Mediterranean arable, cultivated, pine forest, and woodland whole soils. Using Langmuir sorption isotherms, both pine and woodland locations were described with L-type curves, meaning high surface affinity for Se. Cultivated and arable soil isotherms were described by S-type curves, which suggests adsorbate clustering at the surface. Soils with higher amounts of organic matter sorbed highest Se concentrations. Arable soils contained lower amounts of organic matter with high pH, which are both possible explanations for low sorbed Se. Forest soils contained the highest percent organic matter, and also exhibited the highest sorbed Se (Pezzarossa et al., 1999). On sandy loam whole soils containing montmorillonite, Ahlrichs and Hossner (1987) examined selenate mobility between 2 and 9, and determined selenate was more mobile than selenite, especially at pH 7 and 9. In alkaline soils, selenite was rapidly oxidized to the more mobile selenate (Ahlrichs and Hossner, 1987).

Studies have shown that particle size has a pronounced effect on Se sorption behavior. Vouri et al. (1989) identified a positive correlation for selenate sorption with fine textured soils and increased weathering. Wells (1967) also observed that Se could be best retained by clay-sized particles. In Danish soils, highest percentages of selenite were found on clays and silts while only 5% sorbed to sands (Hamdy and Gissel-Nielsen, 1977).

Calcareous soils predominate the semi-arid portions of the western United States (Goldberg and Glaubig, 1988; Lakin, 1961). It should be noted that the number of sorption sites on calcareous minerals are less than those on iron oxides (Cowan et al., 1990). Very little Se sorption data is available for calcareous soils. In calcareous Punjab whole soils containing iron oxides and ammonium oxalate extractable iron, high selenite retention was observed. A decrease in net positive charge as a function of pH on iron oxide surfaces was noted. This caused decreases in SeO_3^{2-} sorption and increases in preference for the monovalent species, $H_2SeO_3^-$ (Dhillon and Dhillon, 1999). Findings were comparable to a Hamdy and Gissel-Nielsen (1977) study that observed 50% selenite retention on iron oxides within a five-minute period. Soils that lacked extractable iron were not able to retain the same Se concentrations compared with those containing higher amounts. Bonding energy constants were also determined and were negatively correlated with pH (Dhillon and Dhillon, 1999). Deep calcareous sandy soil consisting of 60 to 74% calcium carbonate retained almost twice as much selenite compared with soils low in calcium carbonate. Selenium accumulations mostly occurred at the surface (Jones and Belling, 1967). Goldberg and Glaubig (1988) also observed selenite sorption in calcareous, montmorillonite soils for two initial concentrations at pH values between 2 and 12. Maximum selenite sorption occurred at pH 3 for both selenite concentrations, with sharp declines at pH 6

and plateaus at higher pH. The sorption edges were determined to be similar to Neal et al. (1987), however, Goldberg and Glaubig (1988) observed a larger plateau magnitude.

Phyllosilicate Clays.

Clays play a large role in sorbing Se in soils. Montmorillonite, kaolinite, and vermiculite have exhibited adsorptive capacity for both selenite and selenate (Missana et al., 2009; Goldberg and Glaubig, 1988; Bar-Yosef and Meek, 1987; Hamdy and Gissel-Nielsen, 1977). Using a two-site non-electrostatic model, Missana et al. (2009) observed decreases in sorbed selenite with increasing pH (3-8) for montmorillonite and illite, with a plateau above pH 8. Using the constant capacitance model for montmorillonite and kaolinite, Goldberg and Glaubig (1988) observed a similar increase in sorption at low pH and a decrease at higher pH. Selenite sorption maximum was twice as high for kaolinite compared with montmorillonite (Goldberg and Glaubig, 1988).

Hamdy and Gissel-Nielsen (1977) studied selenite sorption on a variety of clay minerals at environmentally relevant pH values. The type of clay and pH had significant influence on Se sorption. Kaolinite, for example, sorbed a greater amount of Se than vermiculite and montmorillonite. Vermiculite sorbed more Se than montmorillonite. Variations in Se sorption were attributed to differences in clay mineral structures. Compared with montmorillonite and vermiculite, kaolinite contains 4 additional hydroxyl groups and 4 less deprotonated hydroxyl groups per crystal unit. Kaolinite also has a lower silica/oxide (SiO_2/R_2O_3) ratio, which controls selenite sorption. The seat of the negative charge also differs for vermiculite surfaces. This is found in the tetrahedral layer of the mineral, while the charge is located in the octahedral layer for montmorillonite (Grim, 1953). Maximum sorption was also determined to occur between pH 3 and 5 for all clays, and a decline was observed above neutral pH (Hamdy and Gissel-Nielsen,

1977). This was also observed by Bar-Yosef and Meek (1987) for kaolinite and vermiculite. They noted adsorption decreases with increasing pH but was insignificant above pH 8. More selenite sorbed to kaolinite than selenate (Bar-Yosef and Meek, 1987).

Minimal selenate adsorption was noted on kaolinite above pH 8 and above pH 3 on illite surfaces by Goldberg (2014). No adsorption maxima were observed as well. A maxima at pH 5 was identified for selenite on kaolinite and pH 4 for illite (Goldberg, 2013; Goldberg, 2014). More selenite was adsorbed onto clay mineral surfaces in comparison with selenate (Goldberg, 2013; Goldberg, 2014). Also, stronger adsorption was noted for both Se species on oxides in comparison with clay surfaces. In contrast with illite, Goldberg (2014) notes that greater adsorption of Se species on kaolinite was due to edge charge. The Triple Layer Model (TLM), which describes surface complexes, indicated that both Se species formed outer-sphere surface complexes on kaolinite and inner-sphere complexes on illite (Goldberg, 2013; Goldberg, 2014). For the clays Na and Ca-montmorillonite, no selenate sorption was observed (Goldberg, 2014).

Oxide Minerals.

Aluminum Oxides

Aluminum oxide minerals are commonly found in soils and can provide sorption sites for Se. Goldberg (2013, 2014) indicated a broad adsorption maximum up to pH 7 and 8 for selenate and selenite, respectively, on an amorphous Al oxide surface. Using the TLM, outer-sphere adsorption best described both Se species on the amorphous Al oxide surface. This indicates that sorption is weaker than on Fe oxides (Goldberg, 2013; Goldberg, 2014).

Peak (2006) examined selenate and selenite adsorption mechanisms at the aluminum oxide/water interfaces using extended X-ray absorption fine structure (EXAFS) spectroscopy

(Figure 2.3). Corundum (α-Al_2O_3; HAO) and hydrous aluminum oxide (HAO) were chosen as sorptive surfaces. The author determined that differences in crystalline structure affected surface complexation, possibly due to changes in the corundum surface. At pH 3.5, outer-sphere complexation was observed for selenate on corundum, and inner-sphere monodentate complexation was observed at pH 4.5 and above. Selenite formed a combination of outer and inner-sphere bidentate-binuclear surface complexes on HAO, while selenate formed only outer-sphere complexes. It is possible that certain aluminum oxide minerals can form bayerite layers upon hydration, which reduce surface chemical interactions. It is also important to note that Se behaves differently on aluminum compared with iron surfaces, and iron surfaces were more reactive with Se oxyanions. This may be due to differences in surface stabilities, especially under acidic conditions. Certain aluminum oxides are considered less thermodynamically stable compared with iron oxides and have reported to spontaneously transform into other aluminum species (Peak, 2006).

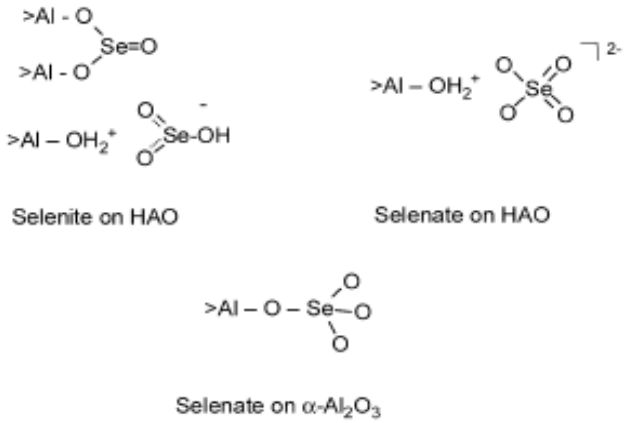

Figure 2.3. Selenite and selenate adsorption mechanisms on a corundum (α-Al_2O) surface and selenate adsorption on a hydrous aluminum oxide (HAO) surface from Peak (2006).

Wijnja and Schulthess (2000) examined mechanisms of selenate adsorption on a different aluminum oxide surface, γ-Al_2O_3, using complementary data sets from two vibrational spectroscopic methods: Raman and attenuated total reflectance Fourier transform infrared (ATR-

FTIR) spectroscopy. Both techniques can assist researchers in determining ion adsorption mechanisms through deducing molecular structures. Vibrational characteristics of selenate were identified, which indicated that the tetrahedral symmetry would reduce in response to coordination with metal surfaces. Using Raman spectroscopy, free selenate was the predominant species observed in all spectra, indicating outer-sphere complexation for pH between 4 and 7. The spectra also indicated small fractions of inner-sphere complexed Se to be present at pH <6. Overall, both Raman and ATR-FTIR spectra were in agreement with selenate outer-sphere complexation on aluminum oxides and small fractions of monodentate inner-sphere complexation (Wijnja and Schulthess, 2000).

Iron Oxides

Iron oxides are common soil minerals that are important for controlling Se solubility (Zhang and Sparks, 1990). Selenite, selenourea, and selenomethionine immobilization on an amorphous iron oxyhydroxides were studied by Tam et al. (1995). The authors determined that selenite was more immobile on the surface compared with both selenourea and selenomethioine Se immobilization resulted in small pH increases for all species, thought to be due to displacement of hydroxyl groups from the oxide surface. The amount of immobilized selenite was held constant until pH 9 and then subsequently decreased. This is in agreement with Hingston et al. (1968) and is due to a reduction in positive charge on the iron oxide surface, resulting in a loss in selenite binding sites. Immobilization discontinued once selenite content increased above 30 mg, possibly due to saturation of binding sites. The adsorption isotherm resembled an H-type isotherm, signifying that selenite is strongly adsorbed (Tam et al., 1995).

In particular, goethite exhibits high adsorption capacity for selenite. Because of this, it has been the focus of many Se sorption studies. Between pH 3 and 8, selenite adsorption on iron oxides was constant. This was speculated to be due to surface charge. Below the isoelectric point of $Fe_2(OH)_3$, colloidal particles exhibited a positive charge, allowing for preferential adsorption of anions (Hamdy and Gissel-Nielsen, 1977). Through extracting ^{75}selenite initially added to iron (III) oxide (Fe_2O_3) minerals found in alkaline regions, Hamdy and Gissel-Nielsen (1977) determined that the largest fractions of selenite were not available to plants. This occurrence likely resulted from anion exchange and chemical precipitation (as ferric selenite) with Fe_2O_3.

Previous mechanistic studies have demonstrated selenate sorption onto both oxide and hydroxide surfaces. Spectroscopic techniques, such as EXAFS and ATR-FTIR, are useful for observing bonding mechanisms for a variety mineral surfaces, specifically hematite, goethite, and hydrous ferric oxide (Peak and Sparks, 2002). Su and Suarez (2000) observed adsorption mechanisms using ATF-FTIR and electrophoresis for selenate and selenite on amorphous Fe-oxides and goethite. Mechanisms for adsorption on amorphous iron oxides and goethite were determined based on a decrease in electrophoretic mobility and point of zero charge (PZC) caused by the presence of selenite and selenate. The sorption envelope was affected by changes in pH and Se concentration, the release of hydroxyl ions during adsorption, and the decrease in symmetry of sorbed selenite/selenate. This may signify inner-sphere complexation for both species on amorphous iron oxide and goethite surfaces. Selenate bidentate complexation on amorphous iron oxides was confirmed through ATF-FTIR and DRIFT spectra. The selenite complex with amorphous iron oxide structure was uncertain with ATF-FTIR due to its insensitivity, but DRIFT spectra exhibited bridging bidentate complexation for selenite on goethite. With increased ionic strength and pH, decreased adsorption was observed for selenate.

It should be noted that ionic strength has a more significant effect for selenate sorption compared to selenite (Su and Suarez, 2000).

Goldberg (2013) and (2014) also examined Se adsorption on an amorphous Fe-oxide. Selenate adsorption maxima were noted at lower pH, between 2 and 4. A marked decreased occurred between pH 6 to 7.5, with little adsorption observed above pH 8.5 (Goldberg, 2014). These findings corroborate with work from Peak and Sparks (2002). The authors observed both inner and outer-sphere complexation of selenate on an amorphous Fe-oxide, however, Goldberg (2014) noted mostly inner-sphere adsorption. For selenite, a broad maximum was noted up to pH 8. This occurred as strong inner-sphere complexes (Goldberg, 2013).

Zhang and Sparks (1990) determined a mechanism for selenite and selenate adsorption and desorption on goethite using pressure-jump relaxation. Within the experimental pH range, single relaxations were observed for selenate adsorption. This assumes that selenate anions are adsorbed onto a protonated surface site on goethite, and that adsorption and protonation occur simultaneously. Evidence from computing the intrinsic equilibrium constant using surface complexation modeling suggested that the above mechanism and outer-sphere surface complexation were correct. Additionally, intrinsic rate and equilibrium constants from the kinetic studies and equilibrium studies were in agreement and of the same order of magnitude. The intrinsic forward rate constant was eight orders of magnitude larger than the reverse, indicating that the rate of adsorption is higher than that of desorption. Thus, desorption was concluded to be a rate-limiting step. As for selenite adsorption, double relaxation was observed, and the authors proposed inner-sphere adsorption for selenate on the goethite surface (Zhang and Sparks, 1990). A modified TLM was used to describe selenite and selenate adsorptive behavior. This demonstrated selenite adsorption as monovalent and bivalent selenite-Fe complexes, due to the

existence of selenite as SeO_3^{2-} and $HSeO_3^-$ in suspension. These inner-sphere complexes formed via a two-step process. During the initial step, $HSeO_3^-$, SeO_3^{2-}, and H^+ react with goethite surfaces through electrostatic attraction. Outer-sphere complexes are then formed on the α-layer of the model. The second step occurs on the α-layer, where monovalent and divalent selenite ions substitute for water molecules on the goethite surface. Inner-sphere complexes subsequently form when selenite is bound directly to the surface. The TLM successfully described selenate adsorption as well. It was assumed that selenate adsorption occurred on the β-layer via electrostatic attractions as an outer-sphere complexes (Zhang and Sparks, 1990).

Balistrieri and Chao (1990) also used the TLM to describe selenite adsorption on ferrihydrite. The results suggested that selenite formed binuclear, inner sphere complexes on ferrihydrite surfaces. The surface site heterogeneity of ferrihydrite was noted by a decreasing equilibrium constant with increasing adsorption density for selenite (Balistrieri and Chao, 1990).

Calcium Carbonate.

Although calcium carbonate minerals have less sorption sites compared with iron and aluminum oxide minerals, they are still important sorbents in calcareous systems (Cowan et al., 1990). Work from Aurelio et al. (2010) indicated that calcite is a large sink for Se. Because of its dynamic solubility, calcite sorption and co-precipitation are more likely to occur in soils, even with lower amounts of calcium carbonate present (Heberling et al., 2014). Selenite and carbonate ions are very similar in structure and size. Therefore, they can exchange and form solid solutions readily. Borrero et al. (1988) determined that up to 77% of phosphate, in the form of monopotassium phosphate (KH_2PO_4) from an initial concentration of 20 μM, was adsorbed to calcareous surfaces. Cowan et al. (1990) speculated that, because selenite and phosphates exhibit similar selectivity, similar percentages could be exhibited by selenite.

Using the reference mineral, calcite, selenite sorption increased at low pH, from 6 to 8, and decreased at high values above pH 9. Using a constant capacitance model with montmorillonite and kaolinite, plateaus at neutral pH were no longer present when calcite was removed from the system. This signifies that the influence of calcite on selenite sorption in calcareous soils should be of high interest (Goldberg and Glaubig, 1988). Singh et al. (1981) observed Se sorption and desorption on a number of different soils. Soils contained either high calcium carbonate content (pH 8.1), high organic matter content (pH 7.8), were saline (pH 7.8), or highly alkaline (pH 10.1). These soils were compared with "normal" soils (pH of 7.6), which are considered non-calcareous, non-saline, non-alkaline, and have normal amounts of organic matter. Soils high in organic matter adsorbed the highest percentages of selenate and selenite, followed by calcareous, saline, and alkaline soils. Low Se sorption percentages were observed for alkaline soils, most likely due to higher solubility caused by high pH. Calcareous soils contained 2% more calcium carbonate with similar properties to the normal soils. It was speculated that higher carbonate content facilitated increased sorption. In all observed cases under varying soil conditions, higher concentrations of selenate were adsorbed than selenite at above neutral pH (Singh et al., 1981).

A single sorbate experiment was conducted by Cowan et al. (1990) for selenite on a calcium carbonate surface. According to pH edge data, this occurred via surface exchange. This was concluded because selenite sorption increased with increasing selenite solution concentration, decreasing pH, and decreasing aqueous carbonate concentrations. The pH edge data were modeled using exchange half-reactions in the software, FITEQL. For this model, CO_3^{2-} and HCO_3^- were assumed to be the exchangeable ions on the calcium carbonate surface. The model results suggested that exchange of HCO_3^- was stronger than CO_3^{2-} and exchange of SeO_3^{2-}

was stronger than $HSeO_3^-$. It is possible that ions can alter surface charge on minerals, making them more positive or negative. If this surface is more positive, this will promote Se attraction to the surface. This relates to changes in surface charge and the PZC, where pH values above the PZC promote a negatively charged surface and vise versa. For calcite, the PZC is typically pH 9.

Along with specific adsorption and exchange, Se co-precipitation with carbonate minerals can occur. Under supersaturated conditions, Se co-precipitation with calcite is the dominant sequestration mechanism. At low-supersaturated conditions, a linear increase for the selenite:carbonate ratio in the solid was observed by Heberling et al. (2014). Coprecipitation with calcite occurs through a series of adsorption and entrapment events (Heberling et al., 2014). The mechanism for this occurs through selenite replacement of carbonate in the calcite crystalline structure. This modifies the appearance of growth features (Renard et al., 2013). Previous work has shown that up to 27.6 m*M* Se kg^{-1} of solid was found in precipitates and that up to 7% of total solid could contain Se(IV) (Aurelio et al., 2010; Baur and Johnson, 2003).

Organic Matter.

Selenium species have the capability of interacting with soil organic matter. They can also be incorporated into amino acids by means of microorganisms and plants through the replacement of sulfur (Christensen et al., 1989). Gustafsson and Johnsson (1992) examined acidic forest soils that contained large concentrations of iron oxides, aluminum oxides, and organic matter. A sodium pyrophosphate $Na_4P_2O_7$/NaOH extraction was completed in order to retrieve organic soil fractions. Fulvates were separated from humates and analyzed. The authors hypothesized that high concentrations of selenite would be retained on fulvate. Initially, between 2 and 12% of Se was extracted using monosodium phosphate (NaH_2PO_4). Following this, selenite was extracted again using $Na_4P_2O_7$/NaOH. Because selenite concentrations for the two

extracts were positively correlated, Gustafsson and Johnsson (1992) speculated $Na_4P_2O_7$/NaOH-extracted selenite was bound by hydroxyl surface groups. This meant that the selenite concentration from the initial extraction could be added to selenite from the second extraction, used to calculate total selenite in the hydrophilic fulvate. The authors also determined that Se was present in high amounts in all fulvate fractions. Hydrophobic fulvates contained the highest percentages of Se, especially in the B-horizons of Ulriksdal (SE) soils. From this, Gustafsson and Johnsson (1992) concluded that soil organic matter has a strong ability to sorb Se. They also compared their results to alkaline soils in California from Abrams et al. (1990), which had similar C:Se ratios. Conversely, only 6% of total Se was $Na_4P_2O_7$/NaOH extractable, which was different from observations made by Gustafsson and Johnsson (1992). The authors believe that this was caused by large disparities in both pH and organic matter structure found in the two regions.

Kamei-Ishikawa et al. (2007) observed Se sorption behavior on humic acid. The structure and shape of humic acid can change with varying pH and ionic strength. It is possible that more binding sites could be observed when humic acid is in its spherical form due to the decrease in the solid/liquid ratio. Possible Se adsorptive mechanisms were either specific or non-specific, determined by changes in ionic strength. The concentration of selenite sorbed to humic acid also increased with decreasing solid:liquid ratio (Kamei-Ishikawa et al., 2007).

Competitive Interactions in Soils

Inorganic Anion Competition.

Additional anions present in soil solution may have the ability to compete with Se for adsorption on mineral surfaces. These interactions can affect Se plant bioavailability and hence,

toxicity. Competitors include a variety of common inorganic ligands as well as organic ligands that will be further discussed (Barrow and Whelan, 1989). In particular, sulfate has been shown to inhibit selenate plant uptake through competition due to chemical similarities. This suggests that Se bioavailability could be reversed due to strong inhibitory effects of sulfate. Competition was more pronounced between sulfate and selenate when compared with phosphate and selenite interactions, perhaps because selenate and sulfate are more chemically similar (Hopper and Parker, 1999).

On goethite surfaces, Se mobility occurs under the following conditions: high Se concentrations, alkaline pH, oxidizing conditions, and the presence of other strongly held anions. The following anions were able to compete with selenite and promote mobility: phosphate > silicate > molybdate > bicarbonate/carbonate > fluoride > sulfate (Balistrieri and Chao, 1987). In alkaline soils subjected to low rainfall, selenate is expected to predominate, which is more soluble and available to vegetation. Selenite, however, is not as soluble. Balistrieri and Chao (1990) examined selenite on ferrihydrite, an amorphous iron oxide, in the presence of competing anions. Selenite sorption increases with decreasing pH and increasing ferrihydrite concentration. The sequence for competitive anions at pH 7.0 is as follows: phosphate > silicate > molybdate >> fluoride > sulfate. Phosphate, molybdate, and silicate sorption reflect their relative affinity for the ferrihydrite surface (Balistrieri and Chao, 1990).

Phosphate and fluoride ions sorb more strongly than selenite anions. However, selenite sorption is actually still comparable to phosphate and also molybdate (Hingston et al., 1968). Both selenite and phosphate were able to outcompete and replace hydroxyl, sulfate, and silicate ions through ligand exchange reactions (Hingston et al., 1968; Rajan, 1976). In alluvial soils in San Joaquin Valley, CA, phosphate inhibited selenite sorption (Neal et al., 1987). This may be

due to a resemblance between selenite adsorptive behavior and phosphate (Hingston et al., 1968). Carbonates are also important anions to discuss in terms of competitive interactions. Observations from a Wijnja and Schulthess (2002) study suggested that goethite might have considerable amounts of carbonates adsorbed on its surface. On goethite surfaces, between pH 6 and 8, carbonate facilitated selenate sorption. Maximum sorption of selenate occurred using 0.2 m*M* of carbonate. Carbonates could facilitate oxyanion sorption due to extra protonated reactive sites. However, at elevated pH, carbonate became competitive for goethite sorption sites (Wijnja and Schulthess, 2002).

On aluminum oxide surfaces, interactions between ions may be controlled by both concentration and sorbate binding affinities (Wu et al., 2002). Also possible is that some sites may be anion specific. In a binary system, both selenite and selenate decreased the amount of sorbed molybdate. Compared with sulfate, selenate also exhibited a higher bonding site affinity (Wu et al., 2002). On γ-Al_2O_3, competitive sorption of selenite and selenate with other anions, including molybdate, chromate, and sulfate was observed. Molybdate anions inhibited selenite sorption under acidic conditions, but above pH 6, selenite sorption was stronger. Chromate sorption was inhibited by both sulfate and selenate. Of the anions examined, molybdate was determined as most likely to be retained on oxide surfaces, followed by selenite, selenate, sulfate, and chromate (Wu et al., 2000). The authors determined that anion competition is dependent on not only the strength and type of surface binding but also the binding rate.

Cowan et al. (1990) examined selenite in a binary system with phosphate, sulfate, and magnesium. In the presence of SO_4^{2-} and PO_4^{3-}, selenite sorption was reduced due to either anion competition or site blockage. Selenite sorption was not influenced by Mg because they sorb at different pH values and exchange on different surface sites.

Organic Anion Competition.

Organic anions found in soils and rhizosphere environments can also compete with Se oxyanions for surface sites. Dissolved organic carbon (DOC) species and selenite can compete for sorption sites on hydrous metal oxides. There are a variety of organic acids that facilitate and participate in ligand exchange reactions on soil surfaces. On aluminum hydroxide surfaces and in the presence of a variety of low molecular weight (LMW) dissolved organic carbon (DOC) acids, Dynes and Huang (1997) found that selenite sorption gradually decreased. Acids included the following: oxalic, citric, L-malic, tartaric, succinic, glycolic, L-aspartic, salicylic, *p*-hydroxybenzoic, glycine, formic, and acetic. Direct sorption of these acids caused a loss of selenite sorption sites, with the degree of site loss most influenced by acid concentration and the law of mass action. Selenite sorption depended on the type of DOC acid present, and it is possible that selenite could desorb weakly bound acids, such as acetate, formate, glycinate, salicylate, and *p*-hydroxybenzoate. Acid interactions with surfaces were dependent on the following reasons: location, type, and distance of coordinating groups along with molecular structure and size (Dynes and Huang, 1997). Surface complexation could be prevented by different stereochemical and electrostatic effects from different types of acids (Stumm, 1986). Also, acids that were unable to form surface complexes were not able to successfully compete with selenite for sorption. These acids include the likes of acetate, formate, and glycinate. Acids capable of forming five to six membered chelate rings were considered more stable due to ring structure, and were able to outcompete selenite for surface sites. These acids include oxalate, citrate, and tartrate. Of the DOC acids studied, both citrate and oxalate effectively outcompeted selenite for sorption sites. Citrate was more effective than oxalate only under low concentrations, due to its increased stereochemical and electrostatic surface interactions from its larger molecular

size and more functional groups. Oxalate, however, was able to penetrate more deeply and adsorb to smaller pore surfaces because of its smaller size. Because of this, oxalate and selenite were in competition for sorption onto smaller pores. Oxalate can also form both mono and bidentate surface complexes and selenite can form similar monodentate complexes, thus competition is expected. Because of the ability of organic acids to prevent selenite sorption, Se bioavailability to plants should increase (Dynes and Huang, 1997). Balistrieri and Chao (1987) also examined selenite competition with citrate and oxalate on goethite, and found that both demonstrated an ability to increase selenite mobility. However, citrate was more effective at competing than oxalate (Balistrieri and Chao, 1987).

Humic acids are common soil components with complex mixtures of different structures derived from plants and microorganisms. They also have no defined molecular structure (Kelleher and Simpson, 2006). Kim et al. (2012) determined its effects on selenite sorption onto hematite surfaces. The authors considered adsorbate/adsorbent ratios, pH, and ionic strength effects on sorption for binary and ternary systems. In a ternary system, sorption efficiencies of selenite onto hematite in the presence of humic acid were lower than in a binary system (Se-hematite) at pH values below 8. At pH values above 8, the opposite occurred. Inhibitory effects of humic acid were apparent at low pH, and humic acid facilitated selenite sorption at high pH. In the ternary system, selenite sorption on hematite surfaces increased with high pH but was determined to decrease at low pH. Selenite saturation occurred when humic acid concentrations were above 50 mg L^{-1} and between pH 4.5 and 11.5. This may be explained by competition between humic acid and selenite on surface sites of hematite (Kim et al., 2012). Masset et al. (2000) examined this same interaction but on goethite surfaces. The authors determined that humate ions were able to form inner-sphere complexes with oxide surfaces. A slight decrease in

selenite adsorption suggested competition with humate anions for surface sites. This same occurrence was noted by Tipping (1981) for phosphate and silicate anions. When selenite concentrations were much lower than humic acid, competitive effects between the two were considered negligible (Masset et al., 2000). Tam et al. (1995) also examined the effects of humate on selenite adsorption on an amorphous ferric oxyhydroxides surface and found no effect on selenite immobilization. Compared with uncoated ferric oxyhydroxides, the coated surface percent immobilization was the same. When selenite was introduced above 30 mg, the maximum immobilization capacity that the authors determined, slight increases in immobilization were noted. This may be because humate increases the availability of other sites, through the formation of selenite-humic acid-ferric oxyhydroxide complexes (Tam et al., 1995).

Conclusion

Research interests in Se contamination and phosphate mining have greatly expanded over the past decade, due to the exceedingly high Se accumulations found in semi-arid soils. This has caused Se toxicity in livestock and wildlife. This literature review comprises of previous works that have demonstrated Se adsorptive behavior on organic matter and a variety of mineral surfaces, including 2:1 clay minerals, iron oxides, aluminum oxides, and carbonate minerals. Additionally, both organic and inorganic anions in soil solution can compete with Se for sorption sites, thus promoting Se solubility and bioavailability. This is because Se solubility and sorption on soil surfaces are the foremost processes to understand in order to control Se.

References

Abrams, M.M., Burau, R.G., 1989. Fractionation of selenium and detection of selenomethionine in a soil extract. Commun. Soil Sci. Plant Anal. 20, 221-237.

Ahlrichs, J.S., Hossner, L.R., 1987. Selenate and Selenite Mobility in Overburden by Saturated Flow. Journal of Environmental Quality 16, 95-98.

ATSDR, U., 2003. Toxicological profile for selenium.

Aurelio, G., Fernandez-Martinez, A., Cuello, G.J., Roman-Ross, G., Alliot, I., Charlet, L., 2010. Structural study of selenium(IV) substitutions in calcite. Chem. Geol. 270, 249-256.

Balistrieri, L.S., Chao, T.T., 1987. Selenium Adsorption by Goethite. Soil Sci. Soc. Am. J. 51, 1145-1151.

Balistrieri, L.S., Chao, T.T., 1990. Adsorption of selenium by amorphous iron oxyhydroxide and manganese dioxide. Geochim. Cosmochim. Acta 54, 739-751.

Bar-Yosef, B., Meek, D., 1987. Selenium Sorption By Kaolinite and Montmorillonite. Soil Science 144, 11-19.

Barrow, N.J., Whelan, B.R., 1989. Testing a mechanistic model. VII. The effects of pH and of electrolyte on the reaction of selenite and selenate with a soil. J. Soil Sci. 40, 17-28.

Baur, I., Johnson, C.A., 2003. Sorption of Selenite and Selenate to Cement Minerals. Environ. Sci. Technol. 37, 3442-3447.

Benjamin, M.M., 1983. Adsorption and surface precipitation of metals on amorphous iron oxyhydroxide. Environ. Sci. Technol. 17, 686-692.

Bennett, B.G., 1982. Exposure of man to environmental nickel - an exposure commitment assessment. Sci. Total Environ. 22, 203-212.

Borrero, C., Peña, F., Torrent, J., 1988. Phosphate sorption by calcium carbonate in some soils of the Mediterranean part of Spain. Geoderma 42, 261-269.

Christensen, B.T., Bertelsen, F., Gissel-Nielsen, G., 1989. Selenite fixation by soil particle-size separates. J. Soil Sci. 40, 641-647.

Cobo Fernandez, M.G., Palacios, M.A., Camara, C., 1993. Flow-injection and continuous-flow systems for the determination of Se(IV) and Se(VI) by hydride generation atomic absorption spectrometry with on-line prereduction of Se(VI) to Se(IV). Anal. Chim. Acta 283, 386-392.

Cowan, C.E., Zachara, J.M., Resch, C.T., 1990. Solution ion effects on the surface exchange of selenite on calcite. Geochim. Cosmochim. Acta 54, 2223-2234.

Dhillon, K.S., Dhillon, S.K., 2000. Restoration of Se-Contaminated Soils. in: Iskandar, I.K. (Ed.). Environmental Restoration of Metals-Contaminated Soils. Lewis Publishers, Boca Raton, FL.

Duc, M., Lefevre, G., Fedoroff, M., 2006. Sorption of selenite ions on hematite. J. Colloid Interf. Sci. 289, 556-563.

Dynes, J.J., Huang, P.M., 1997. Influence of Organic Acids on Selenite Sorption by Poorly Ordered Aluminum Hydroxides. Soil Sci. Soc. Am. J. 61, 772-783.

Fordyce, F.M., 2013. Selenium Deficiency and Toxicity in the Environment. in: Selinus, O. (Ed.). Essentials of Medical Geology: Revised Edition. Springer Netherlands, Dordrecht, pp. 375-416.

Geering, H.R., Cary, E.E., Jones, L.H.P., Allaway, W.H., 1968. Solubility and Redox Criteria for the Possible Forms of Selenium in Soils. Soil Sci. Soc. Am. J. 32, 35-40.

Goldberg, S., 2013. Modeling Selenite Adsorption Envelopes on Oxides, Clay Minerals, and Soils using the Triple Layer Model. Soil Sci. Soc. Am. J. 77, 64-71.

Goldberg, S., 2014. Modeling Selenate Adsorption Behavior on Oxides, Clay Minerals, and Soils Using the Triple Layer Model. Soil Science 179, 568-576.

Goldberg, S., Glaubig, R.A., 1988. Anion Sorption on a Calcareous, Montmorillonitic Soil-Selenium. Soil Sci. Soc. Am. J. 52, 954-958.

Grim, R.E., 1953. Clay Mineralogy. McGraw-Hill, New York.

Gustafsson, J.P., Johnsson, L., 1992. Selenium retention in the organic matter of Swedish forest soils. J. Soil Sci. 43, 461-472.

Hamdy, A.A., Gissel-Nielsen, G.G., 1977. Fixation of selenium by clay minerals and iron oxides. 2. Pflanzenernaehr. Bodenkd. 140, 63-70.

Hayes, K.F., Roe, A.L., Brown, G.E., Jr., Hodgson, K.O., Leckie, J.O., Parks, G.A., 1987. In Situ X-ray Absorption Study of Surface Complexes: Selenium Oxyanions on α-FeOOH. Science 238, 783-786.

Heberling, F., Vinograd, V.L., Polly, R., Gale, J.D., Heck, S., Rothe, J., Bosbach, D., Geckeis, H., Winkler, B., 2014. A thermodynamic adsorption/entrapment model for selenium(IV) coprecipitation with calcite. Geochim. Cosmochim. Acta 134, 16-38.

Hingston, F.J., Posner, A.M., Quirk, J.P., 1968. Adsorption of Selenite by Goethite. Adsorption From Aqueous Solution. American Chemical Society, pp. 82-90.

Hopper, J.L., Parker, D.R., 1999. Plant availability of selenite and selenate as influenced by the competing ions phosphate and sulfate. Plant Soil 210, 199-207.

Jacobs, L.W., 1989. Selenium in agriculture and the environment. Soil Science Society of America Special Publication 23.

Jensen, N.L., 1989. "Se" Mineral Facts and Problems. U.S. Bureau of Mines, Washington D.C.

Jones, G.B., Belling, G.B., 1967. The movement of copper, molybdenum, and selenium in soils as indicated by radioactive isotopes. Aust. J. Agric. Res. 18, 733-740.

Kamei-Ishikawa, N., Tagami, K., Uchida, S., 2007. Sorption kinetics of selenium on humic acid. J. Radioanal. Nucl. Chem. 274, 555-561.

Kelleher, B.P., Simpson, A. J. 2006. Humic substances in soils: Are they really chemically distinct? Environ. Sci. Technol. 40: 4605-4611.

Kim, M., Jang, M., Pak, S.K., 2012. Effect of humic acid on the selenite adsorption onto hematite. Recent Researches in Engineering Mechanics, Urban & Naval Transportation and Tourism, 232-236.

Lakin, H.W., 1961. Se contents of soil. Agriculture Handbook 200. United States Department of Agriculture, Washington D.C.

Lakin, H.W., Byers, H.G., 1941. Se occurrence in certain soils in the United States, with a discussion of related topics: fifth report. United States Department of Agriculture, Washington D.C.

Li, H.-F., McGrath, S.P., Zhao, F.J., 2008. Selenium uptake, translocation and speciation in wheat supplied with selenate or selenite. New Phytol. 178, 92-102.

Macy, J.M., Michel, T.A., Kirsch, D.A., 1989. Selenate reduction by a *Pseudomonas* species: a new mode of anaerobic respiration. FEMS Microbiol. Lett., 61: 195–198.

Macy, J.M., Rech, S., Auling, G., Dorsch, M., Stackenbrandt, E. Sly, L.I., 1993. *Thauera selenatis* gen. nov., sp. nov., a member of the beta subclass of *Proteobacteria* with a novel type of anaerobic respiration. Int. J. Syst. Bacteriol., 43: 135–142.

Masscheleyn, P.H., Delaune, R.D., Patrick, W.H., 1990. Transformations of selenium as affected by sediment oxidation-reduction potential and pH. Environ. Sci. Technol. 24, 91-96.

Masset, S., Monteil-Rivera, F., Dupont, L., Dumonceau, J., Aplincourt, M., 2000. Influence of humic acid on sorption of Co(II), Sr(II), and Se(IV) on goethite. Agronomie 20, 525-525.

McKelvey, V.E., Williams, J.S., Sheldon, R.P., Cressman, E.R., Cheney, T.M., Swanson, R.W., 1959. The Phosphoria, Park City, and Shedhorn Formations in the western phosphate field. U.S. Geological Survey Professional Paper 313-A, 47.

McNeal, J.M., Balistrieri, L.S., 1989. Geochemistry and Occurrence of Selenium: An Overview. in: Jacobs, L.W. (Ed.). Selenium in Agriculture and the Environment. Soil Science Society of America and American Society of Agronomy, Madison, WI.

Missana, T., Alonso, U., García-Gutiérrez, M., 2009. Experimental study and modelling of selenite sorption onto illite and montmorillonite clays. J. Colloid Interf. Sci. 334, 132-138.

NAS-NRC, 1983. Selenium in Nutrition: Revised Edition. National Acadamies Press, Washington DC.

Neal, R.H., Sposito, G., Holtzclaw, K.M., Traina, S.J., 1987. Selenite adsorption on alluvial soils: I. Soil Composition and pH Effects and II. Solution composition effects. Soil Sci. Soc. Am. J. 51.

Neal R.H. 1995. ‚Selenium. Blackie Academic & Professional, London.

Oremland, R.S., Switzer Blum J., Culbertson, C.W., Visscher P.T.,Miller, L.G. Dowdle, P. Strohmaier, F.E., 1994. Isolation, growth, and metabolism of an obligately anaerobic, selenate-respiring bacterium, strain SES-3. Appl. Environ. Microbiol., 60: 3011–3019.

Peak, D., 2006. Adsorption mechanisms of Se oxyanions at the aluminum oxide/water interface. J. Colloid Interf. Sci. 303, 337-345.

Peak, D., Sparks, D.L., 2002. Mechanisms of Selenate Adsorption on Iron Oxides and Hydroxides. Environ. Sci. Technol. 36, 1460-1466.

Pezzarossa, B., Piccotino, D., Petruzzelli, G., 1999. Sorption and desorption of selenium in different soils of the mediterranean area. Commun. Soil Sci. Plant Anal. 30, 2669-2679.

Pilon-Smits, E.A.H., 2015. Selenium in Plants. in: Luttge, U., Beyschlag, W. (Eds.). Progress in Botany. Springer International Publishing, Switzerland, pp. 93-107.

Piper, D.Z., 2001. Marine chemistry of the permian phosphoria formation and basin, Southeast Idaho. Economic Geology 96, 599-620.

Presser, T.S., Piper, D.Z., Bird, K.J., Skorupa, J.P., Hamilton, S.J., Detwiler, S.J., Huebner, M.A., 2004. The Cycle of the Phosphoria Formation: From Deposition to Post-Mining Environment. in: Hein, J.R. (Ed.). The Phosphoria Formation: A Model for Forecasting Global Selenium Sources to the Environment. Elsevier, Amsterdam.

Rader, L.F., Hill, W.L., 1936. Occurence of Se in natural phosphates, superphosphates, and phosphoric acid. Journal of Agricultural Research 51, 1071-1083.

Rajan, S.S.S., 1976. Changes in net surface charge of hydrous alumina with phosphate adsorption. Nature 262, 45-46.

Rajan, S.S.S., 1979. Adsorption of selenite, phosphate and sulphate on hydrous alumina. J. Soil Sci. 30, 709-718.

Renard, F., Montes-Hernandez, G., Ruiz-Agudo, E., Putnis, C.V., 2013. Selenium incorporation into calcite and its effect on crystal growth: An atomic force microscopy study. Chem. Geol. 340, 151-161.

Scott, M.J., Morgan, J.J., 1996. Reactions at Oxide Surfaces. 2. Oxidation of Se(IV) by Synthetic Birnessite. Environ. Sci. Technol. 30, 1990-1996.

Shacklette, H.T., Boerngen, J.G., 1984. Element Concentrations in Soils and Other Surficial Materials of the Conterminous United States. U.S. Geological Survey Professional Paper 1270, United States Government Print Office, Washington.

Singh, M., Singh, N., Relan, P.S., 1981. Adsorption and desorption of selenite and selenate selnium on different soils. Soil Science 132, 134-141.

Spallholz, J.E., 1994. On the nature of selenium toxicity and carcinostatic activity. Free Radical Biol. Med. 17, 45-64.

Sparks, D.L., 2003. Environmental Soil Chemistry. Academic Press, San Diego, CA.

Stillings, L.L., Amacher, M.C., 2010. Kinetics of selenium release in mine waste from the Meade Peak Phosphatic Shale, Phosphoria Formation, Wooley Valley, Idaho, USA. Chem. Geol. 269, 113-123.

Stumm, W., 1986. Coordination interactions between soil solids and water - An aquatic chemist's point of view. Geoderma 38, 19-30.

Su, C., Suarez, D.L., 2000. Selenate and Selenite Sorption on Iron Oxides: An Infrared and Electrophoretic Study. Soil Sci. Soc. Am. J. 64, 101-111.

Switzer Blum, J. Bindi A.B., Buzzelli J., Stolz J.F., Oremland, R.S., 1998. *Bacillus arsenicoselenatis* sp. nov.: two haloalkaliphiles from Mono Lake, California, which respire oxyanions of selenium and arsenic. Arch. Microbiol., 171: 19–30.

Tam, S.C., Chow, A., Hadley, D., 1995. Effects of organic component on the immobilization of selenium on iron oxyhydroxide. Sci. Total Environ. 164, 1-7.

Tan Y, Yao R, Wang R, Wang D, Wang G, Zheng S (2016) Reduction of selenite to Se(0) nanoparticles by filamentous bacterium Streptomyces sp. ES2-5 isolated from a selenium mining soil. Microbial Cell Factories 15: 157

Tipping, E., 1981. The adsorption of aquatic humic substances by iron oxides. Geochim. Cosmochim. Acta 45, 191-199.

USEPA, 2002. Drinking Water and Health Consumer Fact Sheet on Selenium.

USGS, 1977. Final Environmental Impact Statement. Development of Phosphate Resources in Southeastern Idaho.

USGS, 2002. Western Phosphate Field, U.S.A.: Science in Support of Land Management. USGS Fact Sheet FS-100-02.

Vouri, E., Vaariskoski, J., Hartikaisen, H., Vakkilaniun, P., Kumpulainen, J., Niinivaara, K., 1989. Sorption of selenate by Finnish agricultural soils. Agric. Ecos. Environ. 25, 111-118.

Wells, N., 1967. Selenium content of soil-forming rocks. New Zeal. J. Geol.and Geop., 10, 198-208.

Wijnja, H., Schulthess, C.P., 2000. Vibrational Spectroscopy Study of Selenate and Sulfate Adsorption Mechanisms on Fe and Al (Hydr)oxide Surfaces. J. Colloid Interf. Sci. 229, 286-297.

Wijnja, H., Schulthess, C.P., 2002. Effect of Carbonate on the Adsorption of Selenate and Sulfate on Goethite. Soil Sci. Soc. Am. J. 66, 1190-1197.

Wu, C.H., Kuo, C.Y., Lin, C.F., Lo, S.L., 2002. Modeling competitive adsorption of molybdate, sulfate, selenate, and selenite using a Freundlich-type multi-component isotherm. Chemosphere 47, 283-292.

Wu, C.H., Lo, S.L., Lin, C.F., 2000. Competitive adsorption of molybdate, chromate, sulfate, selenate, and selenite on γ-Al_2O_3. Colloids Surf. Physicochem. Eng. Aspects 166, 251-259.

Youssef, G.A., El-Assar, S.A., Berekaa, M.M., El-Shaer, M., Stolz, J.F., 2009. Arsenate and Selenate Reduction by Some Facultative Bacteria in the Nile Delta. Journal of Agricultural and Environmental Science 5, 847-855.

Zhang, P., Sparks, D.L., 1990. Kinetics of selenate and selenite adsorption/desorption at the goethite/water interface. Environ. Sci. Technol. 24, 1848-1856.

Zheng S., Su J., Wang L., Yao R., Wang D., Deng Y., Wang R., Wang G., Rensing C., 2014. Selenite reduction by the obligate aerobic bacterium Comamonas testosteroni S44 isolated from a metal-contaminated soil. B.M.C. Microbiol. 14: 204.

Chapter 3: Selenium geochemistry in reclaimed phosphate mine soils and its relationship with plant bioavailability

Abstract

Selenium accumulation in vegetation has resulted in toxicity in livestock in reclaimed phosphate mine soils in Southeastern Idaho. Plant and soil samples were collected from five study sites near phosphate mines. Soil physicochemical properties, Se speciation, and Se distribution from a sequential extraction procedure (SEP) were examined in relation to Se bioavailability. Chemical analyses revealed that the Se-hyperaccumulator (plants that absorb over 1,000 mg Se kg^{-1}_{DM}), western aster (*Symphyotrichum ascendens* (Lindl.)), contained Se exceeding 6,000 mg Se $kg^{-1}_{DM\ (Dry\ Matter)}$. Soil speciation results indicated that selenite (SeO_3^{2-}) was the dominant species with lower quantities of selenate (SeO_4^{2-}) present. This was expanded using an SEP that accounted for six fractions. The highest significant relationship was determined for western aster Se and water-soluble and phosphate-extractable SEP fractions ($R^2 = 0.85$). This relationship decreased once fractions related to carbonate, amorphous Fe-oxides, organic, and residual Se were factored into the analysis. A highly significant relationship between selenate and the water-soluble Se fraction was also observed ($R^2 = 0.83$). Soluble and ligand exchangeable Se were determined to be "bioavailable fractions" for western aster. Thus, simple water extractions can be used as a quick assessment for Se bioavailability and provide a means to identify potential hazardous areas for grazing livestock.

Introduction

Selenium (Se) is a trace element, with levels in natural soils ranging from 0.01 to 2.0 mg Se kg^{-1} (Shacklette and Boerngen, 1984). Elevated levels of Se can result from a variety of anthropogenic processes, such as those associated with phosphate mining in southeast Idaho,

where it is not uncommon to find soil Se levels much higher than normal background levels (McNeal and Balistrieri, 1989). To date, there have been hundreds of reported grazing deaths due to livestock ingesting plants growing on these contaminated soils (Buck and Jones, 2002; Davis et al., 2012; Edmonson et al., 1993; Fessler et al., 2003). Western aster (*Symphyotrichum ascendens* (Lindl.)) is the plant responsible for the vast majority of these deaths in SE Idaho, with toxicity linked to its Se content (Pfister et al., 2013). Pfister et al. (2013) reported western aster tissues reaching levels as high as 4,455 mg Se kg^{-1}_{DM}, while western aster collected from mine wastes have tested as high as 13,000 mg Se kg^{-1}_{DM} (Davis et al., 2011). Western aster is considered a Se-hyperaccumulator. Hyperaccumulator plants are defined as those that uptake over 1,000 mg Se kg^{-1}_{DM} (Dry Matter) in above-ground biomass (White, 2016). Deaths from grazing on this plant occurred on previously reclaimed land, where Se-laden shale overburden was used as a replacement for topsoil prior to 1996 (Buck and Jones, 2002; Davis et al., 2011). Mine reclamation is a process used to stabilize locations that have been disturbed and establish productive vegetation (Richards et al., 1998). During this time, environmental impact assessments did not identify Se levels as a concern in overburden materials. However, land reclaimed after 1996 used the original salvaged topsoil as the topsoil medium (Buck and Jones, 2002). This change in practice was established in accordance with the Bureau of Land Management (BLM) and the Clean Water Act (CWA) in 1996 (Blanchard et al., 2002). In the Blackfoot River (ID, USA), Se levels have exceeded acute (0.02 mg L^{-1}) and chronic (0.005 mg L^{-1}) aquatic life criteria for the state of Idaho for a number of years due to snowmelt and base flow (IDEQ, 2007; Meyers, 2013). Mining throughout this watershed created pathways for contamination of waterways (Knudsen and Gunter, 2004; Meyers, 2013).

Selenium is considered an essential micronutrient to ruminants but becomes toxic at elevated levels (Davis et al., 2012; Davis et al., 2013; Edmonson et al., 1993). There is a narrow range between dietary and toxic dosages of Se in animals. Toxicity typically occurs when animals ingest between 3 to 8 mg Se kg^{-1} of body weight (NAS-NRC, 1983). Because of this, Se toxicity occurs easily and usually between a 24 to 72-h period (Davis et al., 2013; Shortridge et al., 1971).

In soil environments, Se can exist in four oxidation states (+6, +4, 0, and –2). At neutral to alkaline pH and in aerobic environments, the dominant species present are selenate (SeO_4^{2-}) and selenite (SeO_3^{2-}) (Spallholz, 1994; Burau, 1989). Soluble Se oxyanions are of particular concern because of their potential bioavailability or ability to be incorporated into biota (John and Leventhal, 1995; Spallholz, 1994). For example, western aster can take up greater than normal amounts of Se, primarily as selenate and, to a lesser extent, selenite (Spallholz, 1994). This explains its ability to grow on seleniferous soils while nonaccumulating plants cannot (Davis et al., 2013). At high levels, Se phytotoxicity is typically related to Se-induced oxidative stress and distorted protein structures (Gupta and Gupta, 2016).

It is understood that processes at the solid/water interface control the potential bioavailability of trace elements in the environment (Luoma, 1983). Hence, sequential extraction procedures (SEP) are often employed to determine soil components associated with the target element of concern. For this study, we used a SEP described by Amacher (2010). Sequential extraction procedures involve a series of rinses and extractions with increasingly stronger reagents (Martens and Suarez, 1997; Tessier et al., 1979; Zhao et al., 2005). They provide a more detailed understanding of the potential solubility and bioavailability of trace elements compared to the use of total concentrations. The fractions examined, using the

Amacher (2010) procedure, are as follows: water-soluble Se, PO_4^{3-}-extractable Se, carbonate associated Se, amorphous iron oxide associated Se, organic Se, and residual elemental forms of Se. These soil fractions vary in their relation to Se bioavailability to plants. The water-soluble fraction accounts for soluble selenate and some selenite, while the PO_4^{3-}-extractable fraction accounts for Se that is ligand exchangeable (Amacher, 2010). Carbonate-associated Se is removed using ammonium acetate (NH_4AOc), which has previously been used for exchangeable metals by Chapman (1965). Exchangeable metals are considered to be metals that are bound to mineral and organic soil components but can be exchanged with one another (Chapman, 1965). However, it also dissolves carbonate minerals which solubilizes metals (Tessier et al., 1979; Wagemann et al., 1977; Jackson, 1958; Chapman, 1965). Ammonium oxalate ($C_2H_8N_2O_4$), in the dark, was used to extract Se bound to amorphous iron oxides (Amacher, 2010). This reagent was originally employed by Tamm (1922) to remove amorphous iron, aluminum, and silicon oxides from soils. At room temperature and in the dark, this reagent is specific to dissolving amorphous iron oxides (Gleyzes et al., 2002). Previous works indicate that organic Se comprises a large portion of Se in soil, either derived from parent material or partitioned within organic matter (Ryser et al., 2006; Ryser et al., 2005; Stillings and Amacher, 2004; Yamada et al., 1998). In seleniferous soils, large quantities of Se were found in humified organic matter (Moreno Rodriguez et al., 2005). In the Amacher (2010) procedure, potassium persulfate ($K_2S_2O_8$) was used to oxidize organic matter, releasing bound or occluded Se. Residual fractions are accounted for in the final SEP extraction, similar to Martens and Suarez (1997). This fraction is composed of trace elements bound or occluded in minerals that cannot be released for long periods of time (Tessier et al., 1979).

Understanding Se speciation and its various phases in soils is necessary to develop methods to reduce its solubility in contaminated soils. Accordingly, the objectives of this study were to:

(1) Characterize the physicochemical properties of Se present in contaminated soils that affect its bioavailability
(2) Determine Se speciation in soluble and exchangeable soil phases because of its important influence on bioavailability, mobility, and toxicity.
(3) Employ a soil sequential extraction procedure (SEP) that identifies six phases of Se in soils.
(4) Relate Se concentrations from the SEP fractions and speciation to Se uptake in the Se-hyperaccumulator, western aster.

Materials and Methods

Sample Collection

Five study sites associated with phosphate mining operations near Soda Springs, Idaho, USA were chosen. Study sites included three pre-1996 reclaimed locations, Sites A, B, and C, and two sites reclaimed post-1996, D and E (Figure 3.1). Sites reclaimed prior to 1996 used the Se-laden shale overburden as the reclamation soil medium. Those reclaimed after 1996 used the original salvaged topsoil as the reclamation soil medium, as per regulatory changes that are in accordance with the BLM and CWA (Blanchard et al., 2002).

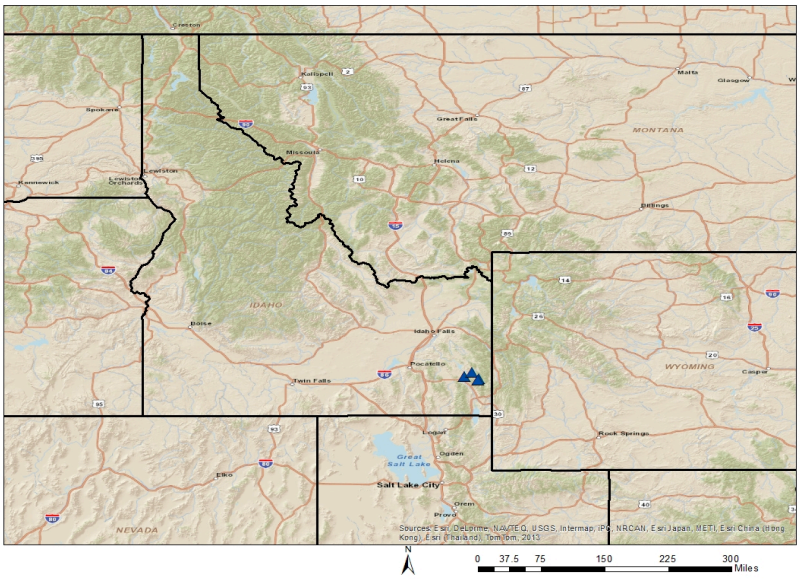

Figure 3.1: State view of five sites in southeastern Idaho. Note: Two sites are superimposed due to close proximity at this magnification.

Sampling transects were established in a Y-shape for the five different locations (Figure 3.2). In total, 78 samples were collected. Sixteen samples were collected from Sites A, B, C, and D locations and fourteen were collected from Site E.

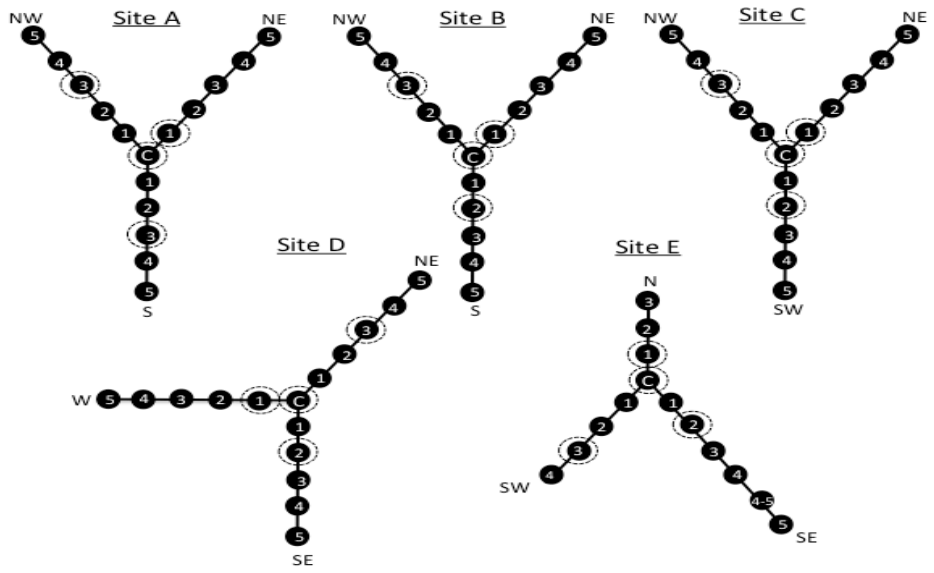

Figure 3.2: Transect sampling diagrams for the five study locations. Black circles indicate soil sampling points, and dashed circles indicate vegetation sampling points. Note: Sites A-D contain 16 sampling points, and Site E contains 14. Diagrams are not to scale.

[a] N = North; S = South; E = East ; W = West; C = Center point

One center point was established at each study site where high Se levels were presumed to occur, determined by the presence of western aster. From the center point, transect lines were extended 30 m in three directions. Soil samples were collected every 6 m in each direction (0-20 cm depth). Soils were placed in plastic sampling bags that were stored in a plastic cooler for transport. Plant and soil samples were taken from the same transect points in order to establish a relationship between plant Se levels and associated soil fractions. Plant samples were collected using a quadrat with dimensions of 0.5 by 1.0 m at four points from each transect. Plants were identified by species by a field botanist, separated into paper bags by species, and washed. Fifty-seven plants were collected from Site A, 35 from Site B, 36 from the Site C, 47 from Site D, and 36 from Site E.

Following collection, soil samples were air-dried at ambient temperature and passed through a 2 mm sieve in order to remove coarse fragments. Prior to plant digestions, shoots were separated from roots and split into two groups. The first half of the shoots was washed with 0.50% sodium laurel sulfate followed by 0.10 *M* HCl. Shoots were then thoroughly rinsed with distilled water. The second half of the shoot was left unwashed. This was completed in order to confirm that Se was resultant of root absorption and not from soil deposition on the plant surface. The two separate halves (shoots) were placed in separate beakers, covered with aluminum foil, and dried for 48 h in a 70°C oven. Once the two halves were dried, shoots were ground in a stainless steel coffee grinder (Capresso Coffee Grinder, Model 501).

Soil Characterization

Soils were analyzed for the physicochemical properties particle size (sand, silt and clay), pH, total organic carbon (TOC), and total inorganic carbon (TIC) in duplicate. Prior to particle

size analyses, soil samples were pretreated for removal of organic matter, carbonates, and secondary free iron oxides. Removal of these components can enhance separation of soil aggregates by decreasing particle coatings and cementing agents (Kunze and Dixon, 1986). Pretreatments for organic matter were completed using hydrogen peroxide and magnesium chloride and for iron oxides using sodium-citrate dihydrate and sodium dithionite as described in procedures modified by Kunze and Dixon (1986). Carbonate pretreatments followed a procedure described by Saffari et al. (2009), using 0.5 *M* HCl. Following pretreatments, particle size was determined using the hydrometer method (Gee and Bauder, 1986). Soils from Sites A, B, C, and D were silt loam and Site E soils were considered a loam.

Soil pH was determined in a 1:1 ratio with water using a pH 718 STAT Titrino (Metrohm, Herisau, Switzerland) equipped with a combination pH electrode (Thomas, 1996). For carbon analyses, samples were ground to a fine powder and analyzed using a TOC analyzer that is capable of measuring TC, TIC, TOC, separately (Skalar Primac^{SLC} TOC Analyzer – Model CS22, De Breda, Netherlands).

Selenium Sequential Extraction Procedure

Sequential extraction procedures generally follow a similar format to the Tessier et al. (1979) procedure. The procedure used in this study was modified by Martens and Suarez (1997) for Se, which was further modified by Amacher (2010).

Six fractions of soil Se were separated through the following sequential extractions. For each sample in duplicate, 0.500 g of air-dried soil was weighed and placed into 50 mL polypropylene centrifuge tubes. The procedure is outlined as follows:

a. Water-soluble Se. The first extraction was completed using 25.0 mL of deionized water, vortex mixed, and shaken for 2 h at 120 cycles/min using an Innova 4230 incubator shaker (New Brunswick Scientific, Edison, NJ). After extractions were complete, samples were centrifuged at 1500 rpm for ten minutes. Supernatants were collected following this (25 mL).

b. Phosphate (PO_4^{3-})-Extractable Se. The second extraction was completed on the residue from step a, using 25.0 mL of pH 7.2 0.01 *M* KH_2PO_4/K_2HPO_4 buffer, vortex mixed and shaken for 2 h at 120 cycles/min. After extractions were complete, samples were centrifuged at 1500 rpm for ten minutes. Supernatants were collected following this (25 mL).

c. Carbonate-Associated Se. The third extraction was completed on residues from step b, using 25.0 mL of pH 5 1 *M* NH_4OAc. This was left stay for 30 min to allow for initial reaction with carbonates to subside. Following this, suspensions were mixed using a vortex mixer and shaken for 24 h at 120 cycles/min. After extractions were complete, samples were centrifuged at 1500 rpm for ten minutes. Supernatants were collected following this (25 mL).

d. Amorphous Iron oxide-Associated Se. The forth extraction was completed on residues from step c, using 25.0 mL of 0.2 *M* $C_2H_8N_2O_4$ + 0.2 *M* oxalic acid ($C_2H_2O_4$) added to samples in the dark. The suspension was mixed using a vortex mixer and shaken for 2 h at 120 cycles/min with the shaker window covered to prevent light from interacting with soil solutions. After extractions were complete, samples were centrifuged at 1500 rpm for ten minutes, and 25 mL supernatants were collected. Following this, 5 mL of oxalate solution was added to centrifuge tubes, the residue was re-suspended using the vortex mixer, and centrifuged again for 5 min at 1500 g. The

final supernatant (5 mL) was collected, added to the initial 25 mL supernatant, and diluted to a 50 mL volume.

e. Organic Se (-II) Compounds. The fifth extraction was completed on residues from step d, using 25.0 mL of 0.1 *M* $K_2S_2O_8$. The suspension was mixed using a vortex mixer. Samples were placed in an oven set to 90 °C for 2 h. After heating, samples were cooled to ambient temperature and centrifuged for 10 min at 1500 g. Following this, an additional 5 mL of $K_2S_2O_8$ was added to the centrifuge tube, re-suspended using the vortex mixer, and centrifuged again for 5 min at 1500 g. The final supernatant (5 mL) was collected, added to the initial 25 mL supernatant, and diluted to a 50 mL volume.

f. Residual Se. The final extraction was completed on residues from step e, using 2.5 mL of concentrated, trace metal grade nitric acid (HNO_3). The suspension was mixed using a vortex mixer and placed in boiling water for 30 min. Following this, samples were cooled to ambient temperature and 20 mL of deionized water was added. Samples were vortex mixed and placed in a boiling water bath for 90 min. Samples were then cooled to ambient temperature again and centrifuged for 10 min at 1500 g. Supernatants were collected following this (25 mL). Deionized water (5 mL) was added to the centrifuge tubes, re-suspended via the vortex mixer, and centrifuged for 5 min at 1500 g. The final supernatant (5 mL) was collected, added to the initial 25 mL supernatant, and diluted to a 50 mL volume.

Following centrifugation, supernatants were filtered and saved for analysis. Residues were washed with 95% ethanol three times in between extractions and left to dry. Samples were analyzed using a Spectro Arcos ICP-AES (SPECTRO Analytical Instruments, Inc., Mahwah,

NJ). Six method blanks were analyzed that corresponded with each fraction, with no detectable Se found.

Selenium Speciation

Selenium speciation was determined for soils in duplicate from two points along each of the five transects. In order to remove soluble and exchangeable forms, Se was extracted from 1.0 g of soil using 25 mL of 0.05 *M* potassium phosphate dibasic (K_2HPO_4) in metal free polycarbonate centrifuge tubes and shaken for 24 h on an incubator shaker. The suspension was centrifuged at 9000 rpm, and the resulting supernatant was filtered through a 0.45 μm nitrocellulose membrane filter (Alam et al., 2000). Prior to IC-ICP-MS analysis, samples were filtered a second time through 0.20 μm syringe filters. The filtrate was analyzed for Se speciation using IC-ICP-MS. The IC system consisted of an Agilent 1200 series quaternary pump (Santa Clara, CA, USA) and a Hamilton PRP X-100 anion exchange column (Reno, NV, USA). The mobile phase used for transporting analytes through the IC column was pH 5 10 m*M* citric acid. The ICP-MS system consisted of an Agilent 7500cx. Instrument calibration was accomplished using prepared sodium selenate and selenite standards. The Se concentrations of the standards were determined against a NIST standard (Inorganic Ventures, Christiansburg, VA, USA) using ICP-MS with quantification using an m/z ratio of 77.

Quality controls for both Se speciation analysis and total Se analysis included blanks, random duplicates and spike recovery. Method detection limits for selenate and selenite were 0.8 and 0.9 ug L^{-1}, respectively (Unrine et al., 2007).

Plant Digestion

Dried plant shoots were digested in a 90 °C heat block using HNO_3. Digested samples were collected and analyzed for Se using a Perkin Elmer NexION 300D ICP-MS (Shelton, CT, USA ; Hall and Winger, 2012). Quality assurance/quality control samples were obtained from a tomato leaf standard, and were digested in order to determine if Se was found in reagents or absorbed during filtration.

Statistics

Statistically significant different between site characterizations were determined using an analysis of variance (ANOVA) and least significant difference (LSD). Additionally, statistically significant differences between SEP fractions for all soils (78 total) from each site were compared using ANOVA and LSD to identify whether Se in SEP fractions differed by site. The six SEP fractions were then related to above ground western aster Se levels in soils from corresponding points along transects. Selenium speciation in ten soils was related to the first two SEP fractions (water-soluble and PO_4^{3-}-extractable). Analyses were completed using simple linear regression in the program, JMP® Pro 11.0.0 statistical software (SAS Institute Inc., 2012). Prior to analyses, the Shapiro-Wilk test confirmed approximate normality among specific data points used in the regression analysis. Following this, a regression equation was generated for western aster Se data from specific transect points and related to the sum of each fraction (water-soluble alone, water-soluble + PO_4^{3-}-extractable Se, water-soluble + PO_4^{3-}-extractable Se + carbonate associated Se, etc.). This was completed in order to compare relative bioavailability among fractions and identify any marked differences between successive phases.

Results

Physicochemical Characteristics of Reclaimed Phosphate Mine Soil

Physicochemical properties of phosphate mine soils derived from overburden waste materials varied by site, which may be indicative of differences in reclamation practices. Physicochemical properties and least significant difference statistical analyses are indicated in Table 3.1. Soils from Sites A, B, and C were reclaimed pre-1996, and Sites D and E were reclaimed after 1996. For example, Site D and E soils exhibited finer textures compared with the coarser textures of Sites A, B, and C. All soils were considered circumneutral to alkaline, with site average pH values ranging from 6.75 to 7.92. Clay percentage means were considered statistically the same for Sites A, B, C and Sites D and E. Sites A, B and C soils were generally higher in pH than Site D and E soils, which was attributed to their higher carbonate content or total inorganic carbon (TIC). However, TIC percentage means were statistically the same for Sites B, and C and Sites A, B, D, and E were considered statistically the same.

Table 3.1: Mean physicochemical properties for soils from the five sites with mean statistical comparisons using the least significant difference (LSD) method.

	n	**pH**	**TOC**[b]	**TIC**	**Sand**	**Clay**	**Silt**
		____	___ g C kg^{-1}___		_____ % _____		
A[a]	32	7.92^{Ac}	30.7^{AB}	10.7^{B}	34^{BC}	6^{B}	60^{A}
B	32	7.81^{AB}	32.7^{AB}	24.4^{AB}	41^{AB}	6^{B}	59^{A}
C	32	7.22^{B}	32.4^{AB}	44.8^{A}	45^{A}	4^{B}	59^{A}
D	32	7.53^{C}	16.8^{B}	3.8^{B}	41^{AB}	19^{A}	41^{B}
E	28	6.75^{D}	46.4^{A}	3.0^{B}	27^{C}	18^{A}	55^{A}

[a]A = Site A; B = Site B; C = Site C; D = Site D; E = Site E
[b]TOC = Total Organic Carbon, TIC = Total Inorganic Carbon
[c]Mean values not connected with same uppercase letter are considered statistically different using LSD and ANOVA ($p<0.05$)

Soil Selenium Sequential Extraction Procedure

The distribution of Se phases in the six SEP fractions and total Se are summarized in Table 3.2, with mean comparisons determined using least significant difference (LSD) results.

Total Se concentration means, determined from the summation of SEP fractions, were highest for soils from Site B (217 mg Se kg^{-1} soil). The second highest mean was also observed in Site C soils (54.7 mg Se kg^{-1} soil). Concentrations were lower for Sites A and E (35.6 and 40.2 mg Se kg^{-1} soil, respectively) and were especially low in soils sampled from Site D (21.1 mg Se kg^{-1} soil). Statistically, the Site B total Se mean differed from Sites A, C, D, and E. Sites D and E soils were reclaimed post-1996 with the original salvaged topsoil that contained low levels of Se compared to sites A, B, and C that were reclaimed pre-1996 using Se rich overburden material (Blanchard et al., 2002).

Table 3.2: Sequential extraction procedure (SEP) fractionation of Se descriptive statistics for minimum, maximum, mean, and standard deviation by site.

		Sites				
		A	**B**	**C**	**D**	**E**
	n	32	32	32	32	28
F1[a]	**Min**	ND[c]	ND	ND	ND	ND
	Max	1.79	10.7	1.63	ND	ND
	Mean	0.35^{Bd}	2.05^{A}	0.53^{B}	ND^{Be}	ND^{B}
	SD[b]	0.52	2.5	0.64	ND	ND
F2	**Min**	ND	ND	ND	ND	ND
	Max	1.23	3.33	1.33	0.82	0.55
	Mean	0.29^{B}	1.41^{A}	0.31^{B}	0.20^{B}	0.19^{B}
	SD	0.33	0.88	0.37	0.18	0.13
F3	**Min**	ND	1.61	ND	ND	ND
	Max	3.78	15.7	9.56	1.80	3.16
	Mean	2.08^{B}	7.50^{A}	2.82^{B}	0.91^{B}	0.92^{B}
	SD	1.15	4.27	3.03	0.35	0.64
F4	**Min**	ND	ND	ND	ND	ND
	Max	3.87	9.74	8.99	ND	10.3
	Mean	2.63^{B}	4.92^{A}	4.04^{AB}	ND^{B}	3.65^{AB}
	SD	0.33	2.49	2.16	ND	2.37
F5	**Min**	ND	3.46	ND	4.29	4.12
	Max	15.9	44.2	35.2	10.6	18.6
	Mean	7.24^{B}	15.0^{A}	8.02^{AB}	6.64^{B}	10.5^{AB}
	SD	3.66	12.7	9.52	1.77	4.53
F6	**Min**	7.10	14.0	ND	5.62	10.9
	Max	36.5	385	130	31.2	35.8
	Mean	23.1^{B}	186^{A}	39.0^{B}	13.3^{B}	24.9^{B}
	SD	8.43	95.0	41.8	7.07	6.29
	Mean Total	35.6^{B}	217^{A}	54.7^{B}	21.1^{B}	40.2^{B}

[a]F1 = Water-Soluble Se; F2 = PO_4^{3-}Extractable Se; F3 = Carbonate Se; F4 = Amorphous Iron Oxide Se; F5 = Organic Se; F6 = Residual Se
[b]SD = Standard deviation
[c]ND indicates Se not detected
[d]Mean values not connected with same uppercase letter are considered statistically different using LSD and ANOVA ($p<0.05$)
[e]For statistical analyses, means that are ND were replaced with LOD/√2

For the individual SEP fractions, we define Se levels up to 2 mg Se kg^{-1} soil as low and between 3 and 15 mg Se kg^{-1} as moderate. Means above 16 mg Se kg^{-1} soil are considered high.

In general, lower levels of Se were observed in water-soluble fractions or were below the limit of detection of the ICP-AES (Table 3.2). Water-soluble Se was not detected (ND) in any of the sixteen soils from both Sites D and E. Nine, eleven, and three of the sixteen soils from Site C, A, and B, respectively, showed no detectable water-soluble Se. The maximum water-soluble Se value was observed at Site B (10.7 mg Se kg^{-1} soil). Soils from Site B also contained maximum Se levels in both the water and PO_4^{3-}-extractable fractions. The Site B water-soluble Se mean was considered statistically different from those observed in Sites A, C, D, and E.

Like the water-soluble Se fraction, PO_4^{3-}-extractable Se was lower than the other examined fractions or was not detected in most soils. Similar to its water-soluble fraction, soils from Site B exhibited the maximum levels of PO_4^{3-}-extractable Se (3.33 mg Se kg^{-1} soil). The Site B mean was also considered statistically different from levels observed in the other sites. Thirteen soils from Sites A and C, and three from Site B contained no detectable Se in the PO_4^{3-}-extractable form. One soil from Site E and two soils from Site D contained no detectable Se in this fraction.

Selenium levels within the carbonate fraction were higher and more appreciable than the water-soluble and PO_4^{3-}-extractable fractions for many of the soils. Again, higher Se values were noted in soils from Site B, especially at the center point (15.7 mg Se kg^{-1} soil), whereas carbonate Se was only detected in three Site D soils and one Site E soil. Site B mean soil Se was also considered statistically different from Se found in the other four sites for this particular fraction.

Levels in the amorphous iron oxide fraction were comparable to carbonate fractions. However, Se associated with amorphous iron oxides was not detected in many of the soils examined. This phase was not observed in any of the soils sampled from Site D. Only one soil sampled from Site A contained Se within this fraction and three from Site E. Interestingly, the

maximum level of Se was indicated in soils from Site E for this fraction (10.3 mg Se kg^{-1} soil). Moderate levels of Se were also observed in Site B soils with a maximum of 9.74 mg Se kg^{-1} soil. Selenium in this fraction was not detected in six and five of the soils sampled from Sites C and B, respectively. For soils with detectable levels of Se associated within this fraction, values were between 3.87 and 10.3 mg Se kg^{-1} soil. Unlike previous fractions, the Site B mean Se was not considered different from Sites C and E. Sites C and E Se amorphous iron oxide mean values were also considered statistically the same as levels found in Sites A and D.

Most of the soils sampled exhibited moderate to high abundances of organic Se, with the exception of six Site C soils and one soil from Site A, where they were not detected. Comparisons between all site means indicated that Sites A, C, D, and E were not considered statistically different. Sites B, C, and E were also not statistically different. The maximum organic Se levels was observed in Site B (44.2 mg Se kg^{-1} soil). Site C soils were also high in organic Se along some segments of the transect line as well, with a maximum value of 35.2 mg Se kg^{-1} soil.

Residual Se was the dominant fraction for many of the soils sampled, having the highest abundance of Se. No detectable Se for this fraction was observed in two of the Site C soils, which were also below detection throughout the entire SEP. Seven of the Site C soils were below 10 mg Se kg^{-1}. Eight out of the sixteen soils sampled from Site B were well above 200 mg Se kg^{-1} soil for residual Se, with a maximum of 385 mg Se kg^{-1} soil observed. Soils from Site B were considered to be statistically different from the other 4 sites. One of the Site C soils from the first northwest point along the transect exceeded 100 mg Se kg^{-1} soil.

Soil Selenium Speciation

Selenium speciation was determined for soils extracted with a PO_4^{3-}-buffer. This extraction includes both water-soluble and exchangeable Se species (Zhao et al. 2005). Overall, selenite predominated with lower levels of selenate present (Figure 3.3). Highest levels of selenite were observed in soils from Site B point NE2 (6.21 mg Se kg-1 soil), and highest selenate levels were observed from the center point of Site B (1.16 mg Se kg^{-1} soil). Intermediate levels of selenite were observed in Sites A and C soils. Lowest levels of selenite were found in Sites D (0.06 mg Se kg^{-1} soil) and E (0.07 mg Se kg^{-1} soil), which are post-1996 reclaimed sites. No selenate was detected in Sites D and E soils.

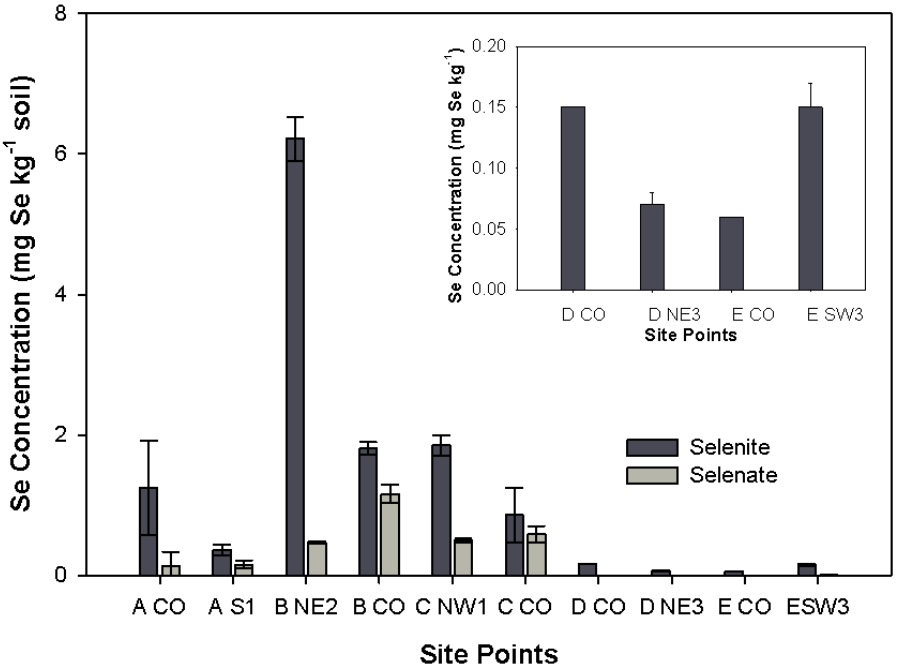

Figure 3.3: Speciation for selenium in soils from two points from each transect (10 samples in duplicate). Insert shows maximized view for Sites D and E.

*A = Site A; B = Site B; C = Site C; D = Site D; E = Site E. Refer to Figure 3.2 for sampling plan diagram for each point.

Selenium speciation results were related to the water-soluble and PO_4^{3-}-extractable SEP fractions using simple linear regression. A statistically significant relationship was observed for selenate and water-soluble Se ($R^2 = 0.83$; $P = 0.0002$; Figure 3.4A) with no significant

relationship observed for selenite ($R^2 = 0.30$; P = 0.1007). A weak relationship was observed for selenate with the PO_4^{3-}-extractable Se fraction ($R^2 = 0.49$; P = 0.0244) and for selenite and PO_4^{3-}-extractable Se ($R^2 = 0.57$; P = 0.0117; Figure 3.4B).

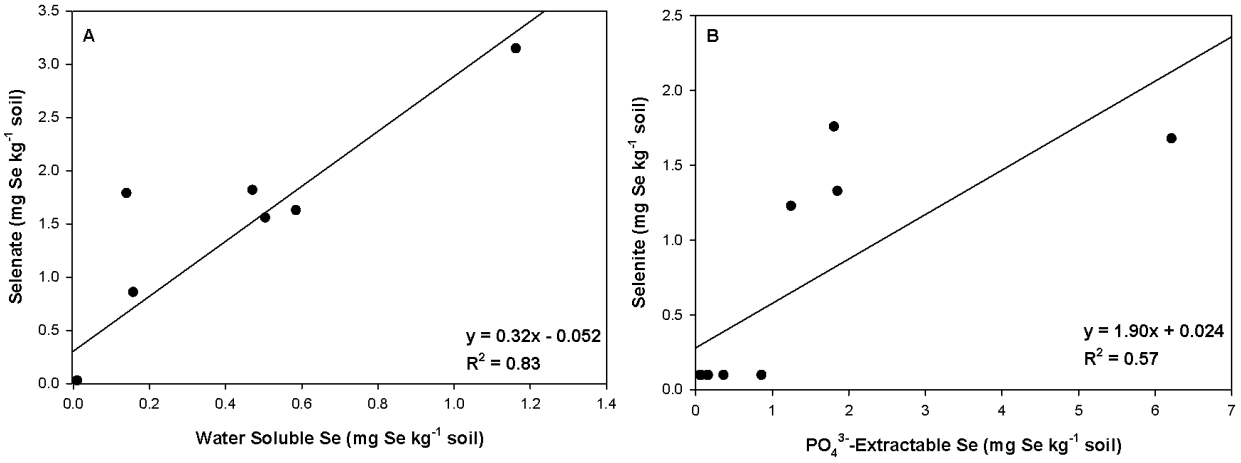

Figure 3.4 A and B: (A) Simple linear regression analysis (*n* = 10) demonstrating the relationship of soil selenate from speciation analyses and the water-soluble selenium fraction from the sequential extraction procedure (SEP) and (B) the relationship of soil selenite from speciation analyses and the phosphate (PO_4^{3-})-extractable fraction from the soil SEP for ten soils analyzed in duplicate

Plant Shoot Selenium Levels

Selenium levels were determined for plants found at the five sites. The only plant species sampled that was considered to be a hyperaccumulator was western aster, which is a native perennial forb. Selenium levels in western aster and other predominating plants found are summarized in Table 3.3. Many of these species are considered Se secondary accumulators and can contain hundreds of mg Se kg^{-1} in shoots (Ellis and Salt, 2003).

Table 3.3: Selenium mean values found in dominant plants observed at the five sites

	Aster[a]	Alfalfa	Bulb.	Brome.	Dand.	Wh.
	mg kg^{-1} dry matter					
A CO[b]	2635	307	353	NP	NP	NP
A NW3	137	107	24.3	NP	80.3	NP
A S2	676	260	107	NP	72.4	NP
A NE1	662	100	34.0	NP	122	NP
B CO	6823	NP	NP	NP	NP	NP
B NW3	2927	364	NP	253	NP	644
B S2	2775	156	29.0	267	NP	NP
B NE1	4189	321	NP	250	NP	NP
C CO	1972	NP	NP	NP	NP	NP
C NW3	1639	NP	NP	NP	NP	NP
C SW2	1520	36.4	NP	NP	NP	NP
C NE1	752	NP	NP	NP	NP	NP
D CO	17.5	23.4	NP	NP	17.8	NP
D NE3	NP[c]	3.46	NP	NP	62.8	NP
D SE2	3.88	7.42	NP	4.21	6.81	10.2
D W1	NP	15.5	NP	NP	7.99	6.49
E CO	NP	23.7	NP	2.24	NP	NP
E SW3	NP	135	NP	21.1	NP	NP
E SE2	NP	17.7	NP	12.9	NP	1.75
E N1	35.9	79.8	NP	9.62	NP	NP

[a]Aster (*S. ascendens),* Alfalfa *(M. sativa),* Bulbous Bluegrass *(*P. bulbosa), Brome Grass (*Bromus*), Dandelion (*Taraxacum*), Wheatgrass (*Agropyron*)
[b]A = Site A; B = Site B; C = Site C; D = Site D; E = Site E; Refer to Figure 3.2 for sampling diagram for each point.
[c] NP indicates plant not present

Overall, Se levels were consistently higher in plants throughout the Site B transect. Of the plants sampled, the western aster species exhibited the highest mean Se levels. The highest value was observed at the center point of Site B (6823 mg Se kg^{-1}_{DM}). In secondary accumulators, the highest mean Se value was observed in crested wheatgrass (*Agropyron cristatum* L. ; 644 mg Se kg^{-1}_{DM}). A high alfalfa (*Medicago sativa* L.*)* mean Se value was also observed along all three lines of this transect, especially at point NW3 (364 mg Se kg^{-1}_{DM}). The highest mean Se value in brome grass was observed at the second southern point along this transect (267 mg kg^{-1}_{DM}).

The other two pre-1996 reclaimed sites, A and C, also contained elevated Se levels in

plant samples. Western asters found at the center point of Site A showed elevated Se levels of 2635 mg Se kg^{-1}_{DM}, while those sampled from Site C were highest at the center point (1972 mg Se kg^{-1}_{DM}). Of the more predominant secondary accumulators, the highest Se levels were observed in bulbous bluegrass (*Poa bulbosa* L.; 353 mg kg^{-1}_{DM} at the Site A center point). Elevated alfalfa levels were also indicated at this same center point as well (307 mg kg^{-1}_{DM}).

Lower plant Se levels were observed in the post-1996 reclaimed sites, D and E. Only two western aster plants were sampled along the Site D transect and one along the Site E transect. The maximum Se values were 35.9 mg Se kg^{-1}_{DM} for Site E and 17.5 mg Se kg^{-1}_{DM} for Site D asters, which also correspond with lower Se soil values measured in these sites.

Western Aster Se and Soil Se Fractionation Relationship

The relationship between the hyperaccumulator, western aster, shoot Se levels, and the six SEP Se fractions was evaluated using simple linear regression. Multiple linear regression was not used for this analysis due to high multicollinearity between SEP fractions. For non-detectable Se values where no values could be determined by ICP-AES, a proxy value of the limit of detection (LOD) divided by the square root of two was used in the analysis. This is a standard replacement technique for values below quantification level, where concentrations are considered small but not known (Hopke et al., 2001). This technique has been shown to reduce the overall error caused by replacement, compared to methods such as replacement with LOD/2 or with zero (Croghan and Egeghy, 2003).

A bivariate regression analysis was completed that involved a progressive summation of the six SEP fractions together (Table 3.4). This was employed in order to identify fractions that promote an increase in Se bioavailability. For water-soluble Se alone, a highly significant

relationship was observed (Table 3.4 and Figure 3.5). This suggests that 81% of Se found in western aster can be explained by the water-soluble fraction of Se in soils. For the summation of water-soluble and PO_4^{3-}-extractable Se, a highly significant positive relationship with a slight increase was also observed (85%).

Table 3.4 Regression equations and correlation coefficients (R^2) for predicting Se shoot levels (*n* = 15) using a progressive summation of the six sequential extraction procedure (SEP) fractions.

	Equation	R^2	P-value[b]
F1[a]	Aster [Se] = 1595x + 321	0.81	<0.0001
F1+F2	Aster [Se] = 1111x + 224	0.85	<0.0001
F1+F2+F3	Aster [Se] = 277x + 288	0.79	<0.0001
F1+F2+F3+F4	Aster [Se] = 196x - 5.15	0.67	0.0002
F1+F2+F3+F4+F5	Aster [Se] = 81.3x + 173	0.57	0.0011
F1+F2+F3+F4+F5+F6	Aster [Se] = 14.5x + 349	0.65	0.0003

[a] Summed fractions; F1 = Water-Soluble; F2 = PO_4^{3-}-Extractable; F3 = Carbonate-Associated; F4 = Amorphous Iron Oxide-Associated; F5 = Organic Selenides; F6 = Residual

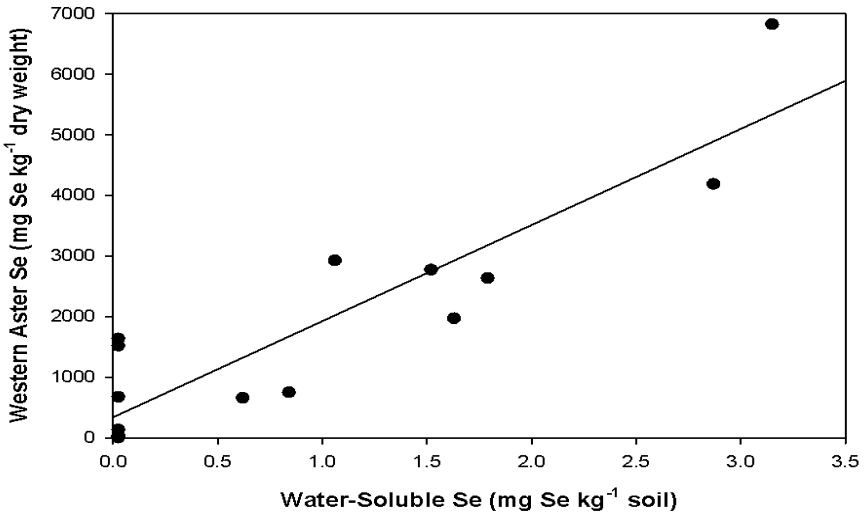

Figure 3.5: Simple linear regression analysis (*n* = 15) demonstrating the relationship of western aster shoot Se levels with the water-soluble fraction from a soil sequential extraction procedure (SEP).

Once carbonate associated Se was summed with the previous two fractions, the relationship decreased. Larger decreases in the relationship were observed once amorphous iron

oxide-associated Se, organic, and residual fractions were summed with the previous fractions. Because the residual fraction acts as a total Se value, this may explain the slight increase in the observed coefficient of determination.

Discussion

Soil Sequential Extraction Procedure

Differences in soil topsoil materials used and soil properties were speculated to affect Se behavior and bioavailability. However, differences in SEP fractions between site were only statistically significant for Site B soils. Higher levels provide an explanation for the correspondingly higher Se levels found in plant shoots, particularly for the water-soluble and PO_4^{3-}-extractable forms of Se. Likewise, non-detectable Se in most of the Sites D and E soils in these fractions also explains lower plant levels as well. According to Zhao et al. (2005), KH_2PO_4 extractions provide an estimate of Se that is available for uptake. Competition from oxyanions, such as phosphate or dissolved organic carbon (DOC) acids, could cause Se to partition into more soluble phases (Dhillon and Dhillon, 2000). Above normal levels of plant-available phosphorus have also been indicate by Bond (1999) in phosphate mines in the western US. Phosphate has also been noted to compete with Se on soil mineral surfaces (Balistrieri and Chao, 1990; Goldberg and Traina, 1987; Neal et al., 1987).

An appreciable abundance of Se within the carbonate SEP fraction indicates that carbonate minerals are possible means of Se sequestration via adsorption or co-precipitation. Selenium is particularly high within this fraction for many soils reclaimed pre-1996, which we speculate may pertain to either high pH or a higher abundance of Se overall. As indicated by Goldberg and Glaubig (1988), selenite sorption increases from pH 6 to 8 and plateaus from pH 8 to 9 on calcite surfaces. The pH in all soils examined were within this range and were especially

high in soils from Site B. According to Zhao et al. (2005), calcium carbonate was the best determinant for decreasing Se bioavailability in soils through Van der Waals surface attraction.

Data also indicate that amorphous iron oxides sequester Se in soils reclaimed pre-1996, particularly at Sites B and C. In general, both selenite and selenate sorb to oxyhydroxides surfaces (Chapman et al., 2010). Soils generally do not sorb selenate above pH 7 on iron oxides (Cornell and Schwertmann, 2003). Work from Balistrieri and Chao (1990) indicates that selenite is largely bound by amorphous iron oxides at pH relevant to our soils (pH 6-8) with subsequent decreases after pH 8. This occurs as strong inner-sphere complexes according to Goldberg (2013). Because of this, we speculate that iron oxide sorbed Se in the soils examined occurs as strong complexes that are not likely bioavailable.

An abundance of Se in the organic fraction was noted, possibly as selenide and/or selenite that are occluded within organic matter (Martens and Suarez, 1997). Residual elemental Se was in the greatest abundance. The abundance of the two aforementioned fractions indicates the presence of Se that has not yet weathered from primary minerals (Ryser et al., 2006). They are not as soluble, have low oxidation potential, and hence, are generally not considered bioavailable (Jacobs, 1989; Neal, 1995). Because of this, we believe that the proportion of both phases is particularly important for soils reclaimed after 1996, suggesting that Se is largely not bioavailable.

Selenium Speciation

Selenite was the dominant species identified in extracts, with appreciable quantities of selenate also indicated in Sites A, B, and C. Selenate was not detected in soils reclaimed after 1996. This corroborates with high plant Se levels in Sites A, B, and C and lower levels in those

from Sites D and E. Higher levels of selenite compared with selenate is also supported by XAFS speciation results in Chapter 4 and also, in work from Ryser et al. (2006). Using μ-XANES and fluorescence microprobe mapping, results from Ryser (2006) indicated that organic Se, elemental Se, and selenite were the dominant species observed in soils from the Conda Mine in Caribou National Forest, ID. Selenate was only dominant in one of the sixteen points of interest for the three soils examined. Ryser et al. (2006) indicated that reduced Se species oxidize to selenate over time. It was speculated that selenate was quickly lost in soils via leaching and/or plant uptake (Ryser et al., 2006).

Strong relationships were identified using regression between water-soluble Se from the SEP and selenate from speciation analyses, indicated in Figure 3.4A. The relationship with selenite was considered insignificant. This corresponds with strong associations of selenite with solid phases at pH <7, while selenate is typically more soluble (Fordyce, 2013). Our findings suggest that selenate comprises a large portion of the water-soluble SEP fraction.

Plant Selenium

Previous work from Zhao et al. (2005) has indicated that Se bioavailability to plants can be verified by examining plant uptake. Hyperaccumulators sampled from Sites A, B, and C were highly elevated in Se. These species can tolerate high quantities of Se and can accumulate thousands of mg Se per kg^{-1}_{DM} (White, 2016). This is thought to be because of the conversion of Se in plants to methylselenocysteine (Freeman et al., 2006). Methylselenocysteine is not as toxic as selenate, which is also taken up by plants (Freeman et al., 2009; de Souza et al., 1998; Neuhierl and Bock, 1996). Secondary accumulating plant species typically do not exceed several hundred mg Se kg^{-1}_{DM}, and therefore, are expected to have lower Se levels than

hyperaccumulators (NAS-NRC, 1983).

Highest plant Se levels in Site B soils were expected as soils from this site also contained the highest Se levels of the five sites. The presence of more hyperaccumulating than nonaccumulating/accumulating plants species in highly seleniferous soils was expected. Nonaccumulators generally do not inhabit seleniferous soils because they can only tolerate Se levels between 10 to 100 μg Se g^{-1}_{DM}, while secondary accumulators can only tolerate levels of around 1 mg Se g^{-1}_{DM} (Dhillon and Dhillon, 2009; Fordyce, 2013; Moreno Rodriguez et al., 2005; Rosenfeld and Beath, 1964; White et al., 2004; White, 2016). Hyperaccumulator tolerance of Se may be related to the Se species stored and area of storage within the plant (de Souza et al., 1998; Freeman et al., 2006; Quinn et al., 2011; Van Hoewyk et al., 2005). These species can store Se as organic methylselenocysteine, while non-accumulators and accumulators store Se as selenate (de Souza et al., 1998; Freeman et al., 2006; Van Hoewyk et al., 2005). Hyperaccumulators also store Se in leaf epidermis and in pollen, ovules, and seeds, while plants that do not hyperaccumulate store Se in leaf vascular tissues (Freeman et al., 2006; Quinn et al., 2011). According to El Mehdawi et al. (2012), hyperaccumulators also exhibit improved growth with increasing supply of Se from soils. This may suggest that these species can benefit from Se uptake via increased anti-oxidant activity (El Mehdawi et al., 2012; Cartes et al., 2005; Hartikainen, 2005).

Western Aster Se and a Soil Sequential Extraction Procedure

The summation of Se in the first two SEP fractions (water-soluble and PO_4^{3-}-extractable Se) exhibited the strongest relationship. Slight decreases in this relationship were observed when carbonate-associated Se was summed with the previous fractions. Work from Zhao et al. (2005)

showed a highly correlated relationship for PO_4^{3-}-extractable Se with plant uptake, with an R^2 value of 0.91 for both field and greenhouse studies. Further decreases in relationships were observed following the inclusion of the amorphous Fe oxide-associated and organic Se. Weak relationships suggest a possible decrease in their contribution to Se bioavailability to western asters and that this fraction is more recalcitrant.

The regression analysis suggests that Se bioavailability increases when Se is water-soluble and PO_4^{3-}-extractable, and begins to decrease with carbonate associations. Carbonate fractions of Se are considered more recalcitrant and require acidification for release. Therefore, the first two fractions were identified as "bioavailable fractions." Our Se speciation results also suggest that selenate is the form of Se present in the water-soluble fraction, and hence, the form taken up by western aster. Several studies have indicated that soil selenate is immediately accumulated by plants in comparison with selenite (Broadley et al., 2006; Fordyce, 2013; Pilbeam et al., 2015). Selenate additions in soils have also resulted in ten-fold more uptake in plant than selenite (Jacobs, 1989; Neal, 1995). Previous work from Sharmasarkar and Vance (1995) have noted strong relationships between grass species and selenate, suggesting that selenate is the main solution species absorbed. Our regression analyses suggest that other fractions of Se in the SEP (after carbonate bound Se extractions) do not greatly contribute to Se bioavailability.

The water-soluble extract, in conjunction with Se levels in shoots of western aster, can be used to identify potentially problematic soils and predicting Se levels in western aster. Simple water extractions can be employed to assess areas where Se levels are particularly toxic in plants to grazing livestock. This can be a useful, quick tool during remediation efforts. For example, a soil water-soluble extract value of 3 mg kg^{-1} would correspond to a predicted Se levels in western

aster of approximately 5000 mg kg^{-1} (Figure 3.5). This level definitely sets a warning threshold that indicates that these areas should be avoided by grazing animals and targeted for remediation.

Conclusion

This study examined Se contamination in soils resulting from previous phosphate mining reclamation practices. Sequential extractions indicated that the dominant phase of Se observed was in the residual fraction, followed by the organic Se fraction. Notable amounts of carbonate- and amorphous iron oxide-associated Se were also observed in soils, demonstrating that a portion of Se was sequestered via adsorption or co-precipitation reactions. Lower levels of water-soluble and PO_4^{3-}-extractable Se were indicated in the SEP. Findings associated with higher abundances of bound forms of Se corroborate with our speciation result because a higher level of selenite was present. Selenite is typically bound or exchangeable. Lower levels of the more soluble Se species, selenate, are also present in speciation results. This corresponds with low abundances of selenate in the water–soluble SEP fraction. A highly significant relationship between selenate and the water-soluble Se fraction was confirmed with a lower, but still significant, relationship observed for selenite and the PO_4^{3-}-extractable Se fraction.

Plant shoot Se levels were reflective of soil Se levels. High levels of Se were found in Se accumulating and hyperaccumulating (western aster) vegetation sampled from Sites A, B, and C, which were reclaimed before 1996. Lower levels were noted for plants sampled from Sites D and E reclaimed post-1996. This was especially true for western aster. Regression data suggests that a strong relationship exists for water-soluble and PO_4^{3-}-extractable Se with increasing plant uptake. This relationship decreases once other SEP fractions are factored into the model and decrease even further with the inclusion of organic Se fractions. Simple water extractions could be beneficial tools, as indicated by the relationship between the water-soluble fraction with

selenate soil speciation and western aster shoot Se. This work identifies a method for quick assessment of Se bioavailability in soils and for relating this to Se accumulation in western aster found in problematic locations.

References

Alam, M.G.M., Tokunaga, S., Maekawa, T., 2000. Extraction of selenium from a contaminated forest soil using phosphate. Environ. Technol. 21, 1371-1378.

Amacher, M., 2010. Sequential Extraction of Selenium. USDA-Forest Service Open File Report, pp. 155-159.

Balistrieri, L.S., Chao, T.T., 1990. Adsorption of selenium by amorphous iron oxyhydroxide and manganese dioxide. Geochim. Cosmochim. Acta 54, 739-751.

Blanchard, T., Baun, C., Stone, L., Gudgell, D., Hayes, J., 2002. Hardrock and Phosphate Mining in Idaho. A report by the Idaho Conservation League and Boulder-Whites Clouds Council.

Bond, M.M., 1999. Characterization and Control of Selenium Releases from Mining in the Idaho Phosphate Region. University of Idaho.

Broadley, M.R., White, P.J., Bryson, R.J., Meacham, M.C., Bowen, H.C., Johnson, S.E., Hawkesford, M.J., McGrath, S.P., Zhao, F., Breward, N., Harriman, M., Tucker, M., 2006. Biofortification of UK food crops with selenium. Nutrition Society, pp. 169-181.

Buck, B.W., Jones, J.L., 2002. Interagency/Industry Coordination To Respond to Selenium Contamination At Phosphate Mines In Southeastern Idaho.

Burau, R.G., 1989. Selenium in Arid and Semiarid Soils. ASCE Journal of Irrigation and Drainage Engineering 115, 42-47.

Cartes, P., Gianfreda, L., Mora, M.L., 2005. Uptake of Selenium and its Antioxidant Activity in Ryegrass When Applied as Selenate and Selenite Forms. Plant Soil 276, 359-367.

Chapman, H.D., 1965. Total Exchangeable Bases. Soil Science Society of America, Inc. and American Society of Agronomy, Inc., Madison, WI.

Chapman, P.M., Adams, W.J., Brooks, M.L., Delos, C.G., Luoma, S.N., Maher, W.A., Ohlendorf, H.M., Presser, T.S., Shaw, D.P., 2010. Ecological Assessment of Selenium in the Aquatic Environment. CRC Press, New York.

Cornell, R.M., Schwertmann, U., 2003. The Iron Oxides: Structure, Properties, Reactions, Occurrences and Uses. Wiley-VCH, Weinheim, Germany.

Croghan, C.W., Egeghy, P.P., 2003. Methods of Dealing with Values Below the Limit of Detection using SAS. Southeastern SAS User Group, St. Petersburg, FL, pp. 22-24.

Davis, T.Z., Stegelmeier, B.L., Green, B.T., Welch, K.D., Panter, K.E., Hall, J.O., 2011. Acute toxicity of selenium compounds commonly found in selenium accumulator plants. CAB International, Cambridge, MA.

Davis, T.Z., Stegelmeier, B.L., Panter, K.E., Cook, D., Gardner, D.R., Hall, J.O., 2012. Toxicokinetics and pathology of plant-associated acute selenium toxicosis in steers. J. Vet. Diagn. Invest. 24, 319-327.

Davis, T.Z., Stegelmeier, B.L., Welch, K., Pfister, J.A., Panter, K.E., Hall, J.O., 2013. Comparative oral dose toxicokinetics of selenium compounds commonly found in selenium accumulator plants. J. Anim. Sci. 91, 4501-4509.

de Souza, M.P., Pilon-Smits, E.A.H., Lytle, C.M., Hwang, S., Tai, J., Honma, T.S.U., Yeh, L., Terry, N., 1998. Rate-Limiting Steps in Selenium Assimilation and Volatilization by Indian Mustard. Plant Physiol. 117, 1487-1494.

Dhillon, K.S., Dhillon, S.K., 2009. Accumulation and distribution of selenium in some vegetable crops grown in selenate-Se treated clay loam soil. Frontiers of Agriculture in China 3, 366-373.

Dhillon, S.K., Dhillon, K.S., 2000. Selenium adsorption in soils as influenced by different anions. J. Plant Nutr. 163, 577-582.

Edmonson, A.J., Norman, B.B., Suther, D., 1993. Survey of state veterinarians and state veterinary diagnostic laboratories for selenium deficiency and toxicosis in animals. J. Am. Vet. Med. Assoc. 202, 865-872.

El Mehdawi, A.F., Cappa, J.J., Fakra, S.C., Self, J., Pilon-Smits, E.A.H., 2012. Interactions of selenium hyperaccumulators and nonaccumulators during cocultivation on seleniferous or nonseleniferous soil – the importance of having good neighbors. New Phytol. 194, 264-277.

Ellis, D.R., Salt, D.E., 2003. Plants, selenium and human health. Curr. Opin. Plant Biol. 6, 273-279.

Fessler, A.J., Moller, G., Talcott, P.A., Exon, J.H., 2003. Selenium toxicity in sheep grazing reclaimed phosphate mining sites. Vet. Hum. Toxicol. 45, 294-298.

Fordyce, F.M., 2013. Selenium Deficiency and Toxicity in the Environment. in: Selinus, O. (Ed.). Essentials of Medical Geology: Revised Edition. Springer Netherlands, Dordrecht, pp. 375-416.

Freeman, J.L., Quinn, C.F., Lindblom, S.D., Klamper, E.M., Pilon-Smits, E.A.H., 2009. Selenium protects the hyperaccumulator Stanleya pinnata against black-tailed prairie dog herbivory in native seleniferous habitats. Am. J. Bot. 96, 1075-1085.

Freeman, J.L., Quinn, C.F., Marcus, M.A., Fakra, S., Pilon-Smits, E.A.H., 2006. Selenium-Tolerant Diamondback Moth Disarms Hyperaccumulator Plant Defense. Curr. Biol. 16, 2181-2192.

Gee, G.W., Bauder, J.W., 1986. Particle-Size Analysis. in: Klute, A. (Ed.). Methods of Soil Analysis: Part 1-Physical and Mineralogical Methods. Soil Science Society of America, Inc. and American Society of Agronomy, Inc., Madison, WI.

Gleyzes, C., Tellier, S., Astruc, M., 2002. Fractionation studies of trace elements in contaminated soils and sediments: a review of sequential extraction procedures. TrAC, Trends Anal. Chem. 21, 451-467.

Goldberg, S., 2013. Modeling Selenite Adsorption Envelopes on Oxides, Clay Minerals, and Soils using the Triple Layer Model. Soil Sci. Soc. Am. J. 77, 64-71.

Goldberg, S., Glaubig, R.A., 1988. Anion Sorption on a Calcareous, Montmorillonitic Soil-Selenium. Soil Sci. Soc. Am. J. 52, 954-958.

Goldberg, S., Traina, S.J., 1987. Chemical modeling of anion competition on oxides using constant capacitance model-mixed ligand approach. Soil Sci. Soc. Am. J. 51, 929-932.

Gupta, M., Gupta, S., 2016. An Overview of Selenium Uptake, Metabolism, and Toxicity in Plants. Frontiers in Plant Science 7, 2074.

Hall, J.O., Winger, H., 2012. Toxicology ICP/MS Sample Digestion and Preparation Procedure for Forage & Feed. Utah Veterinary Diagnostic Laboratory.

Hartikainen, H., 2005. Biogeochemistry of selenium and its impact on food chain quality and human health. J. Trace Elem. Med Biol. 18, 309-318.

Hopke, P.K., Liu, C., Rubin, D.B., 2001. Multiple Imputation for Multivariate Data with Missing and Below-Threshold Measurements: Time-Series Concentrations of Pollutants in the Arctic. Biometrics 57, 22-33.

IDEQ, 2007. Selenium project southeast Idaho phosphate mining resource area. Pocatello, ID.

Jackson, M.L., 1958. Soil Chemical Analysis. Prentice-Hall, Englewood Cliffs, N.J.

Jacobs, L.W., 1989. Selenium in agriculture and the environment. Soil Science Society of America Special Publication 23.

John, D.A., Leventhal, J.S., 1995. Chapter 2: Bioavailability of metals. in: du Bray, E.A. (Ed.). Preliminary compilation of descriptive geoenvironmental mineral deposit models. U.S. Department of the Interior - U.S. Geological Survey Denver, CO.

Knudsen, A.C., Gunter, M.E., 2004. Chapter 7: The effects of weathering on the mineralogy of the phosphoria formation, Southeast Idaho. in: James, R.H. (Ed.). Handbook of Exploration and Environmental Geochemistry. Elsevier Science B.V., pp. 169-187.

Kunze, G.W., Dixon, J.B., 1986. Pretreatment for Mineralogical Analysis. in: Klute, A. (Ed.). Methods of Soil Analysis: Part 1-Physical and Mineralogical Methods. Soil Science Society of America, Inc. and American Society of Agronomy, Inc., Madison, WI.

Luoma, S.N., 1983. Bioavailability of trace metals to aquatic organisms - A Review. Sci. Total Environ. 28, 1-22.

Martens, D.A., Suarez, D.L., 1997. Selenium Speciation of Soil/Sediment Determined with Sequential Extractions and Hydride Generation Atomic Absorption Spectrophotometry. Environ. Sci. Technol. 31, 133-139.

McNeal, J.M., Balistrieri, L.S., 1989. Geochemistry and Occurrence of Selenium: An Overview. in: Jacobs, L.W. (Ed.). Selenium in Agriculture and the Environment. Soil Science Society of America and American Society of Agronomy, Madison, WI.

Meyers, T., 2013. Remediation scenarios for selenium contamination, Blackfoot watershed, southeast Idaho, USA. Hydrogeology Journal 21, 655-671.

Moreno Rodriguez, M.J., Cala Rivero, V., Jiménez Ballesta, R., 2005. Selenium Distribution in Topsoils and Plants of a Semi-arid Mediterranean Environment. Environ. Geochem. Health 27, 513-519.

NAS-NRC, 1983. Selenium in Nutrition: Revised Edition. National Acadamies Press, Washington (DC).

Neal, R.H., 1995. Selenium. Blackie Academic & Professional, London.

Neal, R.H., Sposito, G., Holtzclaw, K.M., Traina, S.J., 1987. Selenite adsorption on alluvial soils: II. Solution composition effects. Soil Sci. Soc. Am. J. 51.

Neuhierl, B., Bock, A., 1996. On the mechanism of selenium tolerance in selenium-accumulating plants. Purification and characterization of a specific selenocysteine methyltransferase from cultured cells of Astrugulus bisculatus. Eur. J. Biochem. 239, 235-238.

Pfister, J.A., Davis, T.Z., Hall, J.O., 2013. Effect of selenium concentration on feed preferences by cattle and sheep. J. Anim. Sci. 91, 5970-5980.

Pilbeam, D.J., Greathead, H.M.R., Drihem, K., 2015. Selenium, 2nd ed. CRC Press, Boca Raton, FL.

Quinn, C.F., Prins, C.N., Freeman, J.L., Gross, A.M., Hantzis, L.J., Reynolds, R.J.B., Yang, S., Covey, P.A., Banuelos, G.S., Pickering, I.J., Pilon-Smits, E.A.H., 2011. Selenium accumulation in flowers and its effects on pollination. New Phytol. 192, 727-737.

Richards, R.T., Chambers, J.C., Ross, C., 1998. Use of Native Plants on Federal Lands: Policy and Practice. Journal of Range Management 51, 625-632.

Rosenfeld, I., Beath, O.A., 1964. Selenium: Geobotany, Biochemistry, Toxicity and Nutrition. Academic Press, New York.

Ryser, A.L., Strawn, D.G., Marcus, M.A., Fakra, S., Johnson-Maynard, J.L., Möller, G., 2006. Microscopically Focused Synchrotron X-ray Investigation of Selenium Speciation in Soils Developing on Reclaimed Mine Lands. Environ. Sci. Technol. 40, 462-467.

Ryser, A.L., Strawn, D.G., Marcus, M.A., Johnson-Maynard, J.L., Gunter, M.E., Möller, G., 2005. Micro-spectroscopic investigation of selenium-bearing minerals from the Western US Phosphate Resource Area. Geochem. Trans. 6, 1-11.

Saffari, M., Yasrebi, J., Karimian, N., Shan, X.Q., 2009. Effect of Calcium Carbonate Removal on the Chemical Forms of Zinc in Calcareous Soils by Three Sequential Extraction Methods. Research Journal of Biological Sciences 4, 858-865.

Shacklette, H.T., Boerngen, J.G., 1984. Element Concentrations in Soils and Other Surficial Materials of the Conterminous United States. U.S. Geological Survey Professional Paper 1270, United States Government Print Office, Washington.

Sharmasarkar, S., Vance, G.F., 1995. Characterization and correlation of soil and plant selenium in some range and coal mine environments of Wyoming. Commun. Soil Sci. Plant Anal. 26, 2577-2591.

Shortridge, E.H., O'Hara, P.J., Marshall, P.M., 1971. Acute Selenium Poisoning in Cattle. New Zeal. Vet. J. 19, 47-50.

Spallholz, J.E., 1994. On the nature of selenium toxicity and carcinostatic activity. Free Radical Biol. Med. 17, 45-64.

Stillings, L., Amacher, M., 2004. Selenium attenuation in a wetland formed from mine drainage in the Phosphoria Formation, southeast Idaho. Life Cycle of the Phosphoria Formation: From Deposition to the Post-Mining Environment. Elsevier B.V., Amsterdam.

Tamm, O., 1922. Eine method zur bestimmung der anorganischen komponenten des gelkomplex in boden. Medd. Statens Skogforsokanst. 19, 385-404.

Tessier, A., Campbell, P.G.C., Bisson, M., 1979. Sequential extraction procedure for the speciation of particulate trace metals. Anal. Chem. 51, 844-851.

Thomas, G.W., 1996. Soil pH and Acidity. American Society of Agronomy, Madison, WI.

Unrine, J.M., Jackson, B.P., Hopkins, W.A., 2007. Selenomethionine biotransformation and incorporation into proteins along a simulated terrestrial food chain. Environ. Sci. Technol. 41, 3601-3606.

Van Hoewyk, D., Garifullina, G.F., Ackley, A.R., Abdel-Ghany, S.E., Marcus, M.A., Fakra, S., Ishiyama, K., Inoue, E., Pilon, M., Takahashi, H., Pilon-Smits, E.A.H., 2005. Overexpression of AtCpNifS enhances selenium tolerance and accumulation in *Arabidopsis*. Plant Physiol. 139, 1518-1528.

Wagemann, R., Brunskill, G.J., Graham, B.W., 1977. Composition and Reactivity of Some River Sediments from Mackenzie Valley, NWT Canada. Environ. Geol. 1, 349-358.

White, P., Bowen, H., Parmaguru, P., Fritz, M., Spracklen, W.P., Spiby, R.E., Meacham, M.C., Mead, A., Harriman, M., Trueman, L.J., Smith, B.M., Thomas, B., Broadley, M.R., 2004. Interactions between selenium and sulphur nutrition in *Arabidopsis thaliana*. J. Exp. Biol. 55, 1927-1937.

White, P.J., 2016. Selenium accumulation by plants. Ann. Bot. 117, 217-235.

Yamada, H., Yumei, K., Aso, T., Hiroshi, U., Fujimura, T., Yonebayashi, K., 1998. Chemical forms and stability of selenium in soil. Soil Sci. Plant Nutr. 44, 385-391.

Zhao, C.Y., Ren, J.H., Xue, C.Z., Lin, E., 2005. Study on the relationship between soil selenium and plant selenium uptake. Plant Soil 277, 197-206.

Chapter 4: Selenium speciation in phosphate mine soils and evaluation of a sequential extraction procedure using XAFS

Abstract

Selenium is a toxic trace element found in soils in the Western US, where the ingestion of Se-hyperaccumulating plants has resulted in mass livestock fatalities. Therefore, a reliable understanding of Se speciation and bioavailability is critical for effective mitigation. Sequential extraction procedures (SEP) are often employed to examine Se phases and speciation in contaminated soils. However, they may be limited by experimental conditions. We examined the validity of a SEP using X-ray absorption fine structure (XAFS) spectroscopy for both whole soils (no extractions) and a sequence of extracted soils (using the SEP). The sequence included progressive steps of removal of soluble, PO_4^{3-}-extractable, carbonate, amorphous Fe-oxide, crystalline Fe-oxide, organic, and residual forms of Se. For whole soils, XANES linear combination fitting (LCF) show that elemental and organic Se species predominated, with lower amounts of Se(IV) present that were related to carbonate and Fe-oxides. Oxidized Se species were more elevated than previous SEP results from ICP-AES suggested. For soils from the SEP sequence, XANES LCF results indicated only partial recovery of carbonate, Fe-oxide and organic Se. This suggests that not all Se was removed during their designated extractions, possibly due to lack of mineral solubilization or reagent specificity. Selenium fractions associated with amorphous and crystalline Fe-oxides were reduced in amount or removed after step 5 (using 0.04 *M* hydroxylamine HCl) for most soils examined. XAFS results indicate that partial dissolution of solid phases may occur during the extraction process. This paper demonstrates why precautions should be taken to ensure full recovery of trace elements during extraction to improve the validity of said procedures. Mineralogical and chemical

characterizations should be completed prior to SEP implementation in order to identify extractable phases or mineral components that may influence the extraction effectiveness. In combination with synchrotron analyses, SEPs can be appropriately tailored for reliable quantification of speciation in contaminated soils.

Introduction

Selenium is an essential and toxic trace element found in elevated concentrations in seleniferous regions. In soils where bioavailable forms are present, vegetation can accumulate Se at toxic levels. Western aster (*Symphyotrichum ascendens* (Lindl.)), prince's plume (*Stanleya pinnata* (Pursh)), and two-grooved milkvetch (*Astragalus bisulcatus* (Hook)) are three examples of hyperaccumulators that can absorb thousands of mg Se kg^{-1} on a dry weight basis (Davis et al., 2012; Freeman et al., 2007; Freeman et al., 2006). In particular, foraging livestock exhibit Se toxicity following the ingestion of Se hyperaccumulating vegetation (Fessler et al., 2003).

Seleniferous soils throughout the Western Phosphate Resource Area (WPRA) of the United States are attributed to the mining of the Phosphoria Formation. This is primarily due to previous reclamation practices and associated waste rock. Prior to 1996, middle waste shale material that contained elevated levels of Se, was generally re-deposited onto the surface after mining. This material contained reduced Se species, selenide (Se(-II)) and elemental Se (Se(0)), which are not immediately soluble or mobile (Desborough et al., 1999). The exposure of reduced Se species to weathering conditions promotes oxidation to the more soluble species, selenate (Se(VI); SeO_4^{2-}) and selenite (Se (IV); SeO_3^{2-} ; McNeal and Balistrieri, 1989). Selenate is the more bioavailable species of the two oxidized forms due to its solubility under typical soil pH and low pK_a values ($pK_a1 = -3$; $pK_a2 = 1.9$; Masscheleyn et al., 1990). In contrast, Se(IV) is typically strongly sorbed onto mineral surfaces, such as clays, oxides, and carbonates (Duc et al.,

2006; Goldberg and Glaubig, 1988; Hayes et al., 1987; Rajan, 1979; Su and Suarez, 2000). This is because Se(IV) has a higher pK_a1 of 2.5 and a pK_a2 of 7.3 than Se(VI) (Goldberg, 2011).

Selenium speciation and bioavailability are a function of soil pH, redox conditions, and soil mineralogical composition (Geering et al., 1968; USEPA, 1996). Examining total trace element concentrations is often considered inappropriate when evaluating bioavailability (Tessier et al., 1979). Instead, sequential extraction procedures (SEP) are employed to estimate fractions of trace elements associated with soluble, exchangeable, mineralogical, and organic phases using progressively stronger reagents. Trace metals associated with each of these fractions will often differ greatly in their potential bioavailability to plants, microbial populations, and higher level biological organisms. Sequential extractions are easily accomplished and the chemical reagents used are accessible to most researchers. However, SEPs are often criticized for being operationally defined due to the experimental conditions administered. Several limitations that authors have noted include: issues with target element and solid phase chemical properties (Martin et al., 1987), lack of specificity of reagents for target phases (Jouanneau et al., 1983), partial dissolution of target elements (Sulkowski and Hirner, 2006), and redistribution and readsorption of solubilized elements (Qiang et al., 1994; Shan and Chen, 1993).

In contrast to SEP protocols and methods, synchrotron-sourced spectroscopic techniques provide more detailed insight into trace element associations with a number of mineralogical and organic phases in soils. Several authors have demonstrated the usefulness of XAFS techniques for directly comparing SEP results and using this to evaluate their validity for target phases. Previous studies have indicated that mobile species are better estimated using SEPs, which are often overlooked using XAFS (Scheinost et al., 2002). Scheinost et al. (2002) examined Zn in smelter-contaminated soils using a combination of XAFS and a SEP. XAFS was used to examine

a series of samples that were sequentially extracted for Zn. The authors noted that the SEP failed to identify Zn associated with mineral phases due to precipitation and nonspecific dissolution. This was due to shortcomings of the extraction technique during the SEP. In this example, following extraction (0.2 *M* ammonium-oxalate), XAFS results indicated incomplete dissolution of the Zn-bearing minerals, franklinite and sphalerite. Further, LCF analyses indicated that solubilized Zn was re-precipitated as Zn-oxalate. While the SEP was not able to accurately target Zn associated with mineral phases, it was, however, able to better estimate mobilized Zn species that were not identified by XAFS. This was concluded following soluble Zn extraction, and was identified as bound via outer-sphere complexes by extended x-ray absorption fine structure spectroscopy (EXAFS ; Scheinost et al., 2002). Qin et al. (2014) compared results from an SEP modified from Kulp and Pratt (2004) and XAFS for Se in seleniferous soils. They also determined that SEP results provided useful information related to bioavailable Se fractions that were not observed in the XAFS spectra. In comparison with the SEP, the authors noted distinct differences in conclusions drawn from the Se XAFS data. They observed an overestimation of elemental Se and underestimation of selenides by the SEP. In combination, the two techniques complement each other and provide improved information for identification and quantification of trace element speciation (Qin et al., 2014).

Previous research on Se in soils has demonstrated that synchrotron-sourced X-ray spectroscopic techniques, especially X-ray absorption fine structure (XAFS), are reliable for probing local structures and electronic environments under a wide range of concentrations for bulk samples (Pickering et al., 1995; Koningsberger and Prins, 1988). The main portion of the generated spectra used was the X-ray absorption near edge structure (XANES) region that can be used to identify valence state and coordination geometry of elements of interest (Kelly et al.,

2008). The XANES spectrum occurs between -20 and +50 eV below and above the absorption edge, providing information about oxidation states of the element of interest, any associated ligands, and the immediate coordination environment (Pickering et al., 2013). X-ray absorption spectroscopy is an ideal method for analyzing speciation in soils because it can be completed in situ with no or minimal pretreatments required. Predominant species are also easily identifiable using short-range structural information (Scheinost et al., 2002).

Seleniferous soils within the western United States are dominated by reduced forms of Se (-II and 0) and the oxidized species, Se(IV) (Oram et al., 2008; Pickering et al., 1995; Ryser et al., 2006; Weres et al., 1989). The few synchrotron based investigations into the speciation of Se in these soils have confirmed this and demonstrated that geomorphological setting plays a large role in the oxidation of these primary minerals and their subsequent weathering products. For example, within the Kesterson Reservoir, XAFS results indicated varying forms of Se present based on the geomorphological setting. Selenium species present in a former evaporation pond indicated a predominance of monoclinic elemental Se with Se(IV) as a minor component (Pickering et al., 1995). The speciation of Se changed within dryer upland locations that include semi-arid grasslands and salt flats where the Se speciation was dominated by Se(VI) with elemental Se also present (Weres et al., 1989). In Blackfoot River, ID sediments, selenite, selenides and elemental Se were predominant (Oram et al., 2008). Finally, Ryser et al. (2006) examined soils from the Conda phosphate mine, located east of Soda Springs, ID and is in close proximity to the current soils examined. Results from μ-XANES and fluorescence microprobe mapping indicated a predominance of Se(IV), Se(-II), and elemental Se with only minor amounts of Se(VI) present (Ryser et al., 2006).

This work aimed to improve our understanding of Se speciation in soils systems and to

increase the reliability of SEPs for estimating bioavailable fractions of Se present in seleniferous soils. Demonstrating the usefulness and shortcomings of SEPs is important from a research perspective because they are widely used techniques that can have limitations that reduce their validity. The combination of SEP and synchrotron-based techniques can provide more reliable information regarding Se solid phases present in soils. An evaluation of this procedure will also prove useful from a regulatory perspective and for future remediation efforts in seleniferous locations. The objectives of this work were to:

(1) Examine Se solid-state speciation in bulk phosphate mine soils and associated mineral surfaces

(2) Evaluate the accuracy of a SEP formulated for Se in soils using XANES spectroscopy

(3) Suggest modifications to this SEP using results gleaned from XANES data, determined by its accuracy for examining Se associated with seven target phases

Materials and Methods

Soil Samples.

The soils investigated were collected from three previously mined and reclaimed phosphate mines near Soda Springs, ID, USA. Reclamation was completed prior to 1996 for all three locations. Soil samples were collected at a depth of 0-20 cm. This sampling depth was chosen due to a shallow calcic horizon below this depth, indicating the presence of a wetting front above the water table. The three sites, labeled A, B and C, were reclaimed using middle waste shale material from the Phosphoria Formation. Y-shaped sampling transects were established. Center points were established in locations where high Se concentrations were presumed to occur based on the presence of Se-hyperaccumulating vegetation. Soils were collected in three locations along each line of the transect. Transect lines were extended 30 m in

three directions, and soil samples were collected every 6 m, resulting in 16 soils from each location (A, B, and C) for a total of 48 samples. Soil samples were dried and sieved to 8-mesh (2 mm). Selected physicochemical properties are noted in Table 4.1. Soil mineralogy was determined by powder X-ray diffraction (XRD) using a PANalytical Xpert Pro MPD (Westborough, MA) with Cu kα radiation and a scan rate of 0.02° Θ, from 5 to 90° 2Θ. After raw XRD patterns were collected, XPowder software was employed to conduct peak searches (Martin-Ramos, 2004). Reference d-spacing and relative intensities were obtained from the International Centre for Diffraction Data (ICDD) library card database.

Table 4.1. Average relative abundance of Se in six fractions of a sequential extraction procedure.

		F1[b]			F2			F3			F4			F5			F6		
	n	Min	Max	Mean	Min	Max	Mean	Min	Max	Mean	Min	Max	Mean	Min	Max	Mean	Min	Max	Mean
		Relative Distribution (%)																	
A[a]	5	0	4.8	1.4	0	3.3	0.7	0	10.2	4.6	0	11.7	2.4	14.1	19.4	25.8	66.1	81.5	71.6
B	9	0	2.6	0.9	0	1.1	0.5	0.4	6.7	3.9	0	6.7	4.6	2.8	11.3	25.7	64.5	91.4	76.0
C	6	0	1.6	0.9	0	0.8	0.2	0	6.7	3.8	0	9.0	2.9	0	14.3	24.8	61.4	100	80.5

[a]Site name

[b]F1 = water-soluble Se, F2 = PO_4^{3-}-extractable Se, F3 = Carbonate Se, F4 = Iron oxide Se, F5 = organic Se, F6 = Residual/Elemental Se

Samples were chosen for XAFS analysis based on total Se data. Briefly, soils were digested for analysis on a hotplate using a mixture of HNO_3, H_2O_2, and HCl (Hossner, 1996). Total Se was variable, ranging from 3.73 to 435 mg Se kg^{-1}. Soils collected from Site A exhibited the lowest concentration of total Se, ranging from 22.9 to 37.1 mg Se kg^{-1}. Concentrations were highest for soils sampled from Site B, ranging from 117 to 435 mg Se kg^{-1} soil. Soils collected from Site C were also variable and were moderate in comparison with the two previous sites, ranging from 3.73 to 106 mg Se kg^{-1} soil. Of the 48 soils sampled, 20 whole soils were first chosen based on varying levels of total Se and were analyzed using XAFS.

Prior to XAFS analyses, a SEP procedure, described by Amacher (2010) and modified from Martens and Suarez (1997), was employed. Extracts were analyzed for Se using ICP-AES (SPECTRO Analytical Instruments, Inc., Mahwah, NJ). This procedure consisted of six Se fractions: 1) water-soluble Se, 2) PO_4^{3-}-extractable Se, 3) Se associated with carbonates, 4) Se associated with amorphous Fe-oxides, 5) organic Se, and 6) residual elemental Se. Extraction results from this procedure can be found in Table 4.1. In order to substantiate our results from the whole soils analysis, six soil samples (seven subsamples each) from the initial twenty soils were re-analyzed under a progressive, stepwise SEP approach for XANES analysis (Table 4.2A and B).

Table 4.2A. Sequential extraction procedure summary for selenium in calcareous soils

	Fraction	Extractants	Conditions
F1[a]	Water-Soluble	Deionized water	Shaken 2 h at 120 rpm, 20°C
F2	PO_4^{3-}-Extractable	0.01 *M* KH_2PO_4/K_2HPO_4 buffer	Shaken 2 h at 120 rpm, 20°C
F3	Carbonate	pH 5, 1.0 *M* $NH_4CH_3CO_2$	Shaken 24 h at 120 rpm, 20°C
F4	Amorphous Fe/Al Hydrous Oxides	0.2 *M* $C_2H_8N_2O_4$ and $H_2C_2O_4$	Shaken 2 h at 120 rpm in the dark, 20°C
F5	Crystalline Fe/Al Oxides	0.04 *M* Hydroxylamine HCl in 25% (v/v) HAOc	Heat to 96°C for 6 h with occasional agitation
F6	Organic	0.1 *M* $K_2S_2O_8$	Heated to 90°C for 2 h
F7	Residual	Concentrated HNO_3	30 minutes in water bath at 95°C; diluted to 25 mL, and heated again for 1.5 h

Table 4.2B. Stepwise scheme for a sequential extraction procedure (SEP) employed for XANES analysis

Subsample	Extraction
1	F1[a]
2	F1, F2
3	F1, F2, F3
4	F1, F2, F3, F4
5	F1, F2, F3, F4, F5
6	F1, F2, F3, F4, F5, F6
7	F1, F2, F3, F4, F5, F6, F7

[a]F1: Water-soluble; F2: PO_4^{3-}-Extractable; F3: Carbonate-Associated; F4: Amorphous Fe-Oxide-Associated; F5 = Crystalline Fe-Oxide-Associated; F6 = Organic Se; F7 = Elemental Se

Prior to XAFS analyses, samples were air-dried and sieved to 325-mesh (<45μm). Twenty whole soils were analyzed by bulk in-situ XAFS. The six soils used in the second XAFS analyses were prepared in the same manner as whole soils and were extracted using the SEP. They were chosen due to discrepancies indicated in the initial XAFS analyses in comparison with phases identified in the SEP using ICP-AES.

XAFS Reference Compounds.

Selenium salt reference compounds, L-selenomethionine, L-selenocysteine, and gray elemental Se were purchased from Alfa Aesar and Acros Organics. Reference compounds for Se(IV) and Se(VI) sorbed onto ferrihydrite were prepared through sorbing 0.01 *M* sodium selenite and sodium selenate at pH 4.5 onto ferrihydrite in batch reactors. Two-line ferrihydrite was synthesized using the procedure described by Schwertmann and Cornell (2000). The surface area was determined from a BET N_2 isotherm using a Quantachrome Automated Gas Sorption System *(*Model Autosorb 1, Quantachrome Corp., Boynton Beach, FL) and was 258 $m^2\ g^{-1}$. Reference compounds for Se(IV) and Se(VI) sorbed onto calcite were prepared in batch reactors

by adding 0.01 *M* sodium selenite or selenate at pH 8.0 with ground calcite (Excalibur Mineral Company, Charlottesville, VA). Reference compounds for Se(IV) and Se(VI) co-precipitated with calcite were prepared using the procedure described by Aurelio et al. (2010). Monoclinic red Se was synthesized from a procedure described by Ebels et al. (2006). XANES spectra for the aforementioned reference compounds are shown in Figure 4.1.

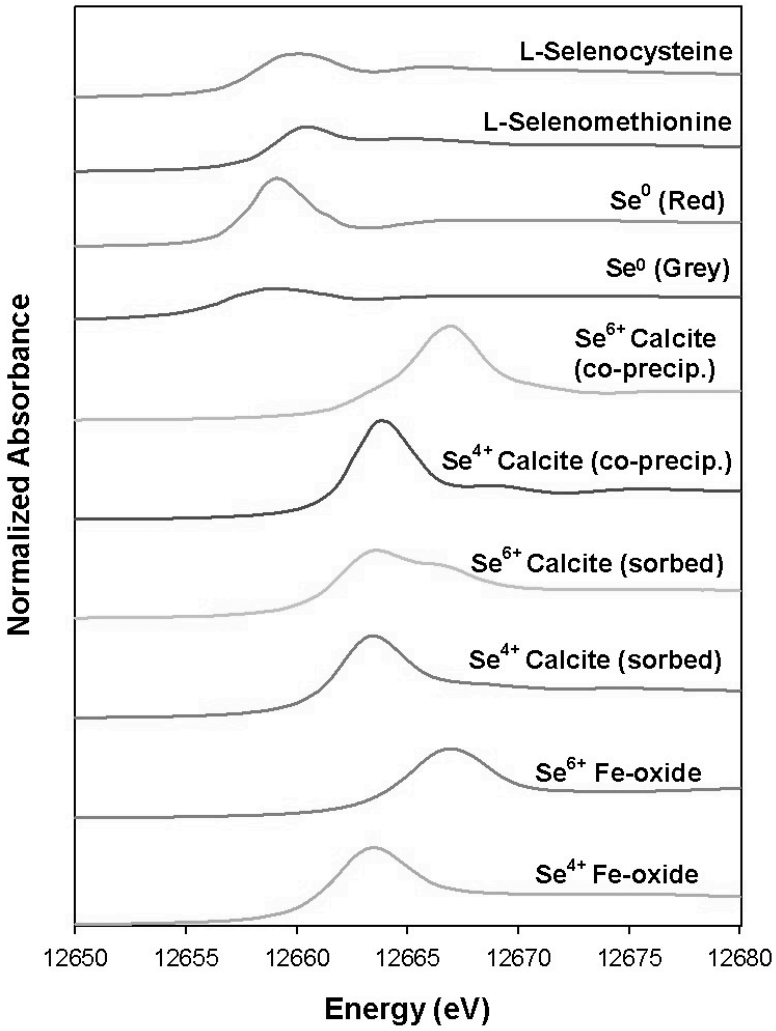

Figure 4.1. Selenium K-edge XANES spectra for 10 reference compounds.

Sequential Extraction Analysis.

Six of the twenty soils (two soils from Sites A, B, and C each) that were first analyzed with XAFS were re-evaluated in order to examine the specificity of extractions for their targeted phases. A progressive-approach to the SEP procedure described by Amacher (2010) was employed. Each of the six samples were divided into seven subsamples. This procedure accounts for six fractions, with modifications. An extraction for Se associated with crystalline oxide using hydroxylamine hydrochloride was supplemented into the procedure, which is described by Tessier et al. (1979). The extraction scheme for each subsample is listed in Table 4.2A and the sequence for all steps is found in Table 4.2B. In between extractions, residues were washed three times with 5 mL 95% ethanol and re-centrifuged. After each extraction scheme was completed, subsamples were analyzed using XAFS in order to determine whether the particular target phases of Se were removed.

X-ray Absorption Spectroscopy.

X-ray absorption fine structure analyses were completed at DND CAT (DuPont-Northwestern-Dow Collaborative Access Team) beamline 5-BM-D, equipped with a double Si (111) monochromator, at the Advanced Photon Source, Argonne National Laboratory (Lemont, IL). Soil samples were compressed into 13 mm pellets using a hand held IR press and sealed between two pieces of Kapton® tape prior to analysis. Spectra were obtained at the Se k-edge energy of 12658 eV, and scans were collected from -200 to 1000 eV above the k-edge. Data collection was completed in fluorescence mode using two solid state Vortex ME4 Silicon Drift detectors. The synchrotron was operated at 7.0 GeV at a nominal 100 mA top-up fill current. The energy of the incident beam was calibrated to a Se foil standard.

A minimum of three and maximum of five XANES spectra were collected, merged, calibrated, and normalized using the software program, Athena, in the computer package IFEFFIT (Ravel and Newville, 2005). Normalization was completed through fitting a first order polynomial from -150 to 30 eV below the edge and either a second or third order polynomial to the spectra from 50-150 to 300-500 eV above the edge. The Se absorption edge (E_o) was determined using the maximum of the first derivative of the signal. Using Athena, linear least-squares combination fitting (LCF) of the XANES region of the spectra was applied to soil spectra along with a combination of the aforementioned reference compounds. The energy range used for the fit was -20 eV below to +30 eV above the Se edge. The quality of fits of reference compounds to the soil spectra were indicated by the goodness of fit parameters, R-factor and χ-square values.

Linear least-squares combination fitting provides quantitative information through fitting combinations of reference compounds to Se spectra. For whole soils, fits were compared to ICP-AES results from a SEP described by Amacher (2010). Using these results, the fits were analyzed first with reference compounds consistent with the SEP. Reference compounds with low contributions (<5%) were removed from the fit. The goodness-of-fit for soils was evaluated by the lowest χ-square and R-factor values with a minimum of reference compounds that were identified in the ICP-AES SEP results. The R-factor is defined as the sum of the squares of the differences between data and the fit at each data point divided by the sum of the squares of each data point. Values below 0.05 are considered to be reasonable fits. The χ-square value is defined as the sum of the square of the difference of predicted fits and data points, divided by uncertainty at these data points (Kelly et al., 2008). If the fits were considered to be poor, other reference compounds that were not identified in the SEP were incorporated into the fit. Comparisons

between XANES and SEP ICP-AES relative abundances were examined using simple linear regression in the statistical software, JMP® Pro 11.0.0 (SAS Institute Inc., 2012).

Results

Soil Chemical Properties and Mineralogy.

Selenium results from the SEP using ICP-AES are found in Table 4.1. Select chemical properties of bulk soils are listed in Table 4.3. Soil pH was generally alkaline with moderate proportions of total organic (TOC) and inorganic carbon (TIC). Soil pH was compared using a one-way ANOVA analysis and least significant difference (LSD) multiple comparison method in JMP Pro 11.0.0 statistical software. Overall, Sites A and B average soil pH values were not statistically different but were statistically more alkaline than those from Site C.

Table 4.3. Select physicochemical properties for soils from the three study sites

Site	pH	TIC[a]	TOC[b]	Fe	Texture
		g kg^{-1}			
Site A					
SA NW1	7.9	6.8	25.2	17.7	Silt Loam
SA NE5	8.2	6.4	41.6	16.8	Silt Loam
Site B					
SB Center	8.3	10.3	30.1	17.3	Silt Loam
SB NE3	7.2	6.7	34.1	17.9	Silt Loam
Site C					
SC NE1	6.8	3.3	58.7	16.1	Silt Loam
SC NW5	7.4	6.2	44.5	14.5	Loam

[a]TIC = Total Inorganic Carbon
[b]TOC = Total Organic Carbon

Sample mineralogy was determined by powder XRD and revealed that soils generally shared similar composition. Mineralogy was comprised of quartz, carbonate-fluorapatite, dolomite, calcite, and muscovite. Smaller peak intensities related to orthorhombic elemental Se were also indicated. Carbonate-fluorapatite was the only phosphate mineral present in analyzed soils. Iron oxide minerals were difficult to identify in diffractograms. Therefore, iron

concentrations in soils from the three study sites were determined using ICP-AES, which were lower than average US soil concentrations (Shacklette and Boerngen, 1984).

XANES Analysis on Whole Soils.

XANES spectra for the twenty samples examined indicated that Se(0) is the most abundant phase present for all soils. Both elemental forms (red and gray) would be considered to make up the residual fraction (F6) associated with the SEP. Linear combination fitting in the XANES region revealed that elemental Se comprised of between 25 and 80% of total Se in soils. In comparison, this is somewhat lower but still close to percentages indicated by the SEP (Table 4.1; 61-100%). This is not unexpected since Se(0) was identified in the X-ray diffractograms. For many of the soils, organic Se(-II) comprised the second largest fraction and were identified as the second most abundant phase in both the SEP and XANES analysis (0-25%, and 8-23%, respectively; Table 4.1 and 4.4). Elemental and organic species of Se are expected in soils in the WPRA because the two occur in mine waste rock from the middle waste shale region of the Phosphoria Formation (Ryser et al., 2006; Ryser et al., 2005). XANES results indicated that many of the soils examined contained oxidized Se (Se(IV)) species (Table 4.4). XANES results were comparable for both Se(IV) associated with ferrihydrite (5 to 41%) and co-precipitated with calcite (4 to 40%). Selenate was not observed in any of the examined soils. Sequential extraction results suggest that this is because the relative abundance of water-soluble Se, which is the likely fraction where Se(VI) would be observed, is too low (<5%) to be reliably quantified in the XANES region (Table 4.1).

Table 4.4. XANES linear least-squares combination fits for 20 samples with compounds used to create reference spectra

Sample	Reference Compounds								
	Se^{IV}-Fh*	Se^{IV}-Ca	Se^{VI}-Ca	Se^{IV}-Co-Ca	Se-Cys.	Se-Me.	Se Gray	Se Red	R-Factor
	Fractional Abundance								
Site A (n= 5)									
SA NE2	0.34	-	-	0.24	-	0.12	0.12	0.35	0.0039
SA NE5	0.30	-	-	0.21	-	0.06	0.23	0.23	0.0048
SA NW1	0.41	-	-	0.23	0.10	-	-	0.25	0.00097
SA NW3	0.39	0.30	-	-	-	-	0.15	0.15	0.0054
SA Center	0.09	0.26	0.14	0.19	-	-	0.16	0.26	0.0016
Site B (n=9)									
SB NE2	0.05	-	-	0.06	-	0.17	0.34	0.41	0.00020
SB NE3	0.05	-	-	0.09	0.08	0.13	0.25	0.42	0.00019
SB NE5	0.15	-	-	0.07	0.18	-	0.20	0.38	0.000018
SB NW1	0.07	-	-	0.11	0.31	-	0.19	0.36	0.000015
SB NW2	0.06	-	-	0.08	-	0.21	0.32	0.34	0.00023
SB NW4	0.07	-	-	0.08	0.22	-	0.30	0.36	0.00013
SB S2	-	-	-	0.10	0.32	-	0.23	0.37	0.00026
SB S5	0.20	-	-	0.13	0.15	-	0.16	0.35	0.00047
SB Center	0.06	-	-	0.08	-	0.18	0.34	0.34	0.00027
Site C (n=6)									
SC SW1	0.24	-	-	0.13	0.17	-	0.21	0.24	0.00082
SC NE1	0.22	-	-	-	0.19	-	0.29	0.38	0.00069
SC NE4	-	-	-	0.40	-	0.15	0.75	0.05	0.099
SC NW2	0.25	-	-	0.16	-	0.21	0.13	0.29	0.00069
SC NW5	0.29	-	-	0.04	0.09	-	0.31	0.28	0.0020
SC Center	0.24	0.06	-	-	0.21	-	0.24	0.26	0.00016

*Fh = Ferrihydrite; Ca = Calcite (sorbed); Co-Ca = Coprecipitated with calcite; Cys. = Cysteine; Me. = Methionine

Linear combination fittings for two soils from Site A and one from C also showed the presence of Se associated with calcite that was not identified in the SEP (Table 4.4). XANES results indicated that four samples from Site A, one from Site B, and one from Site C showed Se associations with ferrihydrite present in XANES LCF results that were not indicated by the SEP. For particular soils, goodness of fit parameters greatly improved following the incorporation of

the Se(IV)-ferrihydrite reference into the LCF. For example, the initial R-factor for Site A point NW1 was 0.0025. With the inclusion of the Se(IV)-ferrihydrite species, this resulted in an average R-factor improvement of 61.2% and a relative standard deviation of 64.7% (R-factor = 0.00097). Spectral lines in the XANES region confirmed the presence of sorbed forms of Se(IV) in soils where they were previously unaccounted for.

XANES results indicate that Se(IV) is associated with several solid phases, either adsorbed onto Fe-oxides, carbonates, and/or coprecipitated with carbonates (Table 4.4). In general, there was improved agreement for site C between the two techniques than there was for Sites A and B (Figure 4.2 A-D). Secondly, there was little agreement between the carbonate vs. Fe-oxide Se phases. XANES results were higher in adsorbed/co-precipitated oxidized forms of Se than the SEP results indicated. In particular, this occurred for soils from Sites A and C.

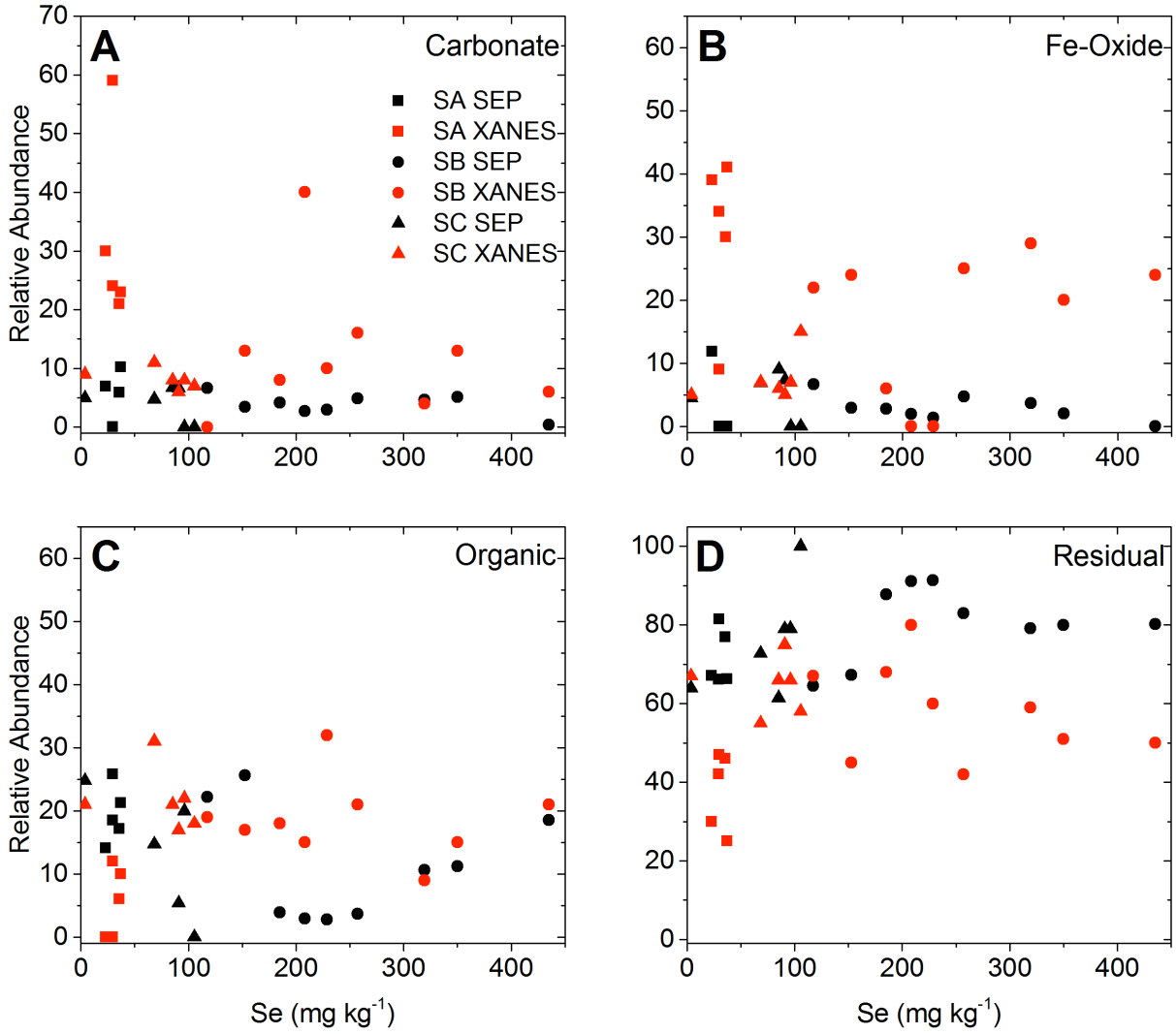

Figure 4.2A-D. Shows relative agreement between sequential extraction procedure and XANES relative abundances (%) as a function of total Se for soils from Sites A (SA), B (SB), and C (SC). Each plot corresponds with (A) carbonate, (B) Fe-oxide, (C) organic and (D) residual fractions.

Comparable abundances were noted for Se(IV) sorbed to ferrihydrite and co-precipitated with calcite, indicated from XANES results. Abundances were related to results from the SEP to evaluate similarities and differences between the predicted Se speciation directly (Figure 4.3) and as a function of the total Se present in the soils (Figure 4.2). Initial evaluations of Figures 4.2 and 4.3 reveal differences in the predicted speciation of Se based on the two techniques used.

The LCF indicates that Se(IV) is associated with several solid phases, either adsorbed onto Fe-oxides, carbonates, and/or coprecipitated with carbonates (Figure 4.2 A and B). However, Figures 4.3 highlights the main inconsistencies between ICP-AES SEP and XANES results, indicating that the Amacher (2010) SEP greatly under-predicts carbonate and Fe-oxide-associated Se. Comparisons were also further evaluated using simple linear regression for all soils examined (Table 4.5A) and for soils by site (Table 4.5B) to identify site dependences on predictability between the two techniques. Simple linear regression analyses were completed for the twenty soils examined in order to identify whether SEP relative abundance results from ICP-AES and XANES were predicative of one another. For Fe-oxide associated phases, results indicated that the two techniques were not predictive of one another overall (p-values > 0.10; Table 4.5A). Additionally, no significant relationships were identified for calcite or organic Se phases as well (p-value > 0.10). A significant relationship between the two techniques was, however, indicated for residual/elemental Se.

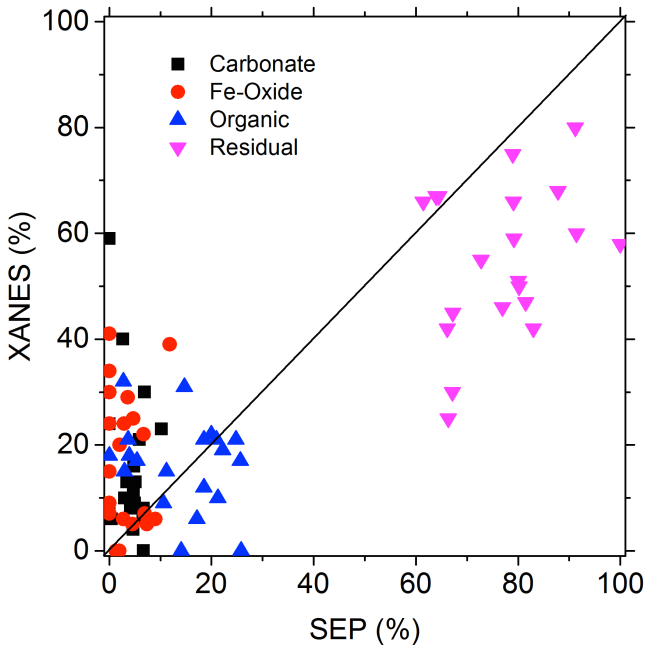

Figure 4.3. Comparison of selenium relative abundances determined by a sequential extraction procedure (SEP) and XANES in a 1:1 ratio for carbonate, iron oxide, organic, and residual forms of Se.

Table 4.5A. Simple linear regression correlation coefficients (R^2) indicating relationships for Se in four phases in soils (n = 20), as determined by XANES and a sequential extraction procedure (SEP) analyzed by inductively coupled plasma-atomic emission spectroscopy (ICP-AES).

	R^2	*p-value*
Iron Oxide Se	0.10	0.1721
Carbonate Se	0.05	0.3659
Organic Se	0.13	0.1245
Residual Se	0.39	0.0031

Table 4.5B. Simple linear regression correlation coefficients (R^2) indicating relationships for Se in several phases, as determined by XANES and a sequential extraction procedure (SEP) analyzed by inductively coupled plasma-atomic emission spectroscopy (ICP-AES) group by site.

		Iron Oxide		**Carbonate**		**Organic**		**Residual**	
Site	*n*	R^2	*p-value*	R^2	*p-value*	R^2	*p-value*	R^2	*p-value*
A	5	0.13	0.4650	0.31	0.3307	0.001	0.9593	0.58	0.1330
B	9	0.36	0.0861	0.28	0.1422	0.0001	0.9746	0.07	0.4870
C	6	0.40	0.1798	0.13	0.4867	0.13	0.5836	0.57	0.0833

The difference in the predicted abundance of complexed/coprecipitated phases was not consistent for the three sites. The location of spectral lines (eV) in the XANES and additional spectral features indicate that these species occur mainly as Se(IV) sorbed to ferrihydrite and co-precipitated with calcite. Soils from Site B showed the most agreement between results from ICP-AES SEP data and XANES LCF analyses, although most p-values determined from simple linear regression were not significant (p-value > 0.10). The iron oxide Se fraction for Site B were considered significant. Figure 4.2B for the amorphous Fe-oxide fraction shows agreement mainly for Site C soils with little consistency for Site A, in particular. Regression analyses indicated the highest correlation coefficient for this phase was indicated for soils from Site C followed by Site B (Table 4.5B), however, the relationship for Site C was considered

insignificant (p-value > 0.10). Highest correlation coefficients were noted for Site A followed by Site B for carbonate Se, neither of which were considered significant.

The discrepancy between the predicted residual/elemental fraction was consistent over the range of Se concentrations investigated (Figure 4.2D). More agreement between the two techniques is noted for Sites A and C soils compared with those from Sites B (Table 4.5B). The Site C residual/elemental fraction was considered significant (p-value < 0.10). However, according to Figure 4.3, the SEP consistently predicted that a greater quantity of Se was associated with the residual/elemental fraction. The second most abundant phase in both the SEP and XANES LCFs were organic Se(-II) compounds. However, unlike the residual/elemental fractions, there was little consistency or trend that could be identified between the two methods for this phase (Figure 4.2C and 4.3; Tables 4.5A and B).

The agreement between SEP and XANES results appears to be concentration dependent. Agreement between XANES and SEP results was identified only at concentrations above 300 mg Se kg^{-1} for carbonate and Fe-oxide associated Se. Regression analyses indicated a significant, strong linear relationship ($R^2 = 1$; p-value = <0.0001) between the two techniques for both phases of Se. Relationships were also identified for organic Se ($R^2 = 0.43$; p-value = 0.5456) and residual/elemental Se ($R^2 = 0.45$; p-value = 0.5309); however, high p-values indicated that the relationships were insignificant.

XANES Analysis of a Sequential Extraction Procedure.

Whole soils analyses suggested that there were discrepancies between ICP-AES SEP and XANES results, particularly for sorbed Se. Therefore, soils were extracted using a modified version of the Amacher (2010) procedure and analyzed further using XANES. Following each step of the Amacher (2010) SEP, Se phase removal after extraction and speciation were

evaluated for six of the twenty (two from each site) whole soils. This was accomplished in order to evaluate the effectiveness of the SEP at removing target mineral and organic phases.

XANES spectra for select soils after each step of the modified extraction scheme are shown in Figure 4.4. For all soils examined, changes in spectral features were not observed following the first (water-soluble) and second extractions (PO_4^{3-}-extractable). This is likely because of their negligible concentrations (≤1% of total Se), as demonstrated by the SEP. Therefore, the spectra for soils extracted for the first two SEP fractions were ignored. Speciation results in soluble and exchangeable soil phases identified in Chapter 3 indicated that the two fractions are mainly composed of oxidized Se. A significant relationship was also noted for Se(VI) and water-soluble Se in Chapter 3. Because of the low concentrations indicated by the SEP, it is unlikely that the XANES spectra were sensitive enough for their accurate identification. XANES LCFs and spectral lines also indicate that Se(IV) is the dominant oxidized/sorbed Se species present in all soils examined.

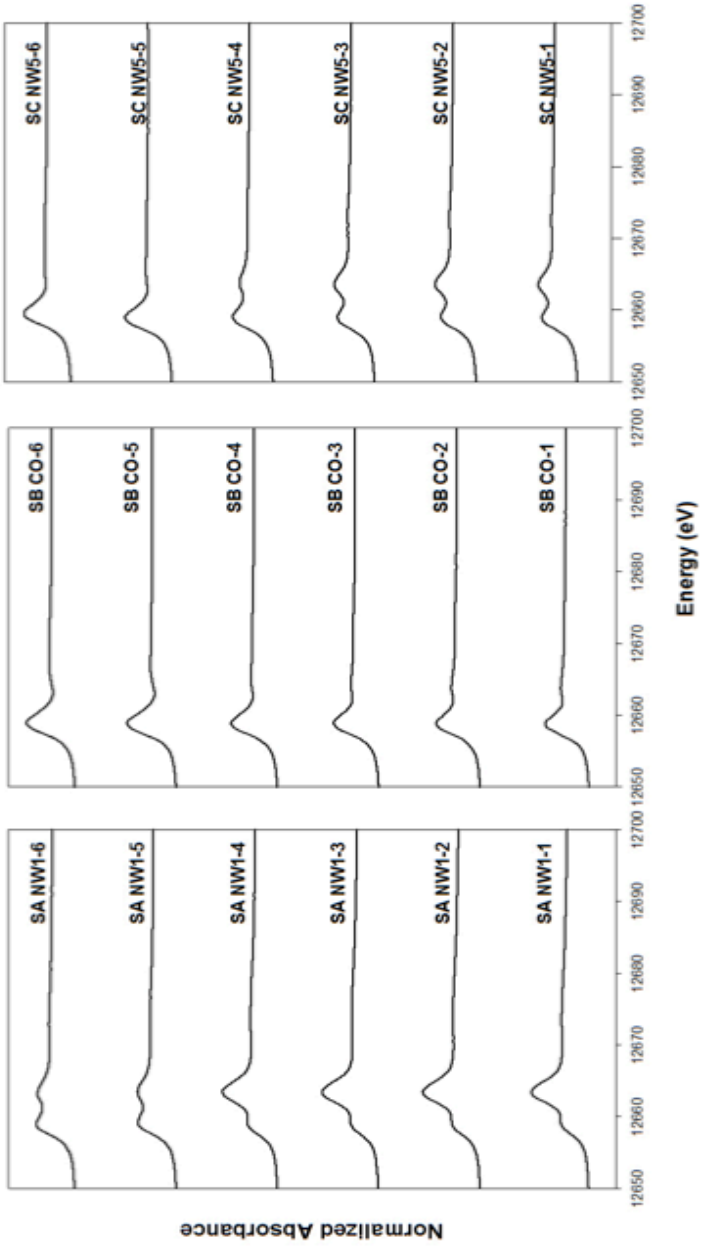

Figure 4.4. Selenium normalized K-edge X-ray absorption near edge structure spectroscopy (XANES) spectra for 6 subsamples from sites A (SA), B (SB), and C (SC) that were extracted for phases of Se. (1) = water-soluble, (2) = PO_4^{3-}-extractable, (3) = carbonate associated, (4) = amorphous iron oxide associated, (5) = crystalline iron oxide associated, (6) = organic selenide.

Site A.

Site A soils were lowest in total Se. Concentrations at points NW1 and NE5 and were 37.1 and 35.7 mg Se kg^{-1} soil, respectively. Sequentially extracted and whole soils XANES LCFs

collectively indicate the presence of Se associated with carbonates in both Site A soils examined. X-ray diffraction patterns and total inorganic carbon (TIC) results also confirmed the presence of carbonate minerals. Peak intensities in diffractograms indicate dolomite is the predominant carbonate mineral present with a less intense calcite peak. Little changes were observed in XANES LCF following the third extraction for carbonate-associated Se.

Following the fourth extraction for amorphous Fe-oxide-associated Se, LCFs indicated that the relative abundance of Se(IV) sorbed to ferrihydrite was not effected by the extraction for the sample from Site A point NW1. Figure 4.5 A and B demonstrate that Se concentrations in this fraction were consistent between whole soils and soils extracted by SEP Steps 3 and 4. After Step 5, the Se(IV)-amorphous Fe-oxide reference compound was reduced even further and slightly more after Step 6 for soils from point NE5.

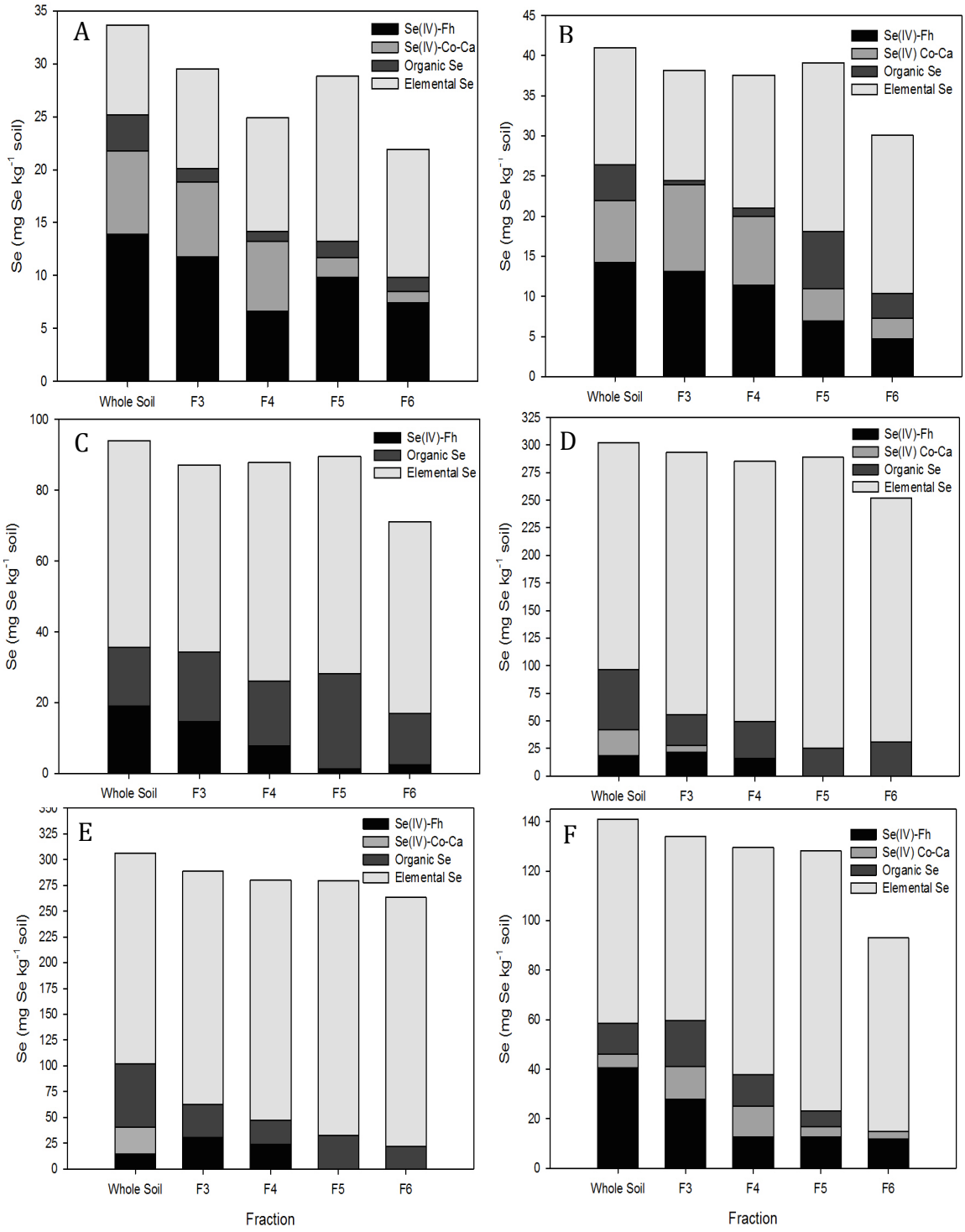

Figure 4.5A-F. Selenium fractionation in whole soil and SEP fractions 3-6 (F3 - F6) identified in XANES linear combination fitting (LCF) for soils from Sites (A) A NW1, (B) A NE5, (C) B NE3 (D) B Center Point (E) C NE1 (F) C NW5.

Organic Se(-II) removal was predicted to occur during Step 6 using potassium persulfate

($K_2S_2O_8$). Figure 4.5 A and B show that no removal of reference compounds from the fit had occurred for both Site A soils during this step in comparison to what was identified in whole soils. When reference compounds were removed from the LCF, goodness of fit parameters increased, indicating that the fit did not improve.

Elemental Se species within the residual fraction were consistent for all soils throughout the extraction scheme. X-ray diffraction patterns also confirmed the presence of gray elemental Se. Linear combination fittings indicate that, following extraction with concentrated HNO_3, little Se was present in soils following this step. However, spectral lines show that the remaining Se was converted from reduced species to Se(VI), which was likely an artifact caused by oxidation with HNO_3 during the extraction. Consequently, Se speciation could not be accurately completed.

Site B.

Site B soils were generally highest in total Se. Concentrations at points NE3 and the center point were 229 and 350 mg Se kg^{-1} soil, respectively. The pH was generally alkaline, due to the presence of carbonate minerals that were confirmed using XRD. X-ray diffractograms indicate intense dolomite peaks with calcite also present.

XANES fit results for Site B soils appear to be more comparable to ICP-AES SEP findings. Figure 4.5 C and D indicates that Se associated with carbonates is completely removed for both soils. X-ray diffraction patterns confirm the presence of calcite in soils, and LCF results suggest that Se(IV) that is co-precipitated in calcite is present. Removal of carbonate associated Se appropriately occurs for point NE3 soils during Step 3. While most Se is removed for soils from the center point, further and complete removal occurs during Step 4 (ammonium oxalate/oxalic acid) according to LCF results.

For Se associated with amorphous and crystalline oxides, complete removal was achieved for both Site B soils (Figure 4.5 C and D). Fits indicated partial removal of this fraction occurred during Step 4 with complete removal achieved during Step 5. Organic Se(-II) is also consistent throughout the extraction procedure, indicating a lack of removal.

Site C.

Site C soils were intermediate in total Se in comparison with soils from the previous two sites. Concentrations in point NE1 and NW5 were 96.0 and 106 mg Se kg^{-1}, respectively. Similar to soils from Site A, a number of discrepancies were noted for Se phases determined in whole soil analyses and those extracted via the SEP that were analyzed in the XANES region. Fit results indicated that soils from point NE1 did not contain carbonate-associated Se, which is in accordance with SEP and XRD results. No obvious diffraction patterns for dolomite or calcite were noted for soils from this point as well. A prominent dolomite peak was present for soils from point NW5 with a less intense calcite peak, demonstrating the presence of sorptive surfaces. The Se(IV) co-precipitated with calcite standard was used in the LCF for extracted soils from point NW5. The relative abundance from the LCF (8%) was near but slightly higher than what was indicated by the SEP ICP-AES results (5%) for Se associated with carbonates.

No carbonate associated Se was found in soils from point NE1. Removal of carbonate Se occurred during an inappropriate step for point NW5 and should have occurred during Step 3 with pH 5 NH_4AOc-HAOc. Relative abundances of Se associated with Fe-oxides were higher in fits than SEP results indicated for both Site C soils. When compared to whole soils, both extracted soils indicated large removals of this fraction during Step 4 (Figure 4.5 E and F). Further removal was noted in soils from point NE1 during Step 5, however, it is possible that this may not be present because of the reduced sensitivity of XANES at low Se concentrations.

A decrease in the relative abundance of organic Se (-II) occurred during Step 5, with complete removal during Step 6 for point NW5 soils noted (Figure 4.5E). Soils from point NE1 showed a reduction in organic Se reference compounds in the LCF following Step 6 but no complete removal (Figure 4.5E). Following the Step 6 extractions, Se reference compounds were manually removed from the LCF for soils from point NE1. This caused a 24% increase in the fit R-factor, signifying no fit improvement and that organic Se compounds may still be present.

Discussion

XANES Analysis on Whole Soils.

According to XANES results, the soils examined for this study contained a predominance of Se(0). Elemental Se is the most abundant form of Se derived from phosphatic shale (Stillings and Amacher, 2010). Soils also contained Se(-II), which may occur as organoselenides and/or ferroselite (an iron selenide), are also present in phosphatic shale (Stillings and Amacher, 2010). Ryser et al. (2006) speculated that because these soils are young and reduced Se species, Se(-II) and Se(0), are present, the existence of primary minerals containing Se in soils is likely. The oxidation of the species, Se(-II) and Se(0), to oxyanions is also a kinetically slow process (Ryser et al., 2006). Bound and co-precipitated forms of oxidized Se were also identified in spectra.

The presence of Se(IV) in XANES LCFs coincides well with μ-XANES work from Ryser et al. (2006) and μ-SXRF work from Oram et al. (2008) who observed a predominance of Se(IV) with lower amounts of Se(VI) in soils from the WPRA. Because of the oxidizing conditions found in semi-arid regions, Se(VI) was thought to predominate, although this has not been confirmed. Ryser et al. (2006) suggests that Se(VI) is rapidly lost in soils through leaching

yet plants throughout this region are accumulating very high concentrations of Se. Based on our XANES LCF data, Se(VI) was not observed in any of the soils examined. It was further speculated that the pH of soils within this region may cause Se(IV) to become more available for plant uptake. The above-normal concentrations of phosphate may also provide surface site competition with Se(IV), causing an increase in Se solubility (Ryser et al., 2006). Several studies have demonstrated that dissolved organic carbon (DOC) acids present in rhizosphere environments can also increase the solubility of sorbed oxyanions (Dynes and Huang, 1995; Dynes and Huang, 1997; Geelhoed et al., 1998; Grafe et al., 2001; Grafe et al., 2002). This was also demonstrated in Chapter 5 with the DOC species, citric acid.

Associations with calcite are expected and are in accordance with soil mineralogy and pH. Sorption results from Goldberg and Glaubig (1988) indicated that, in calcareous soil systems that are above pH 7, Se(IV) should be primarily sorbed onto calcite. It should be noted, however, that the number of sorption sites on calcareous minerals is less than those on Fe-oxides (Cowan et al., 1990). Quantities of Se associated with Fe-oxides in the XANES LCF were in contrast to results from the SEP extraction, which indicated that Fe-oxide bound Se made up approximately 10% or less of the total Se present in any of the soils investigated (Table 4.1). Similar results for carbonate Se were also noted.

Because of discrepancies between XANES LCF and SEP results, it was speculated that other sources (i.e. crystalline forms) of Fe-oxide–sorbed Se were present and unaccounted for by the Amacher (2010) procedure. Ryser et al. (2006) also indicated that reference spectra for Se sorbed to both amorphous and crystalline Fe-oxides were indistinguishable in the XANES region.

Soils with lower abundances of Se under-predict elemental and over-predict bound or co-

precipitated Se(IV) species. However, linear regression analyses for all soils identified a significant relationship between the elemental Se fraction in the SEP identified by ICP-AES and XANES results. This indicates that the two methods are predicative of one another for this particular phase but may also be related to the sensitivity of XANES. Because elemental Se is considered the most abundant phase, it can be more easily identified in XANES spectra. Weak, insignificant relationships between carbonate, Fe-oxide, and organic Se phases were also indicated in the regression analyses. The lower concentrations of these secondary phases may cause difficulties in identifications using XANES. Weak relationships may also indicate that XANES may be identifying target Se phases that were incompletely removed using the SEP.

We have established a concentration dependence of Se for XANES LCF results. Relationships between XANES and SEP results from ICP-AES were significant above concentrations of 300 mg Se kg^{-1} soil. It is important to note that the total abundance of Se present in the soils will have an impact on the ability to resolve specific Se species by analysis of the XANES data. As the concentration of Se decreases, the subsequent decrease in the signal to noise will limit the ability to effectively detect and quantify all of the Se present by LCF analysis of the XANES data. These aforementioned limitations may provide further explanations for discrepancies between XANES and SEP results. Data also suggests that SEP limitations are highly likely and are possibly related to incomplete dissolution of mineral phases during extraction or lack of reagent specificity for target phases.

XANES Analysis of a Sequential Extraction Procedure.

Soil physicochemical properties varied between samples and are speculated to impose differences in removal efficiency and sorbed Se species indicated in XANES spectra. In comparison, Site A soils were lowest, Site B soils were highest, and Site C soils were moderate

in total Se. Lower concentrations of Se will affect the sensitivity of XANES spectra, especially for individual fraction analyses. Speciation results from Chapter 3 indicated that soluble and PO_4^{3-}-extractable Se are mainly composed of oxidized Se. Additionally, a significant relationship was noted for Se(VI) and water-soluble Se. Because of the low concentrations indicated by the SEP, it is unlikely that the XANES spectra were sensitive enough for accurate identification. XANES LCFs and spectral lines also indicate that Se(IV) is the dominant oxidized/sorbed Se species present in all soils examined.

Site A Soils.

Little changes following the third SEP extraction suggests that Se(IV) co-precipitated with calcite, which is identified in the XANES LCF, is not accounted for or effectively removed by the SEP. We speculate that it is also possible that Se could be co-precipitated with other minerals or trace elements that decrease its solubility. Selenite can be strongly bound or co-precipitated to Fe-oxides (Strawn et al., 2002). Merrill et al. (1986) noted that significant quantities of Se(IV) can be co-precipitated with Fe oxyhydroxides. Stillings and Amacher (2004) also found evidence of Se co-precipitated mostly with Fe-oxides in wetland sediments that were receiving phosphate mine drainage. This may provide additional insight into discrepancies related to XANES and SEP results. If Se(IV) is co-precipitated with amorphous Fe-oxides in soils, this may hinder dissolution and recovery of Se during Steps 4 and 5.

Lack of appropriate removal of carbonate fractions may be caused by extractability hindered due to occlusion via co-precipitation with calcite or incomplete carbonate phase dissolution. No current work has examined Se sorption onto dolomite. Previous work, however, reveals that calcite is a large sink for Se (Aurelio et al., 2010). Because of its dynamic solubility, calcite sorption and co-precipitation are more likely to occur in soils, even with lower amounts of

calcium carbonate present (Herberling et al., 2014). When soil solutions are supersaturated with respect to calcite, co-precipitation dominates via a series of adsorption and entrapment events. Below calcite saturation, surface exchange and complexation mechanism will occur (Heberling et al., 2014). Co-precipitated forms of Se are more occluded compared to Se adsorbed to solid phase surfaces, especially on calcite. Because diffractograms identified calcite in soils, which is pedogenic, co-precipitation with Se is a likely mechanism in soils from the three sites. Our LCFs also suggest this reference compound should be utilized in reference spectra for many of the soils examined. The presence of this phase could explain the higher abundance of Se in this fraction in XANES fits compared to SEP ICP-AES data. For soils rich in carbonate minerals (dolomite), Sulkowski and Hirner (2006) observed that the pH rose above the initial extraction value (pH 5) that is generally used for carbonate removal. Because of this, a decrease in desorption and an increase in re-adsorption of target elements occurred. The authors recommended monitoring pH and repetition of using acetic acid until constant pH was achieved. More complete dissolution of carbonates also promoted a 10-fold higher release of Fe from oxides present in soils following hydroxylamine hydrochloride extraction (Sulkowski and Hirner, 2006). Therefore, a second possibility of lack of carbonate mineral dissolution could explain the lack of extractability of Se in our soils and also, the higher abundance of carbonate-associated Se reference compounds in LCFs compared with SEP data. This is imperative to note for future work with SEPs for carbonate-rich soils.

Reductions in Se concentrations for amorphous Fe-oxide associated Se were observed for this soil following Step 4 with no further reductions afterwards. Removal of Se following Step 5 for point NW1 soils signifies the presence and association of Se with crystalline Fe-oxides and also a need for its incorporation into the SEP. Although not indicated in X-ray diffractograms,

Fe-oxide surfaces are likely present.

Removal of organic Se(-II) in Site A soils were not indicated in the LCF following extraction with $K_2S_2O_8$. This suggests that organic Se may still be present in soils. According to Wright et al. (2003), $K_2S_2O_8$ is not specific to just organic Se(-II) compounds, but also metal Se(-II), such as iron selenides. Therefore, it is possible that additional standards may be needed to accurately account for these species. The procedure employed by Wright et al. (2003) also unintentionally solubilized elemental Se. Our results did not indicate any removal of this occurred during the extraction process for any soils analyzed.

For Site A soils, it appears that the SEP failed to completely solubilize several components. Also noted was a possible lack of specificity for $K_2S_2O_8$ for organic Se(-II) species extraction. Further removal of Se associated with Fe-oxides following Step 5 suggests that this fraction is important and should be incorporated into the SEP.

Site B Soils.

Phases identified in XANES regions were in most agreement between whole and sequentially extracted soils from this site. This is contrary to Site A soils, where no carbonate associated-Se was removed. Results for soils from this site indicate a lack of removal of Se(-II) compounds. This suggests that, like soils from Site A, organic Se(-II) compounds were not adequately removed during the extraction process and is, perhaps, due to lack of reagent specificity, ineffectiveness for the target phase examined, or inadequate target phase dissolution possibly caused by pH buffering. However, XANES results indicate that oxidized Se was appropriately extracted in soils from Site B.

Site C Soils.

Linear combination fitting, SEP, and XRD results confirmed the presence of carbonates in soils from point NW5. However, removal of carbonate Se occurred during an inappropriate step. This removal should occur during Step 3 with pH 5 NH_4AOc-HAOc. However, as previously discussed, this indicates that Se is likely more recalcitrant in soils and is not adequately solubilized during the SEP. During extraction, changes in experimental conditions may also occur. Hence, the altered chemistry during extraction may not be sufficient for adequate extraction. Higher relative abundances for Se associated with Fe-oxides than SEP and removal during Steps 4 and 5 suggests that additional forms of Fe-oxides play a part in Se sequestration. Therefore, it is likely that this fraction should be incorporated into SEPs formulated for soils in this region.

Fit results indicated reductions in abundance but lack of complete removal for organic Se(-II) in Site C soils. Combined with the lack of comparability between ICP-AES SEP data and XANES whole soil LCFs along with lack of selenide extractability, it is likely that $K_2S_2O_8$ was unsuccessful at extracting organic Se compounds.

As specified for previously discussed sites, XANES LCFs indicate that organic Se was not adequately removed during the SEP for soils from point NE1 but were for point NW5. The reasoning for this is unclear, considering ICP-AES results for the SEP indicate that point NW5 was highest in Se for this fraction compared with the five other soils examined. As for the oxidized Se fractions, results indicate that Se co-precipitated with calcite was not removed during the SEP. It also appears that Steps 4 and 5 reduce the amount of Se associated with Fe-oxides but complete removal did not occur. Similar findings are noted for Site A and C soils,

however, more accuracy and effectiveness in removal were observed in Site B soils. Possible concentration dependences in removal efficiencies are noted.

Implications for SEPs.

Disparities between XANES LCF whole soil and sequentially extracted soil results suggest that caution should be exerted when employing SEPs for Se or similar oxyanions in soils. This is particularly concerning for oxidized and sorbed species of Se that are more mobile in seleniferous regions. XANES analyses for whole soils indicated that Se was associated with additional forms of Fe-oxides that were not previously accounted for by the unmodified SEP. A lack of carbonate associated Se removal throughout the extraction scheme for many of the soils also suggested that the SEP was not accounting for Se in a more recalcitrant phase. XANES LCFs indicated that organic Se species were also not adequately removed from five out of the six soils. In combination, XANES-SEP results suggest incomplete mineral dissolution or lack of reagent specificity for target phases. Little could be said for the water-soluble and PO_4^{3-}-extractable Se composition because of their low abundance in the soils examined. However, SEP results provide additional insight for these phases not indicated by XANES. Although SEPs are reasonable methods for trace element estimation, the Amacher (2010) procedure fails to reliably quantify Se in several phases.

It is important that SEPs be tailored to soil geochemical composition and mineralogy in order to improve their reliability. Extracting sorbed or co-precipitated Se in carbonate fractions appears to be problematic, especially for soils that are carbonate-rich. Modifications for soils with this particular feature should be made and can include extracting target elements under pH monitored conditions, increasing the extraction liquid:solid ratio, repetition of extractions, or

increasing solute concentrations (Sulkowski and Hirner, 2006; Šurija and Branica, 1995; Tack and Verloo, 1997). Calcium and Mg concentrations can also be monitored during extraction to ensure adequate solubilization during carbonate-associated phase extractions or mineralogy can be re-examined in between phase extractions. Our results also indicated incomplete removal of Se related to Fe-oxides for several soils examined. Previous works have noted the possibility of Fe-oxide-Se co-precipitates in phosphate mine soils that should be further evaluated.

Conclusion

This work examines the distribution of Se in phosphate mine soils using XAFS spectroscopic analyses and an SEP formulated for extraction of various phases of Se. The Se k-edge XANES data was simulated for soils using reference compounds using linear least-squares combination fitting. The XANES spectra provided the most quantitative information for Se speciation in soils, indicating that elemental and organic Se were the largest fractions present. In comparison, lower amounts of sorbed Se(IV) species were present in fits. Using linear regression, significant relationships were only identified between results from a SEP identified by ICP-AES and XANES for the residual/elemental Se fraction. This indicates that the two methods are predicative of one another for this phase, which is likely related to XANES sensitivity. Higher relative abundances of Se related to Fe-oxides in whole soils suggested that an additional phase of Se related to crystalline Fe-oxides was present. With this information, a modified SEP was evaluated for its ability to target specific solid phases for removal. XANES LCFs for extracted soils indicated that only partial dissolution of Se occurred in the carbonate, Fe-oxide, and organic fractions. XANES results indicate that care should be taken when formulating SEPs to evaluate oxyanion contaminants in soils. Sequential extractions should be tailored to prospective soils to be analyzed, with both chemical and mineralogical compositions

known in order to ascertain the most suitable procedure.

References

Amacher, M, 2010. Sequential Extraction of Selenium, USDA-Forest Service Open File Report, pp. 155-159.

Aurelio, G, Fernandez-Martinez, A, Cuello, G J, Roman-Ross, G, Alliot, I, Charlet, L, 2010. Structural study of selenium(IV) substitutions in calcite. Chem. Geol. 270:249-256.

Cowan, C E, Zachara, J M, Resch, C T, 1990. Solution ion effects on the surface exchange of selenite on calcite. Geochim. Cosmochim. Acta 54:2223-2234.

Davis, T Z, Stegelmeier, B L, Panter, K E, Cook, D, Gardner, D R, Hall, J O, 2012. Toxicokinetics and pathology of plant-associated acute selenium toxicosis in steers. J. Vet. Diagn. Invest. 24:319-327.

Desborough, G, DeWitt, E, Jones, J, Meier, A, Meeker, G, 1999. Preliminary Mineralogical and Chemical Studies Related to the Potential Mobility of Selenium and Associated Elements in Phosphoria Formation Strata, Southeastern Idaho, USGS Open File Report, pp. 99-120.

Duc, M, Lefevre, G, Fedoroff, M, 2006. Sorption of selenite ions on hematite. J. Colloid Interf. Sci. 289:556-563.

Dynes, J J, Huang, P M, 1995. Influence of citrate on selenite sorption-desorption on short-range ordered aluminum hydroxides, in: Huang P M (Ed.), Environmental impact of soil component interactions - Metals, other inorganics, and microbial activities. CRC/Lewis Publishers: Boca Raton, FL, pp. 47-61.

Dynes, J J, Huang, P M, 1997. Influence of Organic Acids on Selenite Sorption by Poorly Ordered Aluminum Hydroxides. Soil Sci. Soc. Am. J. 61:772-783.

Ebels, J, Sprik, S, Pietschnig, R, 2006. A Facile Lab Scale Synthesis of Red Selenium, 10th International Electronic Conference on Synthetic Organic Chemistry.

Fessler, A J, Moller, G, Talcott, P A, Exon, J H, 2003. Selenium toxicity in sheep grazing reclaimed phosphate mining sites. Vet. Hum. Toxicol. 45:294-298.

Freeman, J L, Lindblom, S D, Quinn, C F, Fakra, S, Marcus, M A, Pilon-Smits, E A H, 2007. Selenium accumulation protects plants from herbivory by Orthoptera via toxicity and deterrence. New Phytol. 175:490–500.

Freeman, J L, Zhang, L H, Marcus, M A, Fakra, S, McGrath, S P, Pilon-Smits, E A H, 2006. Spatial Imaging, Speciation, and Quantification of Selenium in the Hyperaccumulator Plants Astragalus bisulcatus and Stanleya pinnata. Plant Physiol. 142:124-134.

Geelhoed, J S, Hiemstra, T, Van Riemsdijk, W H, 1998. Competitive Interaction between Phosphate and Citrate on Goethite. Environ. Sci. Technol. 32:2119-2123.

Geering, H R, Cary, E E, Jones, L H P, Allaway, W H, 1968. Solubility and Redox Criteria for the Possible Forms of Selenium in Soils. Soil Sci. Soc. Am. J. 32:35-40.

Goldberg, S, Glaubig, R A, 1988. Anion Sorption on a Calcareous, Montmorillonitic Soil-Selenium. Soil Sci. Soc. Am. J. 52:954-958.

Grafe, M, Eick, M J, Grossl, P R, 2001. Adsorption of Arsenate (V) and Arsenite (III) on Goethite in the Presence and Absence of Dissolved Organic Carbon. Soil Sci. Soc. Am. J. 65:1680-1687.

Grafe, M, Eick, M J, Grossl, P R, Saunders, A M, 2002. Adsorption of Arsenate and Arsenite on Ferrihydrite in the Presence and Absence of Dissolved Organic Carbon. J. Env. Qual. 31:1115-1123.

Hayes, K F, Roe, A L, Brown, G E, Jr., Hodgson, K O, Leckie, J O, Parks, G A, 1987. In Situ X-ray Absorption Study of Surface Complexes: Selenium Oxyanions on α-FeOOH. Science 238:783-786.

Heberling, F, Vinograd, V L, Polly, R, Gale, J D, Heck, S, Rothe, J, Bosbach, D, Geckeis, H, Winkler, B, 2014. A thermodynamic adsorption/entrapment model for selenium(IV) coprecipitation with calcite. Geochim. Cosmochim. Acta 134:16-38.

Jouanneau, J M, Latouche, C, Pautrizel, F, 1983. Analyse critique des extractions sequentielles a travers l'etude de quelques constituants des residus d'attaque critical analysis of sequential extractions through the study of several attack constituent residues. Environmental Technology Letters 4:509-514.

Kelly, S D, Hesterberg, D, Ravel, B, 2008. Analysis of Soils and Minerals Using X-ray Absorption Spectroscopy. SSSA Book Series, no. 5: Madison, WI.

Koningsberger, D C, Prins, R, 1988. X-ray Absorption: Principles, Applications, Techniques of EXAFS, SEXAFS and MES. John Wiley and Sons: New York.

Kulp, T R, Pratt, L M, 2004. Speciation and weathering of selenium in Upper Cretaceous chalk and shale from South Dakota and Wyoming, USA. Geochim. Cosmochim. Acta 68:3687-3701.

Martens, D A, Suarez, D L, 1997. Selenium Speciation of Soil/Sediment Determined with Sequential Extractions and Hydride Generation Atomic Absorption Spectrophotometry. Environ. Sci. Technol. 31:133-139.

Martin, J M, Nirel, P, Thomas, A J, 1987. Sequential extraction techniques: Promises and problems. Mar. Chem. 22:313-341.

Martin-Ramos, D, 2004. XPowder: Departamento de Mineralogia y Petrologia. Universidad de Granada.

Masscheleyn, P H, Delaune, R D, Patrick, W H, 1990. Transformations of selenium as affected by sediment oxidation-reduction potential and pH. Environ. Sci. Technol. 24:91-96.

McNeal, J M, Balistrieri, L S, 1989. Geochemistry and Occurrence of Selenium: An Overview, in: Jacobs L W (Ed.), Selenium in Agriculture and the Environment. Soil Science Society of America and American Society of Agronomy: Madison, WI.

Merrill, D T, Manzione, M A, Peterson, J J, Parker, D S, Chow, W, Hobbs, A O, 1986. Field evaluation of arsenic and selenium removal by iron coprecipitation. J. Water Pollut. Con. F. 58.

Oram, L L, Strawn, D G, Marcus, M A, Fakra, S C, Möller, G, 2008. Macro- and Microscale Investigation of Selenium Speciation in Blackfoot River, Idaho Sediments. Environ. Sci. Technol. 42:6830-6836.

Pickering, I J, Brown, G E, Tokunaga, T K, 1995. Quantitative Speciation of Selenium in Soils Using X-ray Absorption Spectroscopy. Environ. Sci. Technol. 29:2456-2459.

Pickering, I J, Ponomarenko, O, George, G N, La Porte, P F, Strait, K, Gailer, J, Leslie, E M, Spallholz, J, 2013. Synchrotron studies of selenium interactions with arsenic, in: Banuelos G S, Lin Z, Yin X (Eds.), The 3rd International Conference on Selenium in the Environment and Human Health. CRC Press, Hefei, China.

Qiang, T, Xiao-Quan, S, Jin, Q, Zhe-Ming, N, 1994. Trace Metal Redistribution during Extraction of Model Soils by Acetic Acid/Sodium Acetate. Anal. Chem. 66:3562-3568.

Qin, H B, Zhu, J M, Takahashi, Y, Zheng, L R, 2014. Selenium speciation in soils from selenosis area: Comparison between a sequential extraction procedure and XAFS. Taylor & Francis Group: London.

Rajan, S S S, 1979. Adsorption of selenite, phosphate and sulphate on hydrous alumina. J. Soil Sci. 30:709-718.

Ravel, B, Newville, M, 2005. ATHENA, ARTEMIS, HEPHAESTUS: data analysis for X-ray absorption spectroscopy using IFEFFIT. J. Synchrotron Radiat. 12:537-541.

Ryser, A L, Strawn, D G, Marcus, M A, Fakra, S, Johnson-Maynard, J L, Möller, G, 2006. Microscopically Focused Synchrotron X-ray Investigation of Selenium Speciation in Soils Developing on Reclaimed Mine Lands. Environ. Sci. Technol. 40:462-467.

Ryser, A L, Strawn, D G, Marcus, M A, Johnson-Maynard, J L, Gunter, M E, Möller, G, 2005. Micro-spectroscopic investigation of selenium-bearing minerals from the Western US Phosphate Resource Area. Geochem. Trans. 6:1-11.

Scheinost, A C, Kretzschmar, R, Pfister, S, Roberts, D R, 2002. Combining Selective Sequential Extractions, X-ray Absorption Spectroscopy, and Principal Component Analysis for Quantitative Zinc Speciation in Soil. Environ. Sci. Technol. 36:5021-5028.

Schwertmann, U, Cornell, R M, 2000. Iron Oxides in the Laboratory: Preparation and Characterization, Second ed. Wiley-VHC: Weinheim.

Goldberg, S., 2011. Chemical Equilibrium and Reaction Modeling of Arsenic and Selenium in Soils. CRC Press, Boca Raton, FL.

Shacklette, H T, Boerngen, J G, 1984. Element Concentrations in Soils and Other Surficial Materials of the Conterminous United States, U.S. Geological Survey Professional Paper 1270, United States Government Print Office, Washington.

Shan, X, Chen, B, 1993. Evaluation of sequential extraction for speciation of trace metals in model soil containing natural minerals and humic acid. Anal. Chem. 65:802-807.

Stillings, L, Amacher, M, 2004. Selenium attenuation in a wetland formed from mine drainage in the Phosphoria Formation, southeast Idaho. Life Cycle of the Phosphoria Formation: From Deposition to the Post-Mining Environment. Elsevier B.V.: Amsterdam.

Stillings, L L, Amacher, M C, 2010. Kinetics of selenium release in mine waste from the Meade Peak Phosphatic Shale, Phosphoria Formation, Wooley Valley, Idaho, USA. Chem. Geol. 269:113-123.

Strawn, D G, Doner, H, Mavrik, Z, McHugo, S, 2002. Microscale investigation into the geochemistry of arsenic, selenium, and iron in soil developed in pyritic shale materials. Geoderma 108:237-257.

Su, C, Suarez, D L, 2000. Selenate and Selenite Sorption on Iron Oxides: An Infrared and Electrophoretic Study. Soil Sci. Soc. Am. J. 64:101-111.

Sulkowski, M, Hirner, A V, 2006. Element fractionation by sequential extraction in a soil with high carbonate content. Appl. Geochem. 21:16-28.

Šurija, B, Branica, M, 1995. Distribution of Cd, Pb, Cu and Zn in carbonate sediments from the Krka river estuary obtained by sequential extraction. Sci. Total Environ. 170:101-118.

Tack, F M, Verloo, M G, 1997. Determination of the acid extractable metal fraction in a sediment with a high carbonate content: a critical evaluation, in: Prost R (Ed.), Contaminated soils: Third International Conference on the Biogeochemistry of Trace Elements. INRA Editions, Paris, Paris, pp. 167-173.

Tessier, A, Campbell, P G C, Bisson, M, 1979. Sequential extraction procedure for the speciation of particulate trace metals. Anal. Chem. 51:844-851.

USEPA, 1996. EPA Environmental Assessment Sourcebook. Ann Arbor Press, Inc.: Chelsea, Michigan.

Weres, O, Jaouni, A, Tsao, L, 1989. The distribution, speciation and geochemical cycling of selenium in a sedimentary environment, Kesterson Reservoir, California, U.S.A. Appl. Geochem. 4:543-563.

Wright, M T, Parker, D R, Amrhein, C, 2003. Critical Evaluation of the Ability of Sequential Extraction Procedures To Quantify Discrete Forms of Selenium in Sediments and Soils. Environ. Sci. Technol. 37:4709-4716.

Chapter 5: Adsorption of selenite and selenate on ferrihydrite in the presence and absence of dissolved organic carbon

Abstract

This study examines the adsorption of selenite (Se(IV)) and selenate (Se(VI)) on synthetic two-line ferrihydrite in the presence and absence of two low molecular weight (LMW) dissolved organic carbon (DOC) species, citric acid (CA) and salicylic acid (SA). Surface charge potential measurements of ferrihydrite were also examined, which suggest possible Se adsorption mechanisms. Sorption was completed in batch reactor systems at environmentally relevant pH. Our results indicate that CA was competitive with both Se(IV) and Se(VI) for sorption sites on ferrihydrite. This was especially evident at pH 5-7 for Se(IV) and pH 5-6 for Se(VI). Little competition was observed for both Se species in the presence of SA. In the presence of Se(IV) and Se(VI), upwards of 32% of CA adsorption was reduced between pH 5-8. Salicylic acid sorption was almost completely suppressed in the presence of Se(IV) throughout the entire pH range examined, with minimal sorption occurring at pH 5. In the presence of Se(VI), the largest reduction in SA sorption occurred at pH 5-6. Minimal shifts in the surface potential of ferrihydrite at higher pH values suggest that Se(VI) and SA form weak, outer sphere complexes. However at pH values of 5 and 6 there is a shift in the surface potential to more negative values, indicting possible formation of stronger complexes. Larger shifts in surface potential for Se(IV) and CA suggest the formation of strong, inner sphere complexes. This work demonstrates the ability of LMW DOC species (particularly CA) to increase Se(IV) and Se(VI) solubility through surface site competition.

Introduction

Seleniferous soils have caused concern throughout the Western United States and other seleniferous regions throughout the world. In the Western Phosphate Resource Area (WPRA) of the US, soils often contain elevated levels of Se resulting from previous phosphate mining reclamation practices where Se-rich backfill was used as topsoil material. This material contains elevated levels of the oxyanions, selenite [Se(IV)] and selenate [Se(VI)]. Selenite is generally more strongly adsorbed to soil mineral surfaces in comparison with Se(VI), which is more soluble and bioavailable (McNeal and Balistrieri, 1989). A number of cases of ruminant acute toxicity and fatalities have been documented over the past century, largely due to the ingestion of vegetation that accumulates bioavailable Se (Wyoming Board of Sheep Commissioners, 1908; Davis, 1972; Davis et al., 2012). Selenium bioavailability to vegetation may be influenced by competing anions, some of which are dissolved organic species that are present in the rhizosphere zone in soils. Many studies have indicated that Se sorption can be reduced by the presence of other inorganic species via competition. These include SO_4^{2-}, PO_4^{3-}, SiO_4^{4-}, MoO_4^{2-}, CrO_4^{2-}, and CO_3^{2-}(Rajan and Watkinson, 1976; Neal et al., 1987; Barrow and Whelan, 1989; Balistrieri and Chao, 1990; Hopper and Parker, 1999; Wu et al., 2000; Wijnja and Schulthess, 2002). Wu et al. (2002) determined that these interactions were controlled by concentration and binding affinity.

Although there is very little research that examines Se behavior with low molecular weight (LMW) dissolved organic carbon (DOC) that are naturally present in soils, they can evoke competitive interactions. Organic carbon acids are abundant in rhizosphere environments in both agriculture and forest systems, where they can be found in concentrations as high as 1 m*M* (Stevenson, 1967; Fox and Comerford, 1990). These acids can increase bioavailability of anions in soils through ligand exchange reactions (Evans and Zelazny, 1990; Dynes and Huang,

1997). Research has indicated sorption of oxyanions, phosphate, arsenate, and arsenite, onto iron oxides may be reduced by DOC species that can compete for surface sites (Geelhoed et al., 1998; Grafe et al., 2001; Grafe et al., 2002). Dynes and Huang (1997) have demonstrated the DOC species, oxalate, citrate, and tartrate, can effectively compete with Se(IV) for sites on aluminum hydroxides. Differences in the competitive behavior of DOC may be caused by stereochemical electrostatic effects, their ability to form surface complexes, or complex formation kinetics (Stumm, 1986; Dynes and Huang, 1995; Dynes and Huang, 1997).

Many studies have indicated that iron oxides play an important role in Se sorption (Balistrieri and Chao, 1987; Zhang and Sparks, 1990; Su and Suarez, 2000; Peak and Sparks, 2002; Duc et al., 2006; Goldberg, 2013; Goldberg, 2014). Ferrihydrite is a common component of semi-arid soils because the conditions provide a conducive environment for its stability (McFadden, 1988). Ferrihydrite ($Fe_5OH_8 \bullet 4H_2O$) is an amorphous to semi-amorphous iron oxide that contains many iron-octahedra with no particular pattern of assembly (Manceau, 1995). These minerals have many A-type terminal hydroxyl functional groups that are preferred by oxyanions (Sposito, 1984; Waychunas et al., 1993; Manceau, 1995).

The objective of this work was to examine the effects of two organic acids (citric and salicylic) on Se(IV) and Se(VI) adsorption onto an amorphous iron oxide, 2-line ferrihydrite. This was accomplished over a pH range common for soils found in calcareous semi-arid locations (pH 5 to 9) in the Western US.

Material and Methods

Adsorbent Preparation.

Amorphous two-line ferrihydrite ($Fe_5OH_8 \bullet 4H_2O$) was prepared according to Schwertmann and Cornell (2000). All chemicals used were ACS reagent grade or better. The

synthesis involved dissolving 40 g of $FeCl_3 \bullet H_2O$ in 500 mL of deionized water in a 1-L plastic beaker. The pH was adjusted to between 7 and 8 with 1 *M* KOH while stirring vigorously. The suspension was centrifuged and the clear supernatant was siphoned off. The suspension that remained was dialyzed in deionized water. The deionized water was changed multiple times daily during dialysis, and the electrical conductivity was measured until it was equal to the deionized water. Following this, ferrihydrite was freeze-dried for preservation.

The Brunauer-Emmett-Teller (BET) N_2-gas adsorption isotherm method was used to determine the specific surface area of ferrihydrite (Quantachrome Autosorb Automated Gas Sorption System Model Autosorb 1, Quantachrome Instruments, Boynton Beach, FL). The surface area was determined to be 258 $m^2\ g^{-1}$, which is consistent with information presented in Schwertmann and Cornell (2000). X-ray diffraction (XRD) data was consistent with ferrihydrite diffractograms presented in Schwertmann and Cornell (2000), indicating pure 2-line ferrihydrite with minimal impurities present (<1%).

Adsorption Edges.

Adsorption edges were measured in order to observe the effect of pH on Se competition with DOC on a two-line ferrihydrite surface. The procedure employed was similar to Grafe et al. (2002) for a ferrihydrite surface. The adsorption of Se(IV) and Se(VI) was measured as a function of pH (5-9) in a background electrolyte solution of 0.01 *M* NaCl at constant adsorptive (1.0 m*M*) and adsorbent (1.0 g ferrihydrite L^{-1}) concentrations. Nitrogen gas-purged ferrihydrite was prepared in 0.01 *M* NaCl in a 500 mL Teflon-lined, flat-bottomed, water-jacketed reaction vessel and allowed to hydrate for a 24 h period. The reaction vessel was covered with a glass lid with entry ports for the pH electrode, a burette tip, a N_2 gas line, and pipette for sampling. The

pH of the suspension was adjusted to 9 using a Brinkmann Metrohm 718 stat Titrino (Westbury, NY) and the drop-wise addition of 0.10 *M* NaOH. Each suspension was well stirred using a magnetic stir bar and stir plate (Thermolyne Type 7200 Stir Light, Columbia, MD). All experiments were conducted at 298±0.1 K and 0.021 MPa pressure under a N_2 environment. This reduces the influence and interactions of CO_2 on adsorptive processes.

After a 24 h period, adsorptives were added into the batch reactor. They were obtained from prepared stock solutions [0.10 *M* Se (IV) and 0.10 *M* Se (VI)] from sodium salts. Citric and salicylic acid stock solutions (0.01 *M*) were prepared by dissolving an appropriate quantity of sodium citrate and sodium salicylate salts in 0.01 *M* NaCl at pH 7.00. The total acidity of both CA and SA were calculated using formula weight and the assumption that only carboxylic functional groups are active at the pH range examined. The total acidity was determined to be 15.62 $mmol_c\ g^{-1}$ for CA and 7.24 $mmol_c\ g^{-1}$ for SA.

Adsorption edges were measured in duplicate for four scenarios. The first scenario involved separate Se and DOC baseline edges. The second scenario followed the addition of Se before DOC species were added. The third scenario followed the addition of DOC before Se was added. The final scenario involved the addition of Se and DOC simultaneously. All scenarios were completed for both Se(IV) and Se(VI). After the addition of adsorptives, the pH was titrated back to 9.00 and allowed to equilibrate for a minimum of 2 h.

The pH of the suspensions was lowered by one full pH unit from pH 9.00 to 5.00 with 0.1 *M* HNO_3 using a pH stat. Following the equilibration period, a 50-mL sample was retrieved from the batch reactor vessel. Samples were retrieved using a Rainin automated E4 XLS digital pipette (Emeryville, CA) and filtered through a 0.45 μm Millipore nitrocellulose membrane filter

(Billerica, MA) into previously acid-washed polypropylene test tubes for Se analyses and amber glass EPA vials, pre-cleaned to meet EPA standards for organic analyses, for TOC analyses.

For baseline and competitive adsorption analyses, samples were divided as follows: 40 mL for total organic carbon (TOC) analysis, 5 mL for Se analysis, and 5 mL for surface potential determinations. Total organic carbon was analyzed using a Phoenix 8000 UV-Persulfate TOC Analyzer (Teledyne Tekmar Company, Mason, OH). Selenium was analyzed using a SPECTRO Acros inductively coupled plasma atomic emission spectrometer (ICP-AES ; SPECTRO Analytical Instruments, Inc., Mahwah, NJ). In addition to Se analyses, Fe concentrations were determined, confirming minimal dissolution of the ferrihydrite surface had occurred.

Surface charge potential.

The surface potential of ferrihydrite was calculated using microelectrophoresis measurements on a Malvern Zetasizer 3000Hsa (Southborough, MA). This was completed for pure ferrihydrite alone and for samples retrieved for the four aforementioned scenarios. Suspensions were retrieved from the batch system every 2 h following pH adjustments. Samples were first injected into the Zetasizer electrophoresis cell using syringes. An electric field was applied to the cell, causing particles in solution to move towards the electrodes. The applied voltage of 100 mV and Henry function ($f(K_a)$) of 1.5 were used, as determined from the quality of the raw data. The reported potential values are the average of five microelectrophoresis measurements completed in duplicate. Changes in surface potential from the original value for pure ferrihydrite were used to suggest adsorption mechanisms for Se and DOC on the ferrihydrite surface.

Results

Individual Adsorption Edges (Figure 5.1).

Individual pH adsorption edges for Se(IV), Se(VI), citric acid (CA), and salicylic acid (SA) on ferrihydrite were used as references for the adsorption of Se and DOC species on ferrihydrite (Figure 5.1). Results were comparable to findings from Balistrieri and Chao (1990), who observed increasing Se sorption with decreasing pH on ferrihydrite for both Se oxyanions. This is due to the low pKa1 value for Se(IV) and Se(VI), where maximum adsorption typically occurs ($pK_a1_{Se(IV)} = 2.5$ and $pk_a1_{Se(VI)} = -3$). The adsorption of Se(VI) should be less than Se(IV) on goethite surfaces, indicated by equilibrium constants and pK_a values (Balistrieri and Chao (1987). This was in agreement with our findings. Overall, individual baseline sorption edges for CA and SA were lower than Se(IV) and higher than Se(VI). Sorbed quantities of CA and SA were also comparable.

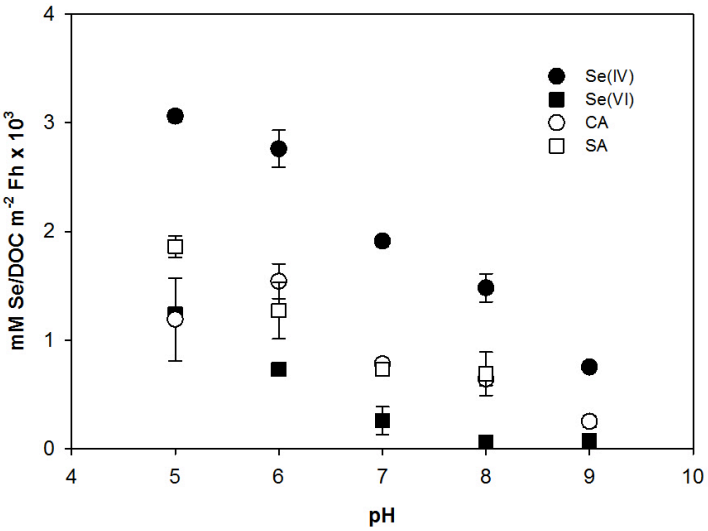

Figure 5.1. Baseline adsorption edges of selenite (Se(IV)), selenate (Se(VI)), citric acid (CA), and salicylic acid (SA) on ferrihydrite ($Fe_5OH_8 \bullet 4H_2O$). Ferrihydrite suspension concentration = 1.00 g L^{-1}, Na_2SeO_3 = 1.0 m*M*, Na_2SeO_4 = 1.0 m*M*, Dissolved organic carbon (DOC) = 1.0 m*M*, background electrolyte = 0.01 *M* NaCl.

Selenite Adsorption in the Presence of Dissolved Organic Carbon (Figure 5.2).

Selenite adsorption was inhibited by CA for all pH values examined (Figure 5.2). No effect on adsorption was observed for Se(IV) in the presence of SA. At pH 5, 32% of Se sorption was inhibited while 31% was inhibited at pH 9 in the presence of CA. Grafe et al. (2002) observed that competition between CA and As(V) was greatest between pH 3 and 5 on ferrihydrite surfaces. Competition between Se(IV) and SA was not apparent. These results are similar to results from Dynes and Huang (1997) who similarly observed that CA effectively outcompeted Se(IV) and there was little competition of Se(IV) with SA on an Al hydroxide surface. While both are able to form chelate rings, CA forms bonds that are stronger (Dynes and Huang, 1995; Dynes and Huang, 1997).

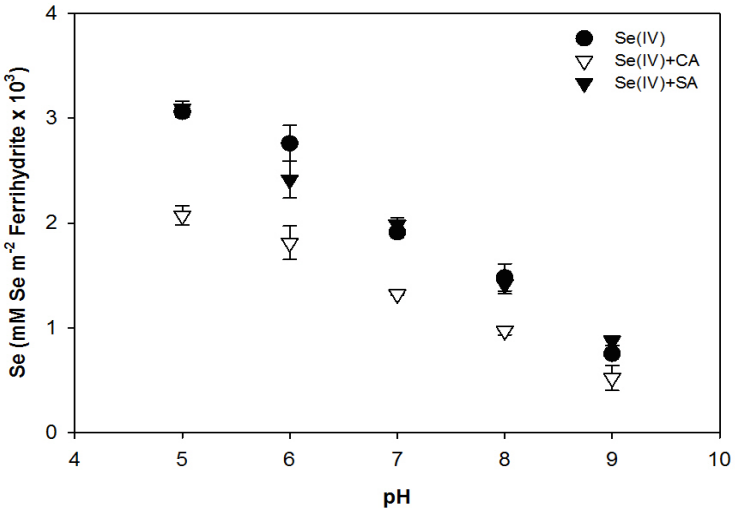

Figure 5.2. The Se(IV) adsorption edge on ferrihydrite ($Fe_5OH_8 \bullet 4H_2O$) in the presence and absence of dissolved organic carbon (DOC): citric acid (CA) and salicylic acid (SA). Ferrihydrite suspension concentration = 1.00 g L^{-1}, Na_2SeO_3 = 1.0 m*M*, Dissolved organic carbon (DOC) = 1.0 m*M*, background electrolyte = 0.01 *M* NaCl.

Selenate Adsorption in the Presence of Dissolved Organic Carbon (Figure 5.3).

At pH 5 and 6, Se(VI) adsorption was inhibited by CA, with more competition occurring at pH 5 (Figure 5.3). At pH 5 and 6, 55 and 38% of Se(VI) adsorption, respectively, was inhibited on the ferrihydrite surface with CA additions. Between pH 7 and 9, minimal Se(VI)

sorption was observed. This is because at more alkaline pH, most Se(VI) is soluble. In the presence of SA, minimal competition occurred at lower pH (5-6). These findings for selenate and CA competition are similar to studies from Grafe et al. (2001) and Grafe et al. (2002) that examine As competition with CA. Those studies observed that As(III) species, which is more soluble than As(V), was greatly inhibited by CA (40 to 45% inhibition) on both goethite and ferrihydrite surfaces.

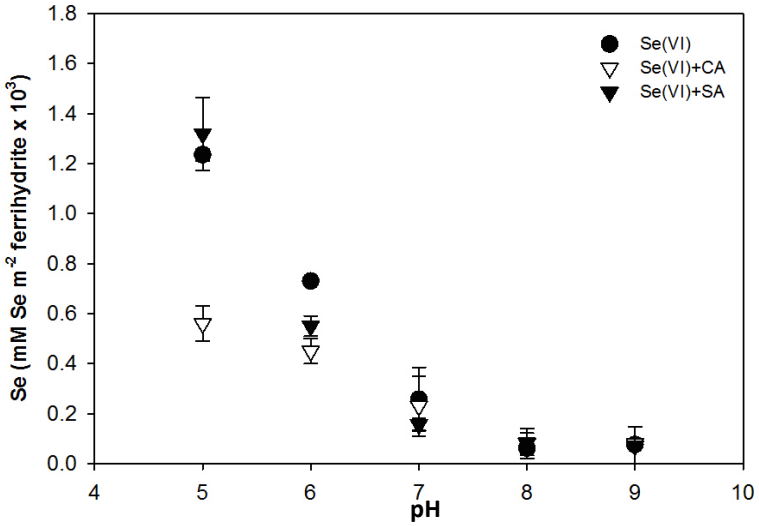

Figure 5.3. The Se(VI) adsorption edge on ferrihydrite ($Fe_5OH_8 \cdot 4H_2O$) in the presence and absence of dissolved organic carbon (DOC): citric acid (CA) and salicylic acid (SA). Ferrihydrite suspension concentration = 1.00 g L^{-1}, Na_2SeO_4 = 1.0 m*M*, Dissolved organic carbon (DOC) = 1.0 m*M*, background electrolyte = 0.01 *M* NaCl.

Dissolved Organic Carbon Adsorption in the Presence of Selenite and Selenate (Figures 5.4 and 5.5).

In the presence of Se(IV), CA adsorption was reduced at pH 5-8, with minimal effects observed above pH 8 (Figure 5.4). Sorption of SA was almost completely suppressed in the presence of Se(IV), except at pH 5, where minimal sorption was observed.

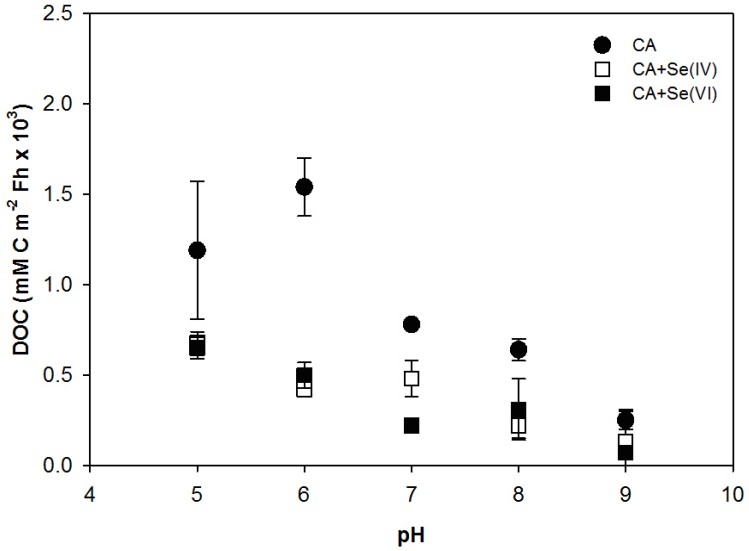

Figure 5.4. Citric acid (CA) adsorption edge on ferrihydrite ($Fe_5OH_8 \cdot 4H_2O$) in the presence and absence of selenium (selenite (Se(IV)) and selenate (Se(VI)). Ferrihydrite suspension concentration = 1.00 g L^{-1}, Na_2SeO_4 = 1.0 m*M*, Dissolved organic carbon (DOC) = 1.0 m*M*, background electrolyte = 0.01 *M* NaCl.

In the presence of Se(VI), reduced CA sorption was observed. This was comparable to Se(IV) competition with CA. Decreases in CA sorption are observed between pH 5-7 (Figure 5.5). Sorption of SA was reduced in the presence of Se(VI), especially between pH 5 and 6. Competition was not as pronounced for Se(VI) compared with Se(IV).

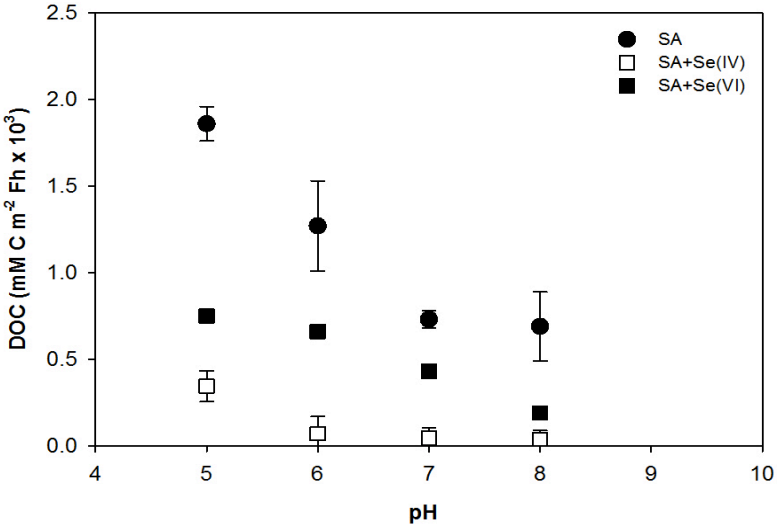

Figure 5.5. Salicylic acid (SA) adsorption edge on ferrihydrite ($Fe_5OH_8 \cdot 4H_2O$) in the presence and absence of selenium (selenite (Se(IV)) and selenate (Se(VI)). Ferrihydrite suspension concentration = 1.00 g L^{-1}, Na_2SeO_4 = 1.0 m*M*, Dissolved organic carbon (DOC) = 1.0 m*M*, background electrolyte = 0.01 *M* NaCl.

Ferrihydrite Surface Potential (Figures 5.6 and 5.7).

The PZC of ferrihydrite with no sorbents present was determined to be at pH 7. Baseline surface potential measurements indicated that the PZC of ferrihydrite shifted to a lower pH due to the presence of Se(IV) and CA (Figure 5.6). The surface potential for CA on ferrihydrite was slightly more negative than Se(IV), overall. Both Se(VI) and SA had little effect on surface charge at higher pH (7-9) (Figure 5.7). At lower pH (5-6), more marked shifts were observed, suggesting that stronger complexes had formed on the ferrihydrite surface.

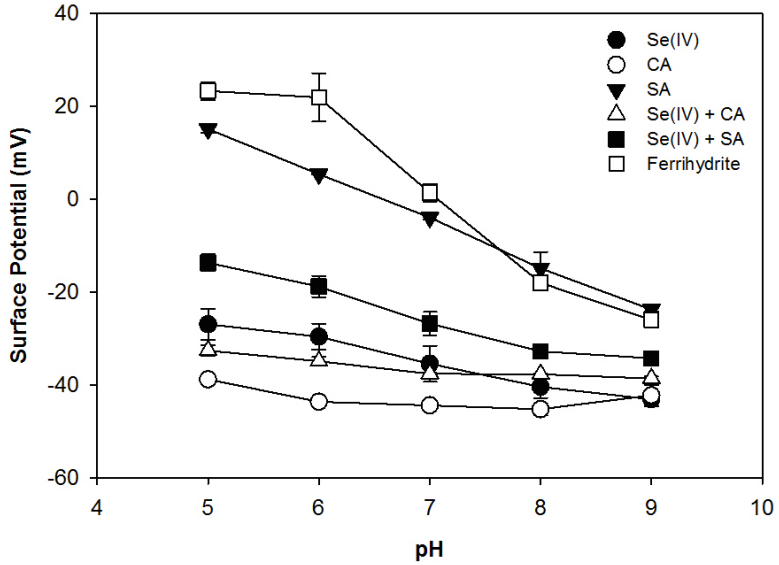

Figure 5.6. Surface potential for ferrihydrite ($Fe_5OH_8 \bullet 4H_2O$) at pH 5-9 alone, with sorbed selenite (Se(IV)), sorbed dissolved organic carbon (DOC), citric acid (CA) and salicylic acid (SA), and with competitive interactions between Se(VI) and DOC. Ferrihydrite suspension concentration = 1.00 g L^{-1}, Na_2SeO_4 = 1.0 m*M*, Dissolved organic carbon (DOC) = 1.0 m*M*, background electrolyte = 0.01 *M* NaCl.

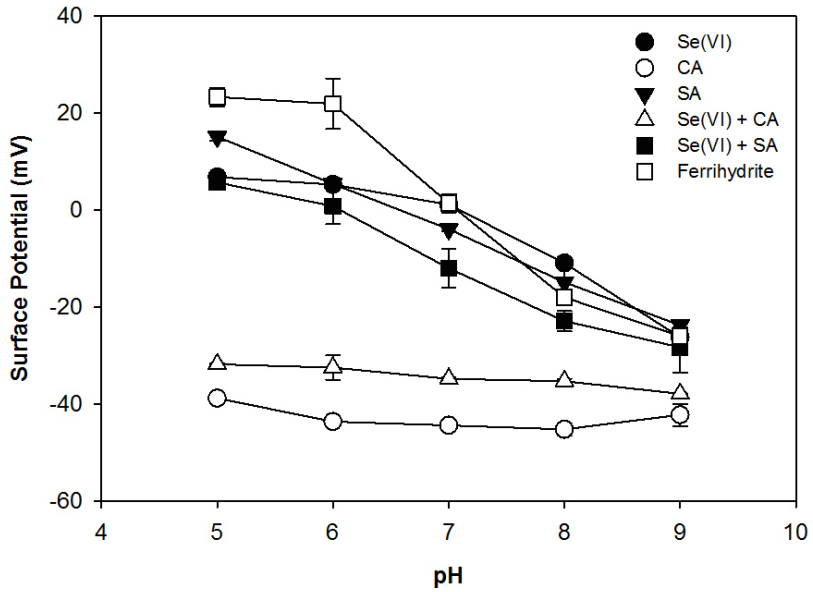

Figure 5.7. Surface potential for ferrihydrite ($Fe_5OH_8 \cdot 4H_2O$) at pH 5-9 alone, with sorbed selenate (Se(VI)), sorbed dissolved organic carbon (DOC), citric acid (CA) and salicylic acid (SA), and with competitive interactions between Se(VI) and DOC. Ferrihydrite suspension concentration = 1.00 g L^{-1}, Na_2SeO_4 = 1.0 m*M*, Dissolved organic carbon (DOC) = 1.0 m*M*, background electrolyte = 0.01 *M* NaCl.

Discussion

Selenite Competitive Behavior with DOC.

Selenite adsorption typically occurs via ligand exchange (Parfitt and Russell, 1977; Zhang and Sparks, 1990; Saeki and Matsumoto, 1994). Numerous authors have indicated Se(IV) has a greater affinity for iron oxides than Se(VI) (Balistrieri and Chao, 1987; Davis and Kent, 1990; Dzombak and Morel, 1990; Cornell and Schwertmann, 2003; Goldberg, 2014; Snyder and Wooyong, 2014). Our results indicate that baseline adsorption of Se(IV) is almost two-fold higher than Se(VI) on ferrihydrite surfaces between pH 5 to 9. Baseline results are confirmed by observations from Balistrieri and Chao (1990), who found Se(IV) sorption increased with decreasing pH and increasing ferrihydrite concentration. The authors also examined Se adsorption using the Triple Layer Model (TLM) (Davis et al., 1978), which is a surface complexation model that accounts for surface site heterogeneity. Balistrieri and Chao (1990)

found that Se(IV) forms strong, inner-sphere complexes on ferrihydrite. Goldberg (2013) and (2014) also examined Se(IV) adsorption on an amorphous Fe-oxide and observed the formation of strong inner-sphere complexes up to pH 8, indicated by a broad adsorption maximum (Goldberg, 2013). Selenate forms inner sphere complexes with type A hydroxyl functional groups, via binuclear bridging, on goethite and hydrous ferric oxides (Manceau and Charlet (1994). However, extended X-ray absorption fine structure (EXAFS) spectroscopic measurements from Hayes et al. (1987) indicate that Se(VI) retains its waters of hydration when sorbed to goethite, forming outer-sphere complexes while Se(IV) is strongly bound via inner-sphere complexation.

In the presence of CA, Se(IV) sorption was reduced, regardless of the order of introduction into the batch reactor system. Competition appears to increase with decreasing pH due to decreases in the amount of available surface sites. For example, at pH 9, 0.75 μmol m^{-2} of Se(IV) occupy reactive sites. Hydrous ferric oxides generally have total reactive surface site densities within the range of 4.36 to 13.07 μmol m^{-2} (Dzombak and Morel, 1990). This indicates that many of the surface sites are not occupied by Se and are in excess. Therefore, competition will not be as pronounced. At pH 5, however, 3.06 μmol m^{-2} of Se(IV) occupied reactive sites. Hence, if Se(IV) occupies more sites, competition with DOC will increase. This also coincides with our findings at lower pH.

Results were similar to Dynes and Huang (1997) for Se(IV) competition with a variety of LMW DOC on an Al hydroxide surface. The concentration, structure, and functionality of DOC were what caused competition with Se(IV). Kinetic studies indicate that ligands with greater negative charge sorbed more quickly and were able to outcompete Se(IV) (Dynes and Huang, 1997).

Citric acid carboxyl groups generally bind to mineral surface hydroxyl groups via ligand exchange reactions (Geelhoed et al., 1998). Our work indicated that CA can effectively compete with Se(IV) for sorption sites at all pH values examined. Similarly, several studies have also reported the competitive nature of CA with other oxyanion species (Balistrieri and Chao, 1987; Geelhoed et al., 1998; Grafe et al., 2001; Grafe et al., 2002; Johnson and Loeppert, 2006).

According to Balistrieri and Chao (1987), CA and Se(IV) have equal affinities for sorption sites on goethite. For DOC anions that are weakly sorbed, higher concentrations are necessary for a comparable decrease in Se(IV) sorption as compared with DOC anions that are strongly sorbed (Balistrieri and Chao, 1987). Several studies report that PO_4^{3-} exhibits comparable sorption behavior and can compete with Se(IV) for the same types of sorption sites, although Se(IV) has a lower site affinity (Rajan and Watkinson, 1976; Hamdy and Gissel-Nielsen, 1977; Balistrieri and Chao, 1987; Ryden et al., 1987). Work from Johnson and Loeppert (2006) found that CA had the greatest effect on mobilizing PO_4^{3-} on ferrihydrite at pH 4. On goethite, Geelhoed et al. (1998) noted that PO_4^{3-} adsorption was most effected by CA at pH below 7, which is similar to our findings for Se(IV). The greatest amount of interaction occurred at pH 5, which is also similar to our findings for Se(IV). Another important factor for sorption was the increased number of binding surface groups on CA in comparison with PO_4^{3-}. Citrate was able to bind with three or four surface groups while PO_4^{3-}, similarly to Se(IV), could only bind with one or two groups (Geelhoed et al., 1998).

Dynes and Huang (1997) note that sorption sites may be lost due to occupation by DOC but also through alterations of surface charge attributed to the presence of sorbed DOC. This is also a function of the amount of DOC present – if higher DOC concentrations are present, they will occupy more binding sites than Se (Dynes and Huang, 1997). Stumm (1986) notes that

bound DOC may hinder the formation of other complexes due to stereochemical and electrostatic effects. For instance, ligands can replace surface hydroxyl groups. If the distance between the oxygen of coordinating groups on ligands were comparable to those of the surface hydroxyl, then they would have site preference (Dynes and Huang, 1997). Dynes and Huang (1997) observed that, in comparison with oxalic acid, CA exhibited more surface coverage due to its larger size and greater number of functional groups.

Few competitive effects were observed for Se(IV) on ferrihydrite in the presence of SA. Yet, CA, was more competitive for surface sites. In contrast, Dynes and Huang (1997) observed Se(IV) competition with both DOC species on an Al hydroxide surface at pH 5. Competition was more pronounced for CA than for SA, which was similar to our observations. At pH 5, SA was not able to form surface ring complexes, which may explain its reduced competition with Se(IV) in comparison with CA (Dynes and Huang, 1997). Dynes and Huang (1997) noted that SA dissolves Al hydroxide surfaces, which could also account for their observations. For this study, dissolved Fe was monitored following each pH adjustment and was found to be minimal.

Evanko and Dzombak (1999) indicated that DOC compounds, like SA, that contain phenolic functional groups in the ortho position, relative to carboxyl groups, have the lowest equilibrium constants for ligand exchange on a goethite surface. Lower equilibrium constants indicate ligand exchange reactions, and hence sorption, are less favorable. DOC containing adjacent carboxylic groups, like CA, had the highest equilibrium constants (Evanko and Dzombak, 1999). Hence, sorption of DOC with higher equilibrium constants is more favorable. This may provide an explanation for differences in DOC competitive behavior.

According to Biber and Stumm (1994), SA forms different surface complexes on different metal oxide surfaces, determined by the surface composition. For instance, on goethite

surfaces, SA forms mononuclear bidentate five-membered chelate complexes but only six-membered pseudo-chelates on aluminum oxides (Yost et al., 1990; Biber and Stumm, 1994). Davis and Leckie (1980) found that SA is weakly adsorbed onto amorphous iron oxides, with behavior similar to SO_4^{2-}. Schnitzer and Khan (1972) noted that carboxylic or phenolic hydroxyl groups located in the ortho position (such as the constituents found on SA) are more reactive with iron oxides. Our results indicate that the observed competitive interactions between Se(IV) and DOC are likely related to binding preference. Minimal differences were observed for the orders of addition scenarios for Se(IV) and DOC in our study. Therefore, it appears that kinetics have little effect on competitive interactions.

Selenate Competitive Behavior with DOC.

Baseline Se(VI) sorption indicated that sorption occurred between pH 5-7, and Se(VI) was predominantly soluble at pH 8-9. At pH 8 and 9, 0.10 and 0.037 μmol m^{-2} surface sites, respectively, were occupied by Se(VI). According to the aforementioned hydrous ferric oxides surface site densities, this indicated that the majority of sites were largely available at the aforementioned pH values due to Se(VI) solubility (Dzombak and Morel, 1990).

In general, Se(VI) does not adsorb onto iron oxides above pH 7 (Cornell and Schwertmann, 2003). Goldberg (2014) also examined Se adsorption on an amorphous Fe-oxide. Adsorption maxima were noted between pH 2 and 4. Similarly to our results, work from Goldberg (2014) indicated that Se(VI) adsorption decreased between pH 6 and 7.5, with little adsorption occurring above pH 8.5. Similar results were also found by Peak and Sparks (2002). Goldberg (2002) noted mostly inner-sphere complexation while Peak and Sparks (2002) observed a mixture of inner and outer-sphere complexes on goethite and hydrous ferric oxide

surfaces. Only inner-sphere complexes were able to form on hematite (Peak and Sparks, 2002). On goethite surfaces, studies with Raman spectroscopy indicate that above pH 6, Se(VI) forms weak outer sphere complexes and inner sphere complexes at pH below 6 (Wijnja and Schulthess, 2000).

To date, no work has examined Se(VI) competitive behavior in the presence of DOC. In the presence of CA, Se(VI) sorption decreased at lower pH (5 and 6) with no competition observed between pH 7 and 9. This observation at higher pH is a result of minimal Se(VI) sorption, and therefore, competition is not expected. Results suggest that sorption inhibition is an important phenomenon that is likely to occur in seleniferous rhizosphere environments when aliphatic DOC, like CA, are present. However, only slight inhibitory effects were observed for the Se(VI) in the presence of SA at pH 5 and 6. Studies from Johnson and Loeppert (2006), Grafe et al. (2001, 2002) and Geelhoed et al. (1998) have observed inhibitory effects of CA on As and P. Little competition from SA and increased competition for CA could be related to differences in functional group configurations, which effect the magnitude of their equilibrium constants for ligand exchange.

Previous studies have indicated that Se(VI) and SO_4^{2-} exhibit similar sorptive behaviors (Davis and Leckie, 1980; Balistrieri and Chao, 1987). Davis and Leckie (1980) noted that comparable amounts of Se(VI) and SO_4^{2-} were sorbed onto amorphous Fe oxyhydroxide. Through additions of forest floor DOC leachate, Vance and David (1992) noted that SO_4^{2-} sorption on Spodosol whole soil surfaces was reduced between 5-22% for the three soils examined. Grafe et al. (2002) examined arsenite competitive sorption with CA on ferrihydrite. Like Se(VI), arsenite is the more soluble species of arsenic (Grafe et al. 2002). Grafe et al. (2002) indicated that arsenite adsorption was reduced between pH 3 and 7 when CA was present.

Similar results were found for Se(VI) between pH 5-7. Similarly to Se(IV), reasons for differences in competitive interactions of DOC with Se(VI) are possibly due to the number of functional groups, their density, and position along with the size of the DOC molecule (Dynes and Huang, 1997; Evanko and Dzombak, 1999; Grafe et al., 2002).

DOC Competitive Behavior with Selenium.

Citric acid sorption decreased with increasing pH according to sorption edge results. Edges followed similar trends to Grafe et al. (2001) and (2002) and Geelhoed et al. (1998) on the Fe-oxides, goethite and ferrihydrite. Increased inhibition of CA on oxyanion adsorption with decreasing pH is also consistent with previous work from Dynes and Huang (1995); Geelhoed et al. (1998); Grafe et al. (2001, 2002). Citric acid sorption was reduced in the presence of Se(IV) and Se(VI). The effects on CA were also comparable between both Se species, with competition most apparent between pH 5 and 6. Both Se species appear to have an inhibitory effect on CA sorption, which suggests that Se species have a greater site preference.

Work from Davis and Leckie (1980) has shown that SA weakly adsorbs to amorphous iron oxides. As previously discussed, lowest equilibrium constants are noted for compounds with phenolic groups in the ortho position, such as SA, relative to the carboxylic group. This is reflected by decreased adsorption of SA in comparison with DOC with higher constants (Evanko and Dzombak, 1999). Currently, no work has examined the effects of oxyanions on SA adsorption. Our results indicate SA sorption decreased with increasing pH. In the presence of Se(IV), SA sorption was almost completely hindered throughout the entire pH range examined. This corresponds with little observed effect of SA on Se(IV) sorption, suggesting that competition is likely caused by a greater preference for surface sites and stronger complexes

formed by Se(IV). Competition appears to be most pronounced for SA in the presence of Se(VI) at pH 5 and 6, when Se(VI) sorption is maximized.

Surface Potential.

Surface charge potentials were determined via electrophoretic measurements and were used to infer reaction mechanisms on mineral surfaces. This was accomplished through identifying shifts in surface potential of metal oxides in the presence of different sorbates (Sposito, 1984). Specifically sorbed positively or negatively charged species on a surfaces can cause a marked shift in the surface potential of metal oxides (Hingston et al., 1972; Anderson and Malotky, 1979).

The surface potential for ferrihydrite was first determined in the absence of any sorbed species present, and the PZC was observed at pH 7. Thus, it should have an increasingly more positive charge below this pH, allowing for sorption of negatively charged oxyanions. Surface potentials for pure ferrihydrite alone and with the implemented competition involving Se and DOC are shown in Figures 5.6 and 5.7.

Little to no shifts in the surface potential were observed in the presence of Se(VI) at higher pH (7-9), however, shifts to lower potentials were noted between pH 5 and 6. This is understandable because at higher pH, Se(VI) is mostly soluble, with more sorption occurring at lower pH values. However, shifts to lower potentials at lower pH for Se(VI) suggests that some inner-sphere complexation may be occurring as well (Hunter, 1981).

Small, slightly more negative differences in the ferrihydrite potential were noted in the presence of SA alone, especially at pH 6. At high pH, a lack of marked shifts in the ferrihydrite surface potential suggests that SA is weakly sorbed through outer-sphere complexes (Hunter, 1981). At lower pH, a reduction in surface potential was observed, suggesting that stronger

complexes are forming. Specific adsorption of anions shifts the surface charge to a lower pH value. For completely dissociated acids, the degree of specific adsorption is directly related to the extent of positive surface charge. For acids that are completely dissociated, most specific adsorption will occur with respect to the extent of the surface positive charge. Minimal specific adsorption will occur at pH that are greater than the PZC for acids that are completely dissociated. For incompletely dissociated acids, adsorption can occur at pH higher than the PZC, but should be near the pK_a of the sorbing acid (Hingston et al., 1972). On Al oxide surfaces, previous work indicates that Se(IV) shifts the PZC to lower pH. Selenite had no effect on a ϒ-Al oxide (Elzinga et al., 2009) but does shift the PZC to a lower pH on gibbsite (Goldberg, 2013). Su and Suarez (2000) observed shifts in the PZC to lower pH for both Se(IV) and Se(VI) following adsorption to an amorphous Fe hydroxide and goethite.

With additions of both Se(IV) and CA, regardless of introduction order or whether they were examined individually, the surface potential measurements became increasingly more negative and the PZC shifted to a lower pH. This marked shift suggested the formation of inner-sphere complexes. With the addition of Se(IV) with SA together, the measured surface potential was markedly higher (more positive) than when Se(IV) and CA were added together but was lower (more negative) in comparison with Se(VI) with SA added together. This suggested that sorbed Se(IV) and CA both contributed to a shift in the PZC, but CA has a greater influence over this than Se(IV).

Reports to date regarding Se(VI) inner vs. outer sphere complex formation on iron oxide surfaces are contradictory. Using dilatometry, Yamaguchi et al. (1999) observed losses in waters of hydration for Se(VI) sorbed to an amorphous iron oxide, suggesting the occurrence of a ligand-exchange reaction. Under neutral pH conditions, Das et al. (2013) determined that Se(VI)

forms inner sphere complexes on ferrihydrite due to its high surface area and ability to disperse in solution. Other analyses by Peak and Sparks (2002) have shown that, at low pH, Se(VI) can form a mixture of outer and inner sphere complexes on goethite and hydrous ferric oxides but only inner-sphere on hematite. While this suggests inner-sphere complex formation, the authors also observed evidence of outer-sphere complexation, as determined by pH edge large dependence on ionic strength (Peak and Sparks, 2002). From attenuated total reflectance (ATR-FTIR) and diffuse reflectance (DRIFT) spectroscopic analyses, Su and Suarez (2000) were able to confirm a mixture of mono- and bidentate inner-sphere complex formation.

Conclusion

This work demonstrates the effectiveness of CA inhibition on Se(IV) and Se(VI) adsorption on ferrihydrite at pH values relevant to seleniferous soils in the Western US. Along with other common organic ligands, CA and SA are important because of their prominence in many rhizosphere environments. Baseline results for Se(IV) indicated sorption occurred throughout the examined pH range (5-9) and increased as pH decreased. Similar results were noted for Se(VI), however, sorption was markedly lower in comparison with Se(IV). In the presence of CA, Se(IV) and Se(VI) sorption inhibition increased with decreasing pH. In the presence of SA, few competitive interactions were observed for Se(IV), and slight competition was observed for Se(VI). The observed competition with CA and lack of competition with SA and Se likely differ because of the effects of phenolic group positions on DOC ligand exchange equilibrium constants. Decreased CA and SA sorption was observed due to Se competition. Discernible shifts in the ferrihydrite point of zero charge (PZC) indicated inner-sphere complex formation for both Se(IV) and CA. Smaller shifts for Se(VI) and SA suggest the formation of

outer-sphere complexes. Competition from CA on Se suggests a likely mechanism for increased Se solubilization in contaminated soil systems. Additionally, it is possible that vegetation that hyperaccumulate Se could facilitate solubilization through inputs of DOC exudates.

References

Anderson, M.A., Malotky, D.T., 1979. The adsorption of protolyzable anions on hydrous oxides at the isoelectric pH. J. Colloid Interf. Sci. 72, 413-427.

Balistrieri, L.S., Chao, T.T., 1987. Selenium Adsorption by Goethite. Soil Sci. Soc. Am. J. 51, 1145-1151.

Balistrieri, L.S., Chao, T.T., 1990. Adsorption of selenium by amorphous iron oxyhydroxide and manganese dioxide. Geochim. Cosmochim. Acta 54, 739-751.

Barrow, N.J., Whelan, B.R., 1989. Testing a mechanistic model. VII. The effects of pH and of electrolyte on the reaction of selenite and selenate with a soil. J. Soil Sci. 40, 17-28.

Biber, M.V., Stumm, W., 1994. An In-Situ ATR-FTIR Study: The Surface Coordination of Salicylic Acid on Aluminum and Iron(III) Oxides. Environ. Sci. Technol. 28, 763-768.

Cornell, R.M., Schwertmann, U., 2003. The Iron Oxides: Structure, Properties, Reactions, Occurrences and Uses. Wiley-VCH, Weinheim, Germany.

Das, S., Jim Hendry, M., Essilfie-Dughan, J., 2013. Adsorption of selenate onto ferrihydrite, goethite, and lepidocrocite under neutral pH conditions. Appl. Geochem. 28, 185-193.

Davis, A.M., 1972. Selenium Accumulation in Astragalus Species. Agron. J. 64, 751-754.

Davis, J.A., James, R.O., Leckie, J.O., 1978. Surface ionization and complexation at the oxide/water interface. I. Computation of electrical double layer properties in simple electrolytes. J. Colloid Interf. Sci. 63, 480-499.

Davis, J.A., Kent, D.B., 1990. Surface complexation modeling in aqueous geochemistry. Min. Soc. Am., Washington D.C.

Davis, J.A., Leckie, J.O., 1980. Surface ionization and complexation at the oxide/water interface. 3. Adsorption of anions. J. Colloid Interf. Sci. 74, 32-43.

Davis, T.Z., Stegelmeier, B.L., Panter, K.E., Cook, D., Gardner, D.R., Hall, J.O., 2012. Toxicokinetics and pathology of plant-associated acute selenium toxicosis in steers. J. Vet. Diagn. Invest. 24, 319-327.

Dynes, J.J., Huang, P.M., 1995. Influence of citrate on selenite sorption-desorption on short-range ordered aluminum hydroxides. in: Huang, P.M. (Ed.). Environmental impact of soil component interactions - Metals, other inorganics, and microbial activities. CRC/Lewis Publishers, Boca Raton, FL, pp. 47-61.

Dynes, J.J., Huang, P.M., 1997. Influence of Organic Acids on Selenite Sorption by Poorly Ordered Aluminum Hydroxides. Soil Sci. Soc. Am. J. 61, 772-783.

Dzombak, D.A., Morel, F.M.M., 1990. Surface complexation modeling: Hydrous ferric oxide. Wiley-Interscience, New York.

Elzinga, E.J., Tang, Y., McDonald, J., DeSisto, S., Reeder, R.J., 2009. Macroscopic and spectroscopic characterization of selenate, selenite, and chromate adsorption at the solid-water interface of gamma-Al2O3. J. Colloid Interf. Sci. 340, 153-159.

Evanko, C.R., Dzombak, D.A., 1999. Surface Complexation Modeling of Organic Acid Sorption to Goethite. J. Colloid Interf. Sci. 214, 189-206.

Evans, A.J., Zelazny, L.W., 1990. Kinetics of aluminum and sulfate release from forest soils by mono- and diprotic aliphatic acids. Soil Sci. 149, 324-330.

Fox, T.R., Comerford, N.B., 1990. Low-Molecular-Weight Organic Acids in Selected Forest Soils of the Southeastern USA. Soil Sci. Soc. Am. J. 54, 1139-1144.

Geelhoed, J.S., Hiemstra, T., Van Riemsdijk, W.H., 1998. Competitive Interaction between Phosphate and Citrate on Goethite. Environ. Sci. Technol. 32, 2119-2123.

Goldberg, S., 2002. Competitive Adsorption of Arsenate and Arsenite on Oxides and Clay Minerals. Soil Sci. Soc. Am. J. 66, 413-420.

Goldberg, S., 2013. Modeling Selenite Adsorption Envelopes on Oxides, Clay Minerals, and Soils using the Triple Layer Model. Soil Sci. Soc. Am. J. 77, 64-71.

Goldberg, S., 2014. Modeling Selenate Adsorption Behavior on Oxides, Clay Minerals, and Soils Using the Triple Layer Model. Soil Sci. 179, 568-576.

Grafe, M., Eick, M.J., Grossl, P.R., 2001. Adsorption of Arsenate (V) and Arsenite (III) on Goethite in the Presence and Absence of Dissolved Organic Carbon. Soil Sci. Soc. Am. J. 65, 1680-1687.

Grafe, M., Eick, M.J., Grossl, P.R., Saunders, A.M., 2002. Adsorption of Arsenate and Arsenite on Ferrihydrite in the Presence and Absence of Dissolved Organic Carbon. J. Env. Qual. 31, 1115-1123.

Hamdy, A.A., Gissel-Nielsen, G.G., 1977. Fixation of selenium by clay minerals and iron oxides. 2. Pflanzenernaehr. Bodenkd. 140, 63-70.

Hayes, K.F., Roe, A.L., Brown, G.E., Jr., Hodgson, K.O., Leckie, J.O., Parks, G.A., 1987. In Situ X-ray Absorption Study of Surface Complexes: Selenium Oxyanions on α-FeOOH. Science 238, 783-786.

Hingston, F.J., Posner, A.M., Quirk, J.P., 1972. Anion adsorption by goethite and gibbsite. J. Soil Sci. 23, 177-192.

Hopper, J.L., Parker, D.R., 1999. Plant availability of selenite and selenate as influenced by the competing ions phosphate and sulfate. Plant Soil 210, 199-207.

Hunter, R.J., 1981. Zeta Potential in Colloid Science. Academic Press. San Diego, CA

Johnson, S.E., Loeppert, R.H., 2006. Role of Organic Acids in Phosphate Mobilization from Iron Oxide. Soil Sci. Soc. Am. J. 70, 222-234.

Manceau, A., 1995. The mechanism of anion adsorption on iron oxides: Evidence for the bonding of arsenate tetrahedra on free Fe(O, OH)6 edges. Geochim. Cosmochim. Acta 59, 3647-3653.

Manceau, A., Charlet, L., 1994. The mechanism of selenate adsorption on goethite and hydrous ferric oxide. J. Colloid Interf. Sci. 168, 87-93.

McFadden, L.D., 1988. Climate influences on rates and processes of soil development in Quaternary deposits of southern California. in: Reinhardt, J., Sigleo, W.R. (Eds.). Paleosols and weathering through geologic time: principles and applications, Special Paper 216. The Geological Society of America, Boulder, CO.

McNeal, J.M., Balistrieri, L.S., 1989. Geochemistry and Occurrence of Selenium: An Overview. in: Jacobs, L.W. (Ed.). Selenium in Agriculture and the Environment. Soil Science Society of America and American Society of Agronomy, Madison, WI.

Neal, R.H., Sposito, G., Holtzclaw, K.M., Traina, S.J., 1987. Selenite adsorption on alluvial soils: I. Soil Composition and pH Effects and II. Solution composition effects. Soil Sci. Soc. Am. J. 51.

Parfitt, R.L., Russell, J.D., 1977. Adsorption on hydrous oxides. IV. Mechanisms of adsorption of various ions on goethite. J. Soil Sci. 28, 297-305.

Peak, D., Sparks, D.L., 2002. Mechanisms of selenate adsorption on iron oxides and hydroxides. Environ. Sci. Technol. 36, 1460-1466.

Rajan, S.S.S., Watkinson, J.H., 1976. Adsorption of selenite and phosphate on an allophane clay. Soil Sci. Soc. Am. J. 40, 51-54.

Ryden, J.C., Syers, J.K., Tillman, R.W., 1987. Inorganic anion sorption and interactions with phosphate sorption by hydrous ferric oxide gel. J. Soil Sci. 38, 211-217.

Saeki, K., Matsumoto, S., 1994. Selenite adsorption by a variety of oxides. Commun. Soil Sci. Plant Anal. 25, 2147-2158.

Schnitzer, M., Khan, S.U., 1972. Humic Substances in the Environment. Marcel-Dekker, New York, NY.

Schwertmann, U., Cornell, R.M., 2000. Iron Oxides in the Laboratory: Preparation and Characterization, Second ed. Wiley-VHC, Weinheim.

Snyder, M., Wooyong, U., 2014. Adsorption Mechanisms and Transport Behavior between Selenate and Selenite on Different Sorbents. Int. J. Waste Resources 4, 144.

Sposito, G., 1984. The surface chemistry of soils. Oxford University Press, New York.

Stevenson, F.J., 1967. Organic acids in soil. in: McLaren, A.D., Peterson, G.H. (Eds.). Soil Biochemistry. Marcel Dekker, New York, pp. 119-146.

Stumm, W., 1986. Coordination interactions between soil solids and water - An aquatic chemist's point of view. Geoderma 38, 19-30.

Su, C., Suarez, D.L., 2000. Selenate and Selenite Sorption on Iron Oxides: An Infrared and Electrophoretic Study. Soil Sci. Soc. Am. J. 64, 101-111.

Vance, G.F., David, M.B., 1992. Dissolved organic carbon and sulfate sorption by spodosol mineral horizons. Soil Sci. 154, 136-144.

Waychunas, G.A., Rea, B.A., Fuler, C.C., Davis, J.A., 1993. Surface chemistry of ferrihydrite: Part 1: EXAFS studies of the geometry of coprecipitated and adsorbed arsenate. Geochim. Cosmochim. Acta 57, 2251-2269.

Wijnja, H., Schulthess, C.P., 2000. Vibrational Spectroscopy Study of Selenate and Sulfate Adsorption Mechanisms on Fe and Al (Hydr)oxide Surfaces. J. Colloid Interf. Sci. 229, 286-297.

Wijnja, H., Schulthess, C.P., 2002. Effect of Carbonate on the Adsorption of Selenate and Sulfate on Goethite. Soil Sci. Soc. Am. J. 66, 1190-1197.

Wu, C.H., Kuo, C.Y., Lin, C.F., Lo, S.L., 2002. Modeling competitive adsorption of molybdate, sulfate, selenate, and selenite using a Freundlich-type multi-component isotherm. Chemosphere 47, 283-292.

Wu, C.H., Lo, S.L., Lin, C.F., 2000. Competitive adsorption of molybdate, chromate, sulfate, selenate, and selenite on γ-Al2O3. Colloids Surf. Physicochem. Eng. Aspects 166, 251-259.

Wyoming Board of Sheep Commissioners, 1908. 10th annual report. Cheyenne, Wyoming.

Yamaguchi, N.U., Okazaki, M., Hashitani, T., 1999. Volume Changes Due to SO2-4, SeO2-4, and H2PO-4 Adsorption on Amorphous Iron(III) Hydroxide in an Aqueous Suspension. J. Colloid Interf. Sci. 209, 386-391.

Yost, E.C., Tejedor-Tejedor, M.I., Anderson, M.A., 1990. In situ CIR-FTIR characterization of salicylate complexes at the goethite/aqueous solution interface. Environ. Sci. Technol. 24, 822-828.

Zhang, P., Sparks, D.L., 1990. Kinetics of selenate and selenite adsorption/desorption at the goethite/water interface. Environ. Sci. Technol. 24, 1848-1856.

Chapter 6: Overall Conclusions

Selenium (Se) is a trace element found in exceedingly high levels in phosphate mine soils in the Western US. Soluble forms are typically absorbed in high quantities by vegetation throughout this region, which can be ingested by ruminants grazing on mine soils. The ingestion of Se-hyperaccumulators, hence, has resulted in a number of livestock fatalities. Because of this, Se geochemical behavior and bioavailability are imperative to examine, especially in relation to the hyperaccumulator, western aster (*Symphyotrichum ascendens* (Lindl.)). The work completed for this dissertation contributes to our understanding of soil Se bioavailability to vegetation, Se speciation and phases in phosphate mine soils, and competitive interactions of dissolved organic carbon (DOC) with Se oxyanions.

In Chapter 3, Se soil geochemistry was examined in contaminated phosphate mine soils using a sequential extraction procedure (SEP) and speciation results for both water-soluble and exchangeable phases. Using simple linear regression, strong relationships were identified for the first two fractions of the SEP (water-soluble and PO_4^{3-}extractable) with plant uptake in western aster. This indicates that water-soluble and PO_4^{3-}-extractable Se most contribute to the bioavailable pool of Se absorbed by plants. Regression analyses for Se speciation and the first two fractions of the SEP indicated that water-soluble Se and selenate species exhibited the strongest significant relationship. The aforementioned relationships indicate the usefulness of water extractions as tools for site assessments. This can facilitate and improve Se remediation throughout this region.

Soil Se speciation and the previously used SEP from Chapter 3 were evaluated by X-ray absorption fine structure (XAFS) spectroscopy in the near edge region. This was completed for both whole and extracted soils. The SEP phases examined included Se sorbed/co-precipitated to

carbonate and Fe-oxide minerals, organic Se, and residual/elemental Se. XAFS analyses of whole soils indicated the presence of fractions of Se that resembled previous SEP findings using ICP-AES. However, sorbed/co-precipitated phases were underestimated by the SEP. Overall, regression analyses indicated that the SEP and XANES techniques, were predicative of one another only for the residual/elemental Se phase. This was likely related to XAFS sensitivity to phases that are more abundant.

Soils were extracted using the SEP and were re-analyzed with XAFS after each step. Results indicated partial dissolution of Se occurred during extractions for sorbed (on carbonate and Fe-oxide minerals) and organic fractions. Therefore, it is advised that soil geochemistry should be fully characterized prior to SEP implementation, and conditions should be monitored during extraction to ensure full recovery of target elements. The formulation of a more accurate and effective SEP for Se in soils can be further evaluated using these recommendations.

In Chapter 5, Se solubility was analyzed in the presence and absence of dissolved organic carbon (DOC) on an amorphous iron oxide surface, ferrihydrite. Citric acid effectively competed with both Se(IV) and Se(VI) at lower pH. This behavior was not observed for salicylic acid. Differences in competitive behavior are likely related to differences in DOC stereochemistry and their ability to form strong surface complexes. In soil systems, it is possible that citric acid, or similar DOC species, can compete with sorbed Se oxyanions, promoting solubilization. This is a possible mechanism for increasing Se bioavailability to Se-accumulating and hyperaccumulating vegetation in rhizosphere environments. It is also possible that plant roots could provide a source of Se-solubilizing DOC from root exudates. This notion can be further examined in future work.

Overall, this research has improved our scientific understanding of Se-affected soils. Relationships that were identified for Se bioavailability to hyperaccumulating vegetation provide

useful tools for future reclamation efforts and helps researchers quickly identify particularly problematic locations. The XAFS evaluation of an SEP provides recommendations that could be useful for formulating a more accurate, effective procedure for targeting phases of oxyanions. Lastly, the highly soluble nature of Se in soils in the western US can be explained by the behavior of DOC species in relation to Se and their effects on Se solubility and adsorption.

Appendix A

Table A. Six fractions of selenium from a sequential extraction procedure (SEP) for all points along five transects.

Transect Point	Water	PO_4^{3-}-Extr.	Carb.	Am. Fe-Oxide	Organic	Residual
SA[a] CO	1.79	1.23	ND	ND	9.61	24.66
SA S1	0.86	ND	ND	ND	3.73	26.34
SA S2	ND[b]	ND	ND	ND	7.41	18.46
SA S3	ND	ND	ND	ND	8.98	15.48
SA S4	ND	ND	2.29	ND	4.58	36.51
SA S5	ND	ND	2.80	ND	4.03	20.75
SA NE1	0.62	0.71	2.82	ND	4.79	32.13
SA NE2	ND	ND	ND	ND	13.15	34.99
SA NE3	ND	ND	2.64	ND	15.86	19.71
SA NE4	1.05	0.83	3.60	ND	9.56	20.09
SA NE5	ND	ND	2.39	ND	6.96	31.24
SA NW1	0.77	ND	3.55	ND	7.38	23.03
SA NW2	ND	ND	3.78	ND	7.01	27.98
SA NW3	ND	ND	2.40	3.87	4.91	22.40
SA NW4	ND	ND	2.51	ND	6.58	9.00
SA NW5	ND	ND	ND	ND	ND	7.11
SB CO	3.15	1.76	15.66	6.34	34.41	245.82
SB S1	1.80	2.23	9.71	4.35	8.53	225.28
SB S2	1.52	1.10	11.55	9.74	36.35	216.11
SB S3	ND	ND	3.01	ND	7.62	45.65
SB S4	ND	ND	2.48	ND	3.46	14.03
SB S5	ND	ND	3.71	ND	4.96	35.87
SB NE1	2.87	1.58	6.59	ND	11.55	164.41
SB NE2	1.82	1.68	1.61	ND	44.15	384.52
SB NE3	1.72	2.64	8.83	3.98	8.21	270.58
SB NE4	0.83	1.56	3.83	ND	9.42	149.28
SB NE5	1.34	1.18	7.9	5.29	7.45	166.68
SB NW1	2.01	1.05	6.83	5.04	7.58	166.85
SB NW2	10.69	3.33	14.87	9.21	11.29	210.48
SB NW3	1.06	0.84	7.6	5.31	6.75	242.43
SB NW4	2.69	1.77	11.03	8.66	25.17	253.26
SB NW5	1.12	1.39	4.65	5.50	13.56	181.41
SC CO	1.63	ND	6.54	7.28	5.33	78.04
SC NW1	1.56	1.33	9.56	6.02	12.83	130.23

SC NW2	0.63	ND	3.27	4.77	10.16	50.26
SC NW3	ND	ND	ND	ND	ND	10.17
SC NW4	0.86	ND	4.61	5.64	7.27	87.30
SC NW5	1.61	0.97	7.00	6.44	35.18	90.87
SC SW1	1.04	0.76	6.68	8.99	20.91	61.17
SC SW2	ND	ND	ND	ND	3.57	9.12
SC SW3	ND	ND	ND	ND	5.00	6.63
SC SW4	ND	ND	ND	ND	ND	9.93
SC SW5	ND	ND	ND	ND	ND	8.19
SC NE1	ND	ND	ND	ND	17.53	69.44
SC NE2	ND	ND	ND	ND	ND	ND
SC NE3	ND	ND	ND	ND	2.85	6.75
SC NE4	ND	ND	ND	ND	ND	2.49
SC NE5	ND	ND	ND	ND	ND	ND
SD CO	ND	ND	ND	ND	5.82	12.38
SD W1	ND	ND	ND	ND	7.66	31.25
SD W2	ND	ND	ND	ND	6.79	11.53
SD W3	ND	ND	1.60	ND	10.61	10.82
SD W4	ND	ND	ND	ND	5.19	10.44
SD W5	ND	ND	ND	ND	5.91	8.97
SD NE1	ND	ND	ND	ND	6.60	15.94
SD NE2	ND	ND	1.50	ND	4.29	6.30
SD NE3	ND	ND	1.77	ND	7.20	5.62
SD NE4	ND	ND	ND	ND	5.58	10.71
SD NE5	ND	ND	ND	ND	5.61	6.95
SD SE1	ND	ND	ND	ND	10.36	20.88
SD SE2	ND	ND	ND	ND	6.95	13.44
SD SE3	ND	0.45	ND	ND	4.76	25.75
SD SE4	ND	0.82	ND	ND	5.58	9.87
SD SE5	ND	ND	ND	ND	7.31	11.4
SE SE1	ND	ND	ND	ND	5.44	22.79
SE SE2	ND	ND	ND	ND	11.27	20.72
SE SE3	ND	ND	ND	ND	18.59	24.82
SE SE4	ND	ND	ND	6.54	14.12	29.62
SE SE4-5	ND	ND	ND	ND	8.43	20.16
SE SE5	ND	ND	ND	ND	4.38	10.89
SE CO	ND	ND	ND	ND	4.13	23.03
SE N1	ND	ND	ND	ND	6.92	30.13
SE N2	ND	ND	ND	ND	6.89	18.88
SE N3	ND	ND	ND	ND	11.26	23.71

SD SW1	ND	ND	ND	ND	13.35	30.02
SD SW2	ND	ND	ND	6.16	15.30	30.74
SD SW3	ND	ND	ND	ND	11.86	26.90
SD SW4	ND	0.55	3.16	10.35	14.98	35.77

[a]SA: Site A; SB: Site B; SC = Site C; SD = Site D; SE = Site E
[b]ND indicates phase not detected

Appendix B

Table B. X-ray diffraction (XRD) d-spacing used to identify minerals in twenty soils used for X-ray absorption near edge structure (XANES) spectroscopy.

	Mineral	*d-spacing*[*]				
Site A						
A NE2	**Quartz**	4.223	**3.328**	2.448	2.276	1.812
	Carb.-Fluorapatite	3.430	3.169	2.787	**2.695**	2.613
	Dolomite	**2.876**	2.182	1.800		
	Gr. Selenium	**3.774**	2.999	2.057	1.991	
A NE5	**Quartz**	4.187	**3.313**	2.440	2.269	1.809
	Carb.-Fluorapatite	7.995	3.420	3.211	3.142	2.778
	Calcite	**3.035**	2.269	1.877		
	Dolomite	**2.889**	2.440	2.180		
	Gr. selenium	**3.753**	2.992	2.051	1.988	
	Muscovite	9.756	4.415	**2.552**		
A NW1	**Quartz**	4.228	**3.325**	2.449	2.276	1.814
	Carb.-Fluorapatite	4.450	3.226	3.150	2.791	
	Dolomite	**2.881**	2.185	1.793		
	Gr. Selenium	**3.781**	2.976	2.054	1.988	
	Muscovite	9.904	4.450	**2.556**		
A NW3	**Quartz**	4.246	**3.338**	2.454	2.278	1.816
	Carb.-Fluorapatite	3.438	3.235	3.055	2.795	**2.698**
	Dolomite	**2.889**	2.192	1.796		
	Muscovite	9.978	4.465	3.000	**2.556**	
	Gr. Selenium	**3.797**	2.999	2.060		
A CO	**Quartz**	4.238	**3.338**	2.447	2.278	1.815
	Carb.-Fluorapatite	3.430	3.235	3.056	2.793	**2.692**
	Dolomite	**2.878**	2.190	1.790		
	Muscovite	8.996	4.449	**2.558**		
	Gr. Selenium	**3.787**	2.995	2.056		
Site B						
B CO	**Quartz**	4.240	**3.332**	2.449	2.276	1.814
	Carb.-Fluorapatite	3.429	2.790	**2.696**	2.621	2.233
	Dolomite	**2.878**	2.189	1.798		
	Muscovite	**2.556**	4.545	3.226	9.922	
	Gr. Selenium	2.992	**3.786**	2.057	1.991	
	Calcite	**3.041**	2.242	1.879		
B NE2	**Quartz**	**3.325**	4.242	2.445	2.273	1.812
	Carb.-Fluorapatite	3.438	2.786	**2.690**	2.611	2.232
	Dolomite	**2.882**	2.187	1.793		
	Muscovite	10.060	4.445	3.219	2.999	**2.556**
	Gr. Selenium	2.986	**3.778**	2.056	1.994	

	Calcite	3.853	**3.042**	1.879		
B NE3	**Quartz**	4.241	**3.333**	2.449	2.276	1.814
	Carb.-Fluorapatite	3.447	3.055	2.791	2.768	**2.695**
	Dolomite	3.227	2.161	1.719	**2.889**	
	Muscovite	9.983	4.990	4.445	2.990	**2.556**
B NE5	**Quartz**	4.240	**3.332**	2.449	2.276	1.814
	Carb.-Fluorapatite	3.429	2.790	**2.696**	2.621	2.233
	Dolomite	**2.882**	2.189	1.798		
	Muscovite	10.062	4.445	3.226	**2.556**	
	Gr. Selenium	**3.786**	2.992	2.057		
B NW1	**Quartz**	4.228	**3.326**	2.449	2.273	1.812
	Carb.-Fluorapatite	3.438	2.763	**2.690**	2.611	2.231
	Dolomite	**2.876**	2.182	1.798		
	Muscovite	**2.556**	4.445	3.219	9.830	
	Gr. Selenium	2.992	**3.786**	2.054	2.007	
B NW2	**Quartz**	4.213	**3.316**	2.445	2.269	1.809
	Carb.-Fluorapatite	3.438	2.757	**2.685**	2.780	2.606
	Dolomite	**2.870**	2.182	1.798		
	Muscovite	9.830	4.425	3.211	**2.552**	
	Gr. Selenium	**3.764**	2.979	2.057		
	Calcite	**3.041**	2.226	1.877		
B NW4	**Quartz**	4.243	**3.327**	2.447	2.274	1.813
	Carb.-Fluorapatite	4.020	3.422	2.787	2.764	**2.692**
	Dolomite	**2.872**	2.187	2.010	1.799	
	Muscovite	9.889	4.446	**2.558**		
B S2	**Quartz**	4.228	**3.325**	2.445	2.272	1.811
	Carb.-Fluorapatite	**2.690**	3.438	3.049	2.762	2.611
	Dolomite	**2.870**	2.185	1.718		
	Muscovite	9.984	4.429	3.210	**2.561**	
	Calcite	**3.041**	1.879	2.283		
B S5	**Quartz**	4.242	**3.333**	2.449	2.276	1.814
	Carb.-Fluorapatite	2.762	**2.690**	3.438	2.786	2.616
	Dolomite	**2.876**	2.185	1.764		
	Muscovite	9.906	4.445	3.211	**2.556**	
	Gr. Selenium	**3.764**	2.993	2.057		
Site C						
C CO	**Quartz**	4.230	**3.326**	2.449	2.276	1.814
	Carb.-Fluorapatite	3.429	3.054	2.788	**2.696**	
	Muscovite	9.830	4.447	3.158	**2.556**	
	Calcite	**3.034**	2.276	1.877		
	Gr. Selenium	2.986	**3.774**	2.057	1.992	
C NE1	**Quartz**	4.226	**3.326**	2.446	2.274	1.813

	Carb.-Fluorapatite	4.019	3.429	3.180	3.048	**2.689**
	Calcite	**3.034**	2.276	1.878		
	Dolomite	**2.889**	2.150	1.810		
	Muscovite	9.907	4.445	3.750	3.638	**2.556**
C NE4	**Quartz**	4.228	**3.330**	2.449	2.274	1.814
	Carb.-Fluorapatite	4.031	3.446	2.786	2.779	**2.696**
	Muscovite	4.445	3.753	3.465	3.200	**2.550**
C NW2	**Quartz**	4.233	**3.325**	2.449	2.274	1.813
	Carb.-Fluorapatite	3.430	3.159	3.050	2.789	**2.695**
	Dolomite	**2.876**	2.190	2.010		
	Muscovite	9.907	4.450	3.680	3.464	**2.551**
C NW5	**Quartz**	4.223	**3.322**	2.449	2.269	1.812
	Carb.-Fluorapatite	3.429	3.165	2.797	**2.690**	2.611
	Calcite	**3.041**	2.276	2.239	1.992	1.876
	Dolomite	**2.870**	2.185	1.809		
	Muscovite	9.906	4.445	2.990	2.860	**2.551**
	Gray selenium	**3.773**	2.994	2.054	1.988	
C SW1	**Quartz**	4.233	**3.328**	2.449	2.272	1.812
	Carb.-Fluorapatite	4.031	3.429	3.165	3.048	1.931
	Calcite	**3.041**	2.276	1.992	1.876	
	Muscovite	9.983	4.445	2.990	**2.556**	1.490

*d-spacing values in bold are those found at 100% intensity